

SPECTRAL CORRELATION TESTS OF AN
EDDY HEAT FLUX PARAMETERIZATION

by

JOHN NEWELL MCHENRY

B.A., DePauw University
(1977)

SUBMITTED IN PARTIAL FULFILLMENT
OF THE REQUIREMENTS FOR THE
DEGREE OF

MASTER OF SCIENCE

at the

MASSACHUSETTS INSTITUTE OF TECHNOLOGY

May, 1980

© Massachusetts Institute of Technology 1979

Signature of Author *John Newell McHenry*
Department of Meteorology
May 9, 1980

Certified by *[Signature]*
Thesis Supervisor

Accepted by *[Signature]*
Chairman, Departmental Committee

WITHDRAWN
FROM
MIT LIBRARIES
LIBRARIES



Room 14-0551
77 Massachusetts Avenue
Cambridge, MA 02139
Ph: 617.253.5668 Fax: 617.253.1690
Email: docs@mit.edu
<http://libraries.mit.edu/docs>

DISCLAIMER OF QUALITY

Due to the condition of the original material, there are unavoidable flaws in this reproduction. We have made every effort possible to provide you with the best copy available. If you are dissatisfied with this product and find it unusable, please contact Document Services as soon as possible.

Thank you.

Some pages in the original document contain pictures, graphics, or text that is illegible.

No Page numbered 28 authors mistake.

SPECTRAL CORRELATION TESTS OF AN
EDDY HEAT FLUX PARAMETERIZATION

by

JOHN NEWELL MCHENRY

Submitted to the Department of Meteorology
on May 9, 1980 in Partial Fulfillment of the
Requirements for the Degree of Master of Science

ABSTRACT

A two-layer model processes eight years of twice daily geopotential height data to compute the total eddy flux of sensible heat and its combination of predictors in a parameterization representative of those used in climate models. The parameterization assumes that the eddy flux is proportional to a stability coefficient, X , times the square of the meridional temperature gradient. Zonal Fourier decomposition and temporal analysis of covariance are employed to determine the correlation spectra of the parameterization, thereby testing its validity for various zonal spatial and temporal scales. This procedure is performed for four 10 degree wide latitude bands centered at 35, 45, 55, and 65 degrees north.

The results show that the parameterization models the seasonally forced zonally averaged eddy flux well, in agreement with previous studies, and reveals additional seasonal forcing on a few other large zonal scales as well. We cannot determine whether the stability coefficient improves the parameterization in comparison with another which does not include it.

Baroclinic adjustment, whereby the eddies adjust the gradient as a result of baroclinic instabilities, is revealed in the negative correlations found on short time scales. It is shown that adjust-

ment may be occurring on zonal scales as small as the relevant zonal scale of the eddies themselves. By identifying the most favored time scale as that scale which exhibits the most negative correlation for a given zonal scale, we can show that that time scale retrogresses as the eddy size decreases. Eventually the eddies become too small, and hence too short-lived, to be observed. We identify four days as an overall favored time scale in which baroclinic eddies adjust the gradient.

THESIS SUPERVISOR: Edward N. Lorenz

TITLE: Professor of Meteorology

ACKNOWLEDGEMENTS

I would like to thank Professor E.N. Lorenz who advised the research and writing of this thesis. Professor Peter H. Stone also provided considerable feedback during the course of the project.

Thanks also are extended to Maurice Blackman for providing spherical harmonic data tapes and a program for converting grid point geopotential heights into spherical harmonics. In addition, the consultants at the NCAR computing facility were invaluable in lending advice on the use of NCAR's CDE 7600 and peripheral devices. Diana Spiegel should also be mentioned for her help in debugging programs and using the department's Harris terminal system.

Finally, thanks go out to Isabel Kole who drafted the figures.

TABLE OF CONTENTS

	<u>Page</u>
TITLE	1
ABSTRACT	2
ACKNOWLEDGEMENTS	4
TABLE OF CONTENTS	5
LIST OF TABLES	7
LIST OF FIGURES	8
CHAPTER ONE. INTRODUCTION	11
1.1 The Eddy Flux Parameterization Problem	11
1.2 Forced Versus Free Eddy Behavior and Baroclinic Adjustment	13
1.3 Objectives of this Research	14
CHAPTER TWO. MODELLING THE EDDY FLUX AND ITS PREDICTORS	17
2.1 Choice of Specific Parameterization for Study and Analysis Method	17
2.2 A Two-Layer Format for Processing Geopotential Height Data	22
2.2.1 Critical Shear	23
2.2.2 Mass-Weighted Meridional Temperature Gradient	24
2.2.3 Actual Shear	24
2.2.4 Eddy Flux	26
CHAPTER THREE. DATA ACQUISITION AND ANALYSIS	29
3.1 Data Sources and Description	29
3.2 Initial Computational Work	30
3.3 Computation by the Two-Layer Model	32
3.4 Spectral Decomposition and Analysis of Variance	44
3.4.1 Fourier Analysis in Latitude Bands	47
3.4.2 Poor Mans Time Spectral Analysis	48
CHAPTER FOUR. DESCRIPTION OF CORRELATION SPECTRA	51
4.1 Determination of Degrees of Freedom and Description of Spectral Tables	51

	<u>Page</u>
4.2 Correlation Spectra for Individual Wavenumbers and Time Scales by Latitude Band	65
4.3 Correlation Spectra for the Sum over all Wavenumbers	91
4.4 Correlation Spectra for the Sum over all Time Scales	96
4.5 Total Correlations by Latitude Band	101
4.6 Variance and Covariance Spectra	101
 CHAPTER FIVE. DISCUSSION OF RESULTS AND CONCLUSIONS	 104
5.1 Forced and Free Regimes	104
5.2 Baroclinic Adjustment: A Free Regime Process	105
5.3 Validity of the Eddy Flux Parameterization: Eddy Flux Predictors	109
 CHAPTER SIX. SUGGESTIONS FOR CONTINUING RESEARCH	 114
6.1 Regional Analysis	114
6.2 Multiple Correlation Studies	117
6.3 General Uses of the Program SPECTRA	118
 APPENDICES	
A. Computer Program SPECTRA: A Listing	119
B. Additional Spectral Output	129
 REFERENCES	 136

LIST OF TABLES

<u>Table</u>		<u>Page</u>
3.1	Two-Layer Model Programming, Programs CRTSHR, DAGRI3	33
3.2	Two-Layer Model Programming, Program FINAL	43
4.1	Degrees of Freedom and 95%, 99% Confidence Limits for Correlation Coefficients	66
5.1	Physical Size of Wavenumber Domain	107
5.2	Correlation Coefficient Comparison: Lorenz (1979) vs. McHenry	112

LIST OF FIGURES

<u>Figure</u>		<u>Page</u>
3.1	Sample Section of an Input Height Grid, 500 mb, Dec. 1, 1962, 00Z	34
3.2	Critical Shear, Sample Output, 5/9/64 00Z	35
3.3	Sample Output $20^{\circ} \Delta T$, 5/9/64 00Z	36
3.4	Sample Output T_1^* , 5/9/64 00Z	37
3.5	Sample Output T_3^* , 5/9/64 00Z	38
3.6	Sample Output, V_1^* , 7/9/66 00Z	40
3.7	Sample Output, V_3^* , 7/9/66 00Z	41
3.8	Sample Output, $U_1 - U_3$, 7/9/66 00Z	42
3.9	Sample Output, $X \cdot (\Delta T)^2$, 4/1/63 00Z	45
3.10	Sample Output, Eddy Flux, 4/1/63 00Z	46
4.1	Components $((A_m, A_m) + (B_m, B_m))_k$ in Analysis of Variance of $X \cdot (\Delta T)^2$ for Latitude Band 1.	53
4.2	Continuation of 4.1	54
4.3	Continuation of 4.1	55
4.4	Components $((C_m, C_m) + (D_m, D_m))_k$ in Analysis of Variance of Eddy Flux for Latitude Band 1	56
4.5	Continuation of 4.4	57
4.6	Continuation of 4.4	58
4.7	Components $((A_m, C_m) + (B_m, D_m))_k$ in Analysis of Covariance of Eddy Flux with $X \cdot (\Delta T)^2$ for Latitude Band 1	59
4.8	Continuation of 4.7	60

List of Figures (continued)

<u>Figure</u>	<u>Page</u>
4.9	61
4.10	62
4.11	63
4.12	67
4.12.1	67
4.12.2	68
4.12.3	69
4.12.4	70
4.12.5	71
4.12.6	72
4.12.7	73
4.12.8	74
4.12.9	75
4.12.10	76
4.12.11	77
4.12.12	78
4.12.13	79
4.12.14	80
4.12.15	81
4.12.16	82
4.12.17	83
4.12.18	84
4.12.19	85
4.12.20	86
4.12.21	87
4.12.22	88
4.12.23	89
4.12.24	90
4.13	91
4.13.1	91
4.13.2	92
4.13.3	93
4.13.4	94
4.14	97
4.14.1	97
4.14.2	98
4.14.3	99
4.14.4	100

List of Figures (continued)

<u>Figure</u>		<u>Page</u>
4.15	Total Correlation Coefficient	102
5.1	Parametric Plot of Preferred Eddy Time Scale in Baroclinic Adjustment	110

CHAPTER ONE

INTRODUCTION

1.1 The Eddy Flux Parameterization Problem

In seeking a closed system of equations to describe climate, the equations of motion along with the thermodynamic equation must be solved in time averaged form. Often the climate is defined as a zonal mean process, and the equations may be spatially averaged as well. Each independent variable is usually thought of as the sum of average and eddy parts which are substituted into the equations, then the equations themselves are averaged. In the case of the mean Navier-Stokes equations, the average product of stochastic variables appears. These terms are known as Reynold's stresses, which describe the transport of turbulent momentum. Similar terms appear in the thermodynamic equation; these are known as eddy heat fluxes. In principle the eddy heat fluxes can be solved for from the original equations. It is, however, a difficult process because the non-linear terms in the momentum equations generate higher order deviations. To get around this closure problem, current research focuses on parameterization of the eddy heat flux in terms of the mean atmospheric structure. Usually the parameterizations include the mean meridional temperature gradient and other quantities derived from the

physical reasons for the existence of the eddies.

Climate models which include the total heat transport must contain parameterizations which accurately measure the contribution of the eddies to that total. Current parameterizations only roughly model the gross eddy transport. The key problem is thus finding improved parameterizations. In order to accomplish this, the physical behavior of the eddies in relation to their predictors must be examined.

Because the eddy behavior is a function of spatial and temporal scales, one parameterization may work well when the averaging time is long, say, several months, but wouldn't work at all for short time scales, say, less than a month. Furthermore, zonal averaging smooths out the contributions of eddies of smaller zonal scale which exist because of locally unstable baroclinic zones. Because differing regions of the earth exhibit differing climates, parameterizations without zonal dependence yield little information for specific geographic regions. Hence no parameterization can capture all of the physics of the growth and decay of eddies.

Solutions to the problem hinge on several approaches. First, what does theory (particularly baroclinic instability theory and scale analysis) suggest? Secondly, what does the data reveal? Finally, how well do particular theories describe the actual behavior of the eddies, and what can we learn about the eddies from them? Our study will focus on answers to this last question.

1.2 Forced Versus Free Eddy Behavior and Baroclinic Adjustment

Much is already known about the behavior of the eddies. Lorenz (1979) showed that for the zonally averaged case, modelling eddy transport as heat diffusion works well only for the meridional planetary scale when the time scale is inclusive of seasonal forcing. For shorter or longer time scales and smaller meridional scales, the variations in eddy flux were free--unrelated to external seasonal forcing--and thus unable to be accounted for by diffusive theory alone. When we speak of free variations, we will be talking about the short period (less than a month) variety.

Stone (1978) has termed the zonally averaged free eddy behavior "baroclinic adjustment." In this process, the eddies grow in response to baroclinic instabilities unrelated to the absolute local value of the temperature gradient--but ultimately affect it by efficiently transporting heat. In contrast for the seasonal case, changes in the sun's inclination force changes in the gradient which force the eddies--a diffusive type transport. Lorenz was the first to identify this difference between forced and free regimes.

Current theories of parameterization are derived for forced variations only and in general apply to the zonally averaged case. Hence, heat transported by eddies as a result of free variations is not well modelled. In most

instances the parameterization seeks to account for the gross effect of the transport due to free variations by defining an eddy diffusivity (in analogy to a thermal diffusivity) which weights the forcing by the gradient. The form of this coefficient may be simple or elaborate depending on which theory was used to derive it.

One by product of these theories, and baroclinic instability theory in general, is the prediction of the relevant zonal scales of the eddies. Held (1978a) suggests, for instance, that the zonal extent of an eddy may depend upon the vertical extent of its associated baroclinic wave. Another by-product is the well-known result that the β -effect serves to stabilize the growth of baroclinic waves. In the two-layer model (Phillips, 1954), β is important in determining the shear at which the model becomes baroclinically unstable. "Two-layer" eddies can grow and transport heat when the actual shear exceeds the critical shear. Both of these considerations have been taken into account in theories which adjust the form of the eddy diffusivity mentioned above.

1.3 Objectives of this Research

By using actual data to test a particular parameterization, much can be learned about (1) the parameterization itself, and (2) the behavior of the eddies in relation to its predictors.

By studying one particular parameterization we are limited in our ability to compare with other parameterizations. However, we can assess its ability to model the eddy flux in comparison to that for which it was designed. To determine how a particular parameterization functions is to determine the spatial and temporal scales over which actual data assess its validity. That is, for what space and time scales is the eddy flux well-positively correlated with its combination of predictors in the parameterization of question?

The eddy behavior in relation to its predictors can be understood, on the other hand, by examining the entire range of correlations through the various space and time scales available in the data base.

Previous studies have concentrated on zonally averaged data. Stone (1978) identified the negative correlations on short time scales between the eddy flux and meridional temperature gradients as baroclinic adjustment, but used only a small data base--three Januaries. Lorenz (1979), although making use of 10 years of twice daily data, again studied the zonally averaged case in looking at meridional scales.

Eddies adjust on short time scales (free variations) and are forced on long time scales. The zonal scale of an eddy can be significantly smaller (determined by the relevant radius of deformation) than the planetary. By studying the zonally-dependent space-time correlation spectrum be-

tween the eddy flux and its predictors, we should be able to observe adjustment on short time scales within several zonal wavenumbers in the form of significant negative correlations. Adjustment has never been observed on scales smaller than wavenumber 0. Also, we should be able to observe forced eddy behavior on seasonal time scales for at least wavenumber 0. No study has sought to tie together adjustment and flux-gradient forcing so succinctly. Furthermore, we can look at the correlation spectrum as a function of latitude and gain knowledge about the relationship between adjustment regimes, forced regimes and the scales of the eddies themselves.

The primary advantage of a spectral correlation test is that it will uncover which zonal spatial scales yield the most significant temporal correlations. Available to us are 10 years of twice daily geopotential height observations at 850 mb, 500 mb and 300 mb (see Section 3.1). By arranging the data in a two-layer format, modelling a parameterization based on the two-layer model and constructing its correlation spectrum as a function of latitude, the free-forced space-time behavior of the "two-layer" eddies should be adequately revealed.

CHAPTER TWO

MODELLING THE EDDY FLUX AND ITS PREDICTORS

2.1 Choice of Specific Parameterization for Study and Analysis Method

In choosing the particular parameterization for this study, we must select one that can be adapted to the two-layer model, since our data are available in that format. The parameter dependences should include meridional temperature gradient and an eddy diffusivity which accounts for the β -effect (because we are interested in latitudinal variations), and which takes into account the zonal scale of the free regime eddies. A priori, then, we choose a parameterization which is likely to reveal the free-forced regime eddy behavior as a function of zonal scale and latitude.

It is convenient to follow Held (1978b). We write the eddy heat flux as

$$\overline{v'\theta'} = -D \frac{\partial \bar{\theta}}{\partial y} \quad (2.1)$$

where D is the eddy diffusivity with units of velocity time length.

$$D = V \cdot L \quad (2.2)$$

Stone (1972) assumes the velocity scale is determined by the vertical shear times the scale height, $V = H \frac{\partial \bar{u}}{\partial z}$ and the length scale is approximated by $L = NH/f$. Here N is the

Brunt-Väisälä frequency, $N \propto \left(\frac{\partial \bar{\theta}}{\partial z} \right)^{1/2}$, and f is the Coriolis parameter. Stone's choice of length scale is the Rossby radius corresponding to the scale height. By the thermal wind relation, $\frac{\partial \bar{u}}{\partial z} \propto \frac{\partial \bar{\theta}}{\partial y}$ so that when D is substituted into (2.1),

$$\overline{v'\theta'} \propto \left(\frac{\partial \bar{\theta}}{\partial y} \right)^2 \left(\frac{\partial \bar{\theta}}{\partial z} \right)^{1/2} \quad (2.3)$$

Because $\beta = \frac{\partial f}{\partial y}$ affects the growth of baroclinic waves, one would expect it to affect the form of the diffusivity (2.2). Held (1978b) has argued using scale analysis that (2.3) should be modified such that

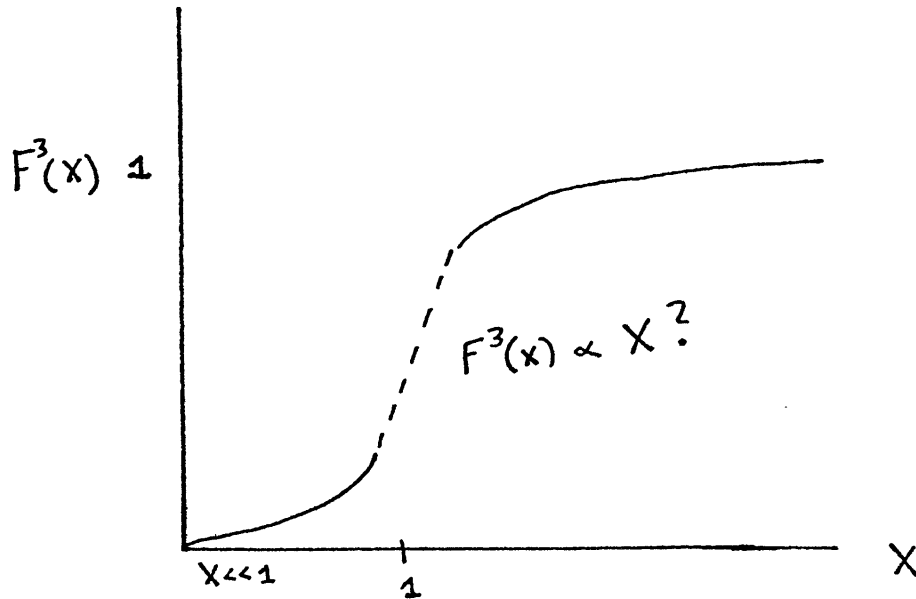
$$\overline{v'\theta'} \propto \left(\frac{\partial \bar{\theta}}{\partial y} \right)^2 \left(\frac{\partial \bar{\theta}}{\partial z} \right)^{1/2} F^3(x) \quad (2.4)$$

where $x = \frac{h}{H}$, H being the scale height, and h is the vertical scale of the most unstable baroclinic mode. This vertical scale is defined by $h = (f^2 \frac{\partial \bar{u}}{\partial z}) / \beta N^2$. When β is small $x \gg 1$; conversely $x \ll 1$ for large β . Held's arguments proceed to deduce the following form for $F^3(x)$ in the limits $\beta \rightarrow$ large and $\beta \rightarrow$ small:

$$F^3(x) = \begin{cases} 1 & \beta \text{ small} \\ x^3 & \beta \text{ large} \end{cases}$$

For small β (β decreases northward) (2.4) reduces to (2.3); for large β (2.4) is changed significantly. The problem

arises because scale analysis doesn't predict the form of $F^3(x)$ for realistic atmospheric values of β . In the real atmosphere, $h \approx H$ so that X is near 1. A plot of F^3 vs. X looks as follows:



Assume for the real atmosphere that $F^3(x) \propto X$. If this is the case, (2.4) becomes

$$\overline{v'\theta'} \propto \left(\frac{\partial \overline{\theta}}{\partial y}\right)^2 \left(\frac{\partial \overline{\theta}}{\partial z}\right)^{1/2} \left(\frac{\partial u}{\partial z}\right) \left(\frac{\partial \theta}{\partial z}\right)^{-1} \quad (2.5)$$

This is a complex parameterization to attempt to study with a large data set. If we ignore the contribution of the static stability to the $1/2$ power in (2.5), it both simplifies the form of the diffusivity and leads us to Saltzman's (1967) parameterization, which says

$$D \propto \left(\frac{\partial \overline{\theta}}{\partial y}\right) \cdot B \quad (2.6)$$

where B is a stability coefficient. In the two layer model, B is directly analogous to X. Thus we choose to test

$$\overline{v'\theta'} \propto \left(\frac{\partial \bar{\theta}}{\partial y}\right)^2 \left(\frac{\partial \bar{u}}{\partial z}\right) \left(\frac{\partial \theta}{\partial z}\right)^{-1} \quad (2.7)$$

both because it is simpler than (2.5) and representative of (2.6). In (2.7), the zonal scale is no longer explicitly NH/f . This is a concession, but we expect it to make little difference in our analysis.

Equation (2.7) is easily adapted to suit a two-layer model. Let subscripts 1 and 3 denote the upper and lower layers respectively. Then $X \propto \left(\frac{\partial \bar{u}}{\partial z}\right) \left(\frac{\partial \theta}{\partial z}\right)^{-1}$ is given by $\frac{U_1 - U_3}{U_c}$, where $U_c = \frac{\beta R(\theta_1 - \theta_3)}{f^2}$ is the critical shear. (See Stone, 1978.) When $(U_1 - U_3)/U_c > 1$ the model is baroclinically unstable and waves may grow. Hence X is just a Saltzman stability coefficient in the two-layer sense.

In order to test (2.7) spectrally, we must be able to compute the instantaneous values of each side as functions of λ, ϕ, t . For the left hand side, we want the mass weighted vertically integrated eddy flux of sensible heat--call it \hat{V}^*T^* . Here $V = [V] + V^*$, $T = T^* + [T]$ where $[()]$ indicates a zonal average. Thus $\hat{V}^*T^*(\lambda, \phi, t)$ is the instantaneous transport desired. Let ΔT be the mass weighted tropospheric temperature gradient. Then

$$\hat{V}^*T^*(\lambda, \phi, t) \propto (\Delta T)^2 \cdot \frac{U_1 - U_3}{U_c} (\lambda, \phi, t) \quad (2.8)$$

Equation (2.8) is appropriate for testing with our data set and accurately represents the physics in (2.7) provided the correlations are not performed point by point. To avoid this, the quantities in (2.8) will each be smoothed latitudinally over the width of 4 independent 10° wide latitude bands. The term $\hat{V^*T^*}$ will represent the average flux through the band. Similarly $(\Delta T)^2$ will be defined as 20° ΔT centered at the band center, and $(U_1 - U_3)/U_c$ will also be smoothed across the band width. The smoothing process, along with a 20° wide ΔT , is necessary because small scale gradients do not force eddy fluxes to any great degree. It also eliminates noise.

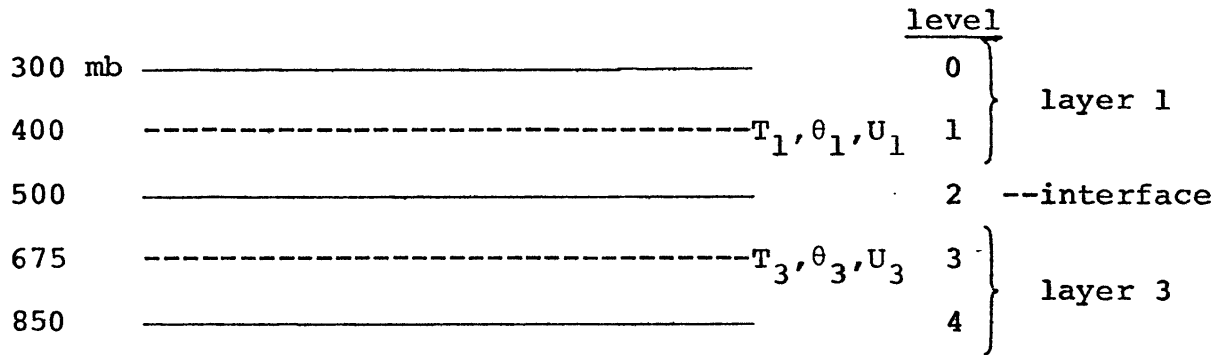
Spectral decomposition of (2.8) will thus take place in 4 latitude bands chosen to be centered at 35° , 45° , 55° , and 65° N. Fast Fourier analysis will be used to compute the zonal Fourier coefficients of each side of (2.8) as functions of time. Then, the poor man's time spectral analysis described by Lorenz (1979) will be used to construct the correlation spectrum of Fourier coefficients as functions of time. Thus, the spatial scales will be resolved as well--the zonally averaged case so often studied just falls out as the wavenumber 0 correlation spectrum. Identically calculated spectra are produced independently for the four latitude bands, allowing interpretation of results to span the midlatitudes. Sections 3.4.1 and 3.4.2 will discuss this analysis in detail.

A priori we can say something about what we expect to learn from studying (2.8). First of all, we would expect it to model forced variations for the zonally averaged case very well. We suspect that the X parameter by itself is not a very good eddy diffusivity, because diffusive assumptions like (2.6) are simpler than those derived from complex baroclinic theory. Because X is on average near 1 (the long-term mean shear approximates the long term critical shear), we can project that for seasonally forced variations our correlations will resemble these between the flux and gradient squared alone. We hope that they would be slightly better, but we have limited means with which to verify this.

We expect that (2.8) will reveal nicely baroclinic adjustment. Because X automatically includes β in its critical shear, we believe the negative correlations indicative of adjustment may be enhanced by the inclusion of X . We expect to be able to detect adjustment for a range of wavenumbers, but perhaps not as well as if the zonal scale were explicitly included as in (2.5). On this last point, however, we can only conjecture.

2.2 A Two-Layer Format for Processing Geopotential Height Data

We seek to compute all of the quantities in (8) using a two-layer model given height data at 300, 500 and 850 mb. We model the atmosphere as follows:



In some sense it is a crude model because there is some eddy transport above 300 mb. (particularly when the tropopause is higher than that) and below 850 mb. We are actually looking at a slice which includes about 80% of the mass of the troposphere

2.2.1 Critical Shear

To compute this we must compute the temperature hydrostatically:

$$T_1 = \left(\frac{g}{R} \right) \frac{\Delta_{0,2} z}{\ln \frac{5}{3}} \quad (2.9)$$

$$T_3 = \left(\frac{g}{R} \right) \frac{\Delta_{2,4} z}{\ln \left(\frac{8.5}{5} \right)} \quad (2.10)$$

where $\Delta_{i,j}$ stands for the height difference between the i, j layers. The potential temperatures θ_1 and θ_3 are just

$$\theta_1 = T_1 \left(\frac{p_s}{p_1} \right)^{R/C_p} \quad (2.11)$$

$$\theta_3 = T_3 \left(\frac{p_s}{p_3} \right)^{R/C_p} \quad (2.12)$$

where $p_1 = 400$ mb, $p_s = 1000$ mb, and $p_3 = 675$ mb. The critical shear, given by $U_c = \frac{\beta R}{f^2} (\theta_1 - \theta_3)$ is then determined as a function of latitude.

2.2.2 Mass Weighted Meridional Temperature Gradient

Let ΔT_i stand for the temperature difference at layer i along a 20° latitude stretch of a given longitude λ_0 . The mass weighted gradient is given by

$$\Delta T_m = \frac{2\Delta T_1 + 3.5 \Delta T_3}{5.5} \quad (2.13)$$

Eq. (2.13) is computed using (2.9) and (2.10).

2.2.3 Actual Shear

We want to compute the velocities U_1 and U_3 in the two layers from the geopotential height data. It is convenient to follow Lorenz (1979) in first computing a geostrophic streamfunction and then getting the velocity fields.

From the divergence equation,

$$\begin{aligned} \frac{\partial \delta}{\partial t} = & -\hat{k} \times \vec{u} \cdot \nabla(f+\zeta) - \omega \frac{\partial \delta}{\partial p} + (f+\zeta)\zeta - \nabla \omega \cdot \frac{\partial \vec{u}}{\partial p} \\ & - \nabla^2 [(gz) + \frac{1}{2} \vec{u} \cdot \vec{u}] + \nabla \cdot \vec{F} \end{aligned} \quad (2.14)$$

include only the terms

$$0 = -\hat{k} \times \vec{u} \cdot \nabla f + f\zeta - \nabla^2 gz \quad (2.15)$$

where $\zeta = \frac{\partial v}{\partial x} - \frac{\partial u}{\partial y} = \mathbf{k} \cdot (\nabla \times \vec{u})$. Assuming that we can represent the velocity by a stream function ψ such that $\vec{u} = \left(-\frac{\partial \psi}{\partial y}, \frac{\partial \psi}{\partial x} \right)$, we have $\nabla \cdot \vec{u} = \delta = 0$. Then $\zeta = \nabla^2 \psi$ by definition. Hence,

$$g\nabla^2 z = (-\hat{k} \times \vec{u}) \cdot \nabla f + f\nabla^2 \psi \quad (2.16)$$

Now $\beta = \frac{\partial f}{\partial y}$ and $\frac{\partial f}{\partial x} = 0$. Then

$$g\nabla^2 z = -u\beta + f\nabla^2 \psi \quad (2.17)$$

$$g\nabla^2 z = \frac{\partial \psi}{\partial y} \beta + f\nabla^2 \psi \quad (2.18)$$

or
$$g\nabla^2 z = \nabla \psi \cdot \nabla f + f\nabla \cdot \nabla \psi = \nabla \cdot (f\nabla \psi) \quad (2.19)$$

Finally,
$$g\nabla^2 z = 2\Omega \nabla \cdot (\sin \phi \nabla \psi) \quad (2.20)$$

A procedure for solving (2.20) for ψ when z is expressed in spherical harmonics is described in Lorenz (1978). Equation (2.20) is more complex than the simple geostrophic relationship $gz = f\psi$ because it includes β effects--this is exactly what we desire.

To get the stream function at levels 1 and 3 we compute

$$\psi_1 = \frac{\psi_0 + \psi_2}{2}, \quad U_1 = \frac{-\partial \psi_1}{\partial y} \quad (2.21)$$

$$\psi_3 = \frac{\psi_2 + \psi_4}{2}, \quad U_3 = \frac{-\partial \psi_3}{\partial y}$$

We can then use a centered finite difference scheme to get the velocities u_1 and u_3 from ψ_1 and ψ_3 . Hence, finally, $(u_1 - u_3)$ is the actual shear desired. Combining the results of (2.21) with the critical shear calculation yields $\frac{u_1 - u_3}{u_c}$, one part of the right hand side of (2.8).

2.2.4 Eddy Flux

We want to compute the total eddy flux representing the integrated value through the depth of the model:

$$\hat{v}^*T^* = \int_{850}^{300} \frac{c_p}{g} v^*T^* dp \quad (2.22)$$

As before $[()] = \frac{1}{2\pi} \int_0^{2\pi} () d\lambda$ so that

$$V^* = V - [V] \quad (2.23)$$

$$T^* = T - [T].$$

T^* is simply computed from (2.9) and (2.10). The choice of a stream function to represent the velocity presupposes a non-divergent field; hence there is no mean meridional signal resolved by this method. This is convenient again because we are only interested in the eddy part of the V field. Hence

$$V_1^* = \frac{\partial \psi_1}{\partial x} \quad (2.24)$$

$$V_3^* = \frac{\partial \psi_3}{\partial x}$$

hold for the eddy velocities at levels 1 and 3. Combining (2.23) and (2.24), we compute the two-layer finite sum representing (2.22):

$$\hat{v}^*T^* = \sum_{i=1}^3 \frac{c_p}{g} v_i^*T_i^*\Delta_i p, \quad \begin{aligned} \Delta_1 &= 200 \\ \Delta_3 &= 350 \end{aligned} \quad (2.25)$$

This completes all of the model equations needed to process the height data into the quantities found in (2.8). The next chapter will discuss data acquisition and handling, the programming of these equations, and the equations and programming of the statistical analysis by spectral decomposition.

CHAPTER THREE

DATA ACQUISITION, MODEL, AND STATISTICAL ANALYSIS

3.1 Data Sources and Description

All the data were derived from synoptic analyses of the 850, 500 and 300 mb geopotential height field made at the National Meteorological Center, although it originated in the different formshaving been stored on tapes at the NCAR computing facility. Initially available to us were previously analyzed height fields at 500, 850 mb in the form of triangularly truncated spherical harmonics (Leight, 1974). The series are defined by:

$$Z(\lambda, \phi, t) = \sum_{n=0}^L \sum_{m=0}^n \left[C_{mn}(t) \cos m\lambda + S_{mn}(t) \sin m\lambda \right] \times P_n^m(\sin \phi) \quad (3.1)$$

Lorenz (1978) documents the spherical harmonic data set at 500 mb completely, the 850 mb set is identical in structure. Here Z is the geopotential height, λ is longitude, ϕ latitude, t time, and P_n^m the associated Legendre function of degree n and order (or wavenumber) m . The series were truncated triangularly at $L = 18$. Maurice Blackmon provided NCAR tapes B6902 and B10618 containing the coefficients C_{mn} and S_{mn} , 100 cosines and 90 sines represent each field.

These two datasets spanned 10 years and 1 month beginning Dec 1, 1962.

In order to employ our model, data was acquired through the NCAR tape library for the 300 mb geopotential heights in 400 word packed binary. Tape C4650 was used; the dataset on this tape began before Dec 1, 1962 and extended through 12z Nov 21, 1971.

3.2 Initial Computational Work

The task of organizing the massive quantity of data (over 13 million data pieces) needed for this study was formidable. Over half the computing time was consumed by this stage of the project. In order to calculate, via the model, the quantities in (2.8) six tapes--3 of the heights themselves and 3 of their spherical harmonic representations--were needed.

The grid size was chosen to be $5^{\circ} \times 5.625^{\circ}$ (latitude x longitude) extending from 25°N to 75°N . This provided 11 latitudes and 64 longitudes. The longitudinal spacing was chosen because fast Fourier analysis is convenient for powers of 2, and in foresight of the upcoming longitudinal Fourier decomposition. The latitudinal range was chosen so that 20° wide ΔT 's were available for the four latitude bands, centered at 35° , 45° , 55° , 65° .

For convenience the length of the study was chosen to begin Dec 1, 1962 and end Nov 21, 1971 so that the datasets

were exactly compatible. This meant that observations were lopped off the beginning of tape C4650, and lopped off the end of the two spherical harmonics tapes.

A program was written to reconstruct the height grids ($5^{\circ} \times 5.625^{\circ}$) from their spherical harmonic coefficients. These grids then became inputs to the parts of the model which used direct heights for calculation. Thus, tapes of the 850 and 500 mb height grids and their spherical harmonic coefficients (4 tapes total) were acquired rather easily.

Producing the raw 300 mb data was much more tedious. Package routines at NCAR were used to unpack the binary data on tape C4650 and convert it to grids like those at the other two levels. It was then discovered that the 300 mb data contained 200 (out of 6556) missing observations. Programs were then written to hydrostatically interpolate the 300 mb heights for the scattered missing observations from the 850 and 500 mb grids, and then insert the interpolated data into their missing slots. Once this was accomplished, we had a complete tape of the 300 mb height grids spanning 6556 observations.

The reverse procedure then had to be undertaken to produce the spherical harmonic coefficients from the height grids at 300 mb. Maurice Blackman provided a program suited for our needs, and after adapting it to our data structure, it was used to accomplish our purpose.

The problems presented by massive quantities of data were significant. For example, the 300 mb spherical harmonics

had to be produced in 5 separate pieces because of the limitations on tape storage capacity. Program efficiency was a high priority because somewhat complex calculations were repeated thousands of times. Hence, small test data sets were constructed and used to test almost every program of significant length. Ensuring that each data set was identically formatted was a must, so that in merging the levels we could be certain that all 3 levels always contained observations made at the same date and hour.

3.3 Computation by the Two-Layer Model

Three programs, named CRTSHR, DAGRI3, and FINAL, were used to compute and store the quantities in (2.8). Table 3.1 describes the functions of the programs CRTSHR and DAGRI3.

Program CRTSHR produced the quantities from the input height grids as shown in Table 3.1. A sample section of an input height grid is shown in Fig 3.1. The programming algorithms used in CRTSHR are quite simple and available from the author.

Sample outputs of critical shear, $20^{\circ}\Delta T$, T_1^* and T_3^* are shown for 5/9/64 at 00Z in figures 3.2 - 3.5 respectively. One item to be noted is that the critical shear is a much stronger function of latitude, due to the β -effect, than longitude. Variations in U_c longitudinally are solely due to static stability differences. Sample outputs were thoroughly checked for consistencies with realistic meteorological

Table 3.1
Two-Layer Model Programming,
Programs CRTSHR, DAGRI3

<u>Quantity</u>	<u>Equation in Text</u>	<u>Input</u>	<u>Produced by Program</u>
Critical Shear	(2.11), (2.12)	Height Grids	CRTSHR
20° Temperate Gradients	(2.13)	Height Grids	CRTSHR
T* Level 1	(2.23), (2.9)	Height Grids	CRTSHR
T* Level 3	(2.23), (2.10)	Height Grids	CRTSHR
V* Level 1	(2.24)	Spherical Harmonics	DAGRI3
V* Level 3	(2.24)	Spherical Harmonics	DAGRI3
Actual Shear	(2.21)	Spherical Harmonics	DAGRI3

02	14	1	0	267414	0	58.0	70.0	70.0
0.0010	574.2	571.6	571.0	570.7	570.4	568.4	565.7	563.3
5.025	572.5	570.5	570.1	569.8	569.5	567.5	564.8	562.4
11.050	570.7	568.7	568.3	568.0	567.7	565.7	563.0	560.6
15.075	570.0	568.0	567.6	567.3	567.0	565.0	562.3	560.0
22.070	568.2	566.2	565.8	565.5	565.2	563.2	560.5	558.2
28.125	570.9	568.9	568.5	568.2	567.9	565.9	563.2	560.9
33.750	575.0	573.0	572.6	572.3	572.0	570.0	567.3	565.0
39.375	575.8	573.8	573.4	573.1	572.8	570.8	568.1	565.8
45.000	575.1	573.1	572.7	572.4	572.1	570.1	567.4	565.1
50.625	570.9	568.9	568.5	568.2	567.9	565.9	563.2	560.9
56.250	570.7	568.7	568.3	568.0	567.7	565.7	563.0	560.7
61.875	567.4	565.4	565.0	564.7	564.4	562.4	559.7	557.4
67.500	575.0	573.0	572.6	572.3	572.0	570.0	567.3	565.0
73.125	575.4	573.4	573.0	572.7	572.4	570.4	567.7	565.4
78.750	583.3	581.3	580.9	580.6	580.3	578.3	575.6	573.3
84.375	586.2	584.2	583.8	583.5	583.2	581.2	578.5	576.2
90.000	583.5	581.5	581.1	580.8	580.5	578.5	575.8	573.5
95.625	582.3	580.3	579.9	579.6	579.3	577.3	574.6	572.3
101.250	580.7	578.7	578.3	578.0	577.7	575.7	573.0	570.7
106.875	578.5	576.5	576.1	575.8	575.5	573.5	570.8	568.5
112.500	576.0	574.0	573.6	573.3	573.0	571.0	568.3	566.0
118.125	575.0	573.0	572.6	572.3	572.0	570.0	567.3	565.0
123.750	576.7	574.7	574.3	574.0	573.7	571.7	569.0	566.7
129.375	560.2	558.2	557.8	557.5	557.2	555.2	552.5	550.2
135.000	583.3	581.3	580.9	580.6	580.3	578.3	575.6	573.3
140.625	585.1	583.1	582.7	582.4	582.1	580.1	577.4	575.1
146.250	587.2	585.2	584.8	584.5	584.2	582.2	579.5	577.2
151.875	590.3	588.3	587.9	587.6	587.3	585.3	582.6	580.3
157.500	585.4	583.4	583.0	582.7	582.4	580.4	577.7	575.4

Fig. 3.1 Sample Section of an Input Height Grid
Dec. 1, 1962, 00Z

CRITICAL SHEAR IN NEELAS FOR SAMPLE 002

0	10	20	30	40	50	60	70	80	90	100
0.030	1.625	1.597	1.554	1.507	1.456	1.402	1.346	1.288	1.229	1.169
0.035	1.630	1.602	1.559	1.512	1.461	1.407	1.351	1.294	1.236	1.177
0.040	1.635	1.607	1.564	1.517	1.466	1.412	1.356	1.299	1.241	1.182
0.045	1.640	1.612	1.569	1.522	1.471	1.417	1.361	1.304	1.246	1.187
0.050	1.645	1.617	1.574	1.527	1.476	1.422	1.366	1.309	1.251	1.192
0.055	1.650	1.622	1.579	1.532	1.481	1.427	1.371	1.314	1.256	1.197
0.060	1.655	1.627	1.584	1.537	1.486	1.432	1.376	1.319	1.261	1.202
0.065	1.660	1.632	1.589	1.542	1.491	1.437	1.381	1.324	1.266	1.207
0.070	1.665	1.637	1.594	1.547	1.496	1.442	1.386	1.329	1.271	1.212
0.075	1.670	1.642	1.599	1.552	1.501	1.447	1.391	1.334	1.276	1.217
0.080	1.675	1.647	1.604	1.557	1.506	1.452	1.396	1.339	1.281	1.222
0.085	1.680	1.652	1.609	1.562	1.511	1.457	1.401	1.344	1.286	1.227
0.090	1.685	1.657	1.614	1.567	1.516	1.462	1.406	1.349	1.291	1.232
0.095	1.690	1.662	1.619	1.572	1.521	1.467	1.411	1.354	1.296	1.237
0.100	1.695	1.667	1.624	1.577	1.526	1.472	1.416	1.359	1.301	1.242
0.105	1.700	1.672	1.629	1.582	1.531	1.477	1.421	1.364	1.306	1.247
0.110	1.705	1.677	1.634	1.587	1.536	1.482	1.426	1.369	1.311	1.252
0.115	1.710	1.682	1.639	1.592	1.541	1.487	1.431	1.374	1.316	1.257
0.120	1.715	1.687	1.644	1.597	1.546	1.492	1.436	1.379	1.321	1.262
0.125	1.720	1.692	1.649	1.602	1.551	1.497	1.441	1.384	1.326	1.267
0.130	1.725	1.697	1.654	1.607	1.556	1.502	1.446	1.389	1.331	1.272
0.135	1.730	1.702	1.659	1.612	1.561	1.507	1.451	1.394	1.336	1.277
0.140	1.735	1.707	1.664	1.617	1.566	1.512	1.456	1.399	1.341	1.282
0.145	1.740	1.712	1.669	1.622	1.571	1.517	1.461	1.404	1.346	1.287
0.150	1.745	1.717	1.674	1.627	1.576	1.522	1.466	1.409	1.351	1.292
0.155	1.750	1.722	1.679	1.632	1.581	1.527	1.471	1.414	1.356	1.297
0.160	1.755	1.727	1.684	1.637	1.586	1.532	1.476	1.419	1.361	1.302
0.165	1.760	1.732	1.689	1.642	1.591	1.537	1.481	1.424	1.366	1.307
0.170	1.765	1.737	1.694	1.647	1.596	1.542	1.486	1.429	1.371	1.312
0.175	1.770	1.742	1.699	1.652	1.601	1.547	1.491	1.434	1.376	1.317
0.180	1.775	1.747	1.704	1.657	1.606	1.552	1.496	1.439	1.381	1.322
0.185	1.780	1.752	1.709	1.662	1.611	1.557	1.501	1.444	1.386	1.327
0.190	1.785	1.757	1.714	1.667	1.616	1.562	1.506	1.449	1.391	1.332
0.195	1.790	1.762	1.719	1.672	1.621	1.567	1.511	1.454	1.396	1.337
0.200	1.795	1.767	1.724	1.677	1.626	1.572	1.516	1.459	1.401	1.342
0.205	1.800	1.772	1.729	1.682	1.631	1.577	1.521	1.464	1.406	1.347
0.210	1.805	1.777	1.734	1.687	1.636	1.582	1.526	1.469	1.411	1.352
0.215	1.810	1.782	1.739	1.692	1.641	1.587	1.531	1.474	1.416	1.357
0.220	1.815	1.787	1.744	1.697	1.646	1.592	1.536	1.479	1.421	1.362
0.225	1.820	1.792	1.749	1.702	1.651	1.597	1.541	1.484	1.426	1.367
0.230	1.825	1.797	1.754	1.707	1.656	1.602	1.546	1.489	1.431	1.372
0.235	1.830	1.802	1.759	1.712	1.661	1.607	1.551	1.494	1.436	1.377
0.240	1.835	1.807	1.764	1.717	1.666	1.612	1.556	1.499	1.441	1.382
0.245	1.840	1.812	1.769	1.722	1.671	1.617	1.561	1.504	1.446	1.387
0.250	1.845	1.817	1.774	1.727	1.676	1.622	1.566	1.509	1.451	1.392
0.255	1.850	1.822	1.779	1.732	1.681	1.627	1.571	1.514	1.456	1.397
0.260	1.855	1.827	1.784	1.737	1.686	1.632	1.576	1.519	1.461	1.402
0.265	1.860	1.832	1.789	1.742	1.691	1.637	1.581	1.524	1.466	1.407
0.270	1.865	1.837	1.794	1.747	1.696	1.642	1.586	1.529	1.471	1.412
0.275	1.870	1.842	1.799	1.752	1.701	1.647	1.591	1.534	1.476	1.417
0.280	1.875	1.847	1.804	1.757	1.706	1.652	1.596	1.539	1.481	1.422
0.285	1.880	1.852	1.809	1.762	1.711	1.657	1.601	1.544	1.486	1.427
0.290	1.885	1.857	1.814	1.767	1.716	1.662	1.606	1.549	1.491	1.432
0.295	1.890	1.862	1.819	1.772	1.721	1.667	1.611	1.554	1.496	1.437
0.300	1.895	1.867	1.824	1.777	1.726	1.672	1.616	1.559	1.501	1.442
0.305	1.900	1.872	1.829	1.782	1.731	1.677	1.621	1.564	1.506	1.447
0.310	1.905	1.877	1.834	1.787	1.736	1.682	1.626	1.569	1.511	1.452
0.315	1.910	1.882	1.839	1.792	1.741	1.687	1.631	1.574	1.516	1.457
0.320	1.915	1.887	1.844	1.797	1.746	1.692	1.636	1.579	1.521	1.462
0.325	1.920	1.892	1.849	1.802	1.751	1.697	1.641	1.584	1.526	1.467
0.330	1.925	1.897	1.854	1.807	1.756	1.702	1.646	1.589	1.531	1.472
0.335	1.930	1.902	1.859	1.812	1.761	1.707	1.651	1.594	1.536	1.477
0.340	1.935	1.907	1.864	1.817	1.766	1.712	1.656	1.599	1.541	1.482
0.345	1.940	1.912	1.869	1.822	1.771	1.717	1.661	1.604	1.546	1.487
0.350	1.945	1.917	1.874	1.827	1.776	1.722	1.666	1.609	1.551	1.492
0.355	1.950	1.922	1.879	1.832	1.781	1.727	1.671	1.614	1.556	1.497
0.360	1.955	1.927	1.884	1.837	1.786	1.732	1.676	1.619	1.561	1.502
0.365	1.960	1.932	1.889	1.842	1.791	1.737	1.681	1.624	1.566	1.507
0.370	1.965	1.937	1.894	1.847	1.796	1.742	1.686	1.629	1.571	1.512
0.375	1.970	1.942	1.899	1.852	1.801	1.747	1.691	1.634	1.576	1.517
0.380	1.975	1.947	1.904	1.857	1.806	1.752	1.696	1.639	1.581	1.522
0.385	1.980	1.952	1.909	1.862	1.811	1.757	1.701	1.644	1.586	1.527
0.390	1.985	1.957	1.914	1.867	1.816	1.762	1.706	1.649	1.591	1.532
0.395	1.990	1.962	1.919	1.872	1.821	1.767	1.711	1.654	1.596	1.537
0.400	1.995	1.967	1.924	1.877	1.826	1.772	1.716	1.659	1.601	1.542
0.405	2.000	1.972	1.929	1.882	1.831	1.777	1.721	1.664	1.606	1.547
0.410	2.005	1.977	1.934	1.887	1.836	1.782	1.726	1.669	1.611	1.552
0.415	2.010	1.982	1.939	1.892	1.841	1.787	1.731	1.674	1.616	1.557
0.420	2.015	1.987	1.944	1.897	1.846	1.792	1.736	1.679	1.621	1.562
0.425	2.020	1.992	1.949	1.902	1.851	1.797	1.741	1.684	1.626	1.567
0.430	2.025	1.997	1.954	1.907	1.856	1.802	1.746	1.689	1.631	1.572
0.435	2.030	2.002	1.959	1.912	1.861	1.807	1.751	1.694	1.636	1.577
0.440	2.035	2.007	1.964	1.917	1.866	1.812	1.756	1.699	1.641	1.582
0.445	2.040	2.012	1.969	1.922	1.871	1.817	1.761	1.704	1.646	1.587
0.450	2.045	2.017	1.974	1.927	1.876	1.822	1.766	1.709	1.651	1.592
0.455	2.050	2.022	1.979	1.932	1.881	1.827	1.771	1.714	1.656	1.597
0.460	2.055	2.027	1.984	1.937	1.886	1.832	1.776	1.719	1.661	1.602
0.465	2.060	2.032	1.989	1.942	1.891	1.837	1.781	1.724	1.666	1.607
0.470	2.065	2.037	1.994	1.947	1.896	1.842	1.786	1.729	1.671	1.612
0.475	2.070	2.042	1.999	1.952	1.901	1.847	1.791	1.734	1.676	1.617
0.480	2.075	2.047	2.004	1.957	1.906	1.852	1.796	1.739	1.681	1.622
0.485	2.080	2.052	2.009	1.962	1.911	1.857	1.801	1.744	1.686	1.627
0.490	2.085	2.057	2.014	1.967	1.916	1.862	1.806	1.749	1.691	1.632
0.495	2.090	2.062	2.019	1.972	1.921	1.867	1.811	1.754	1.696	1.637
0.500	2.095	2.067	2.024	1.977	1.926	1.872	1.816	1.759	1.701	1.642
0.505	2.100	2.072	2.029	1.982	1.931	1.877	1.821	1.764	1.706	1.647
0.510	2.105	2.077	2.034	1.987	1.936	1.882	1.826	1.769	1.711	1.652
0.515	2.110	2.082	2.039	1.992	1.941	1.887	1.831	1.774	1.716	1.657
0.520	2.115	2.087	2.044	1.997	1.946	1.892	1.836	1.779	1.721	1.662
0.525	2.120	2.092	2.049	2.002	1.951	1.897	1.841	1.784	1.726	1.667
0.530	2.125	2.097	2.054	2.007	1.956	1.902	1.846	1.789	1.731	1.672
0.535	2.130	2.102	2.059	2.012	1.961	1.907	1.851	1.794	1.736	1.677
0.540	2.135	2.107	2.064	2.017	1.966	1.912	1.856	1.799	1.741	1.682
0.545	2.140	2.112	2.069	2.022	1.971	1.917	1.861	1.804	1.746	1.687
0.550	2.145	2.117	2.074	2.027	1.976	1.922	1.866	1.809	1.751	1.692
0.555	2.150	2.122	2.079	2.032	1.981	1.927	1.871	1.814	1.756	1

TEMPERATURES FROM SAMPLES COLLECTED AT 0

	45.0	50.0	55.0	60.0	65.0	70.0	75.0
0.000	2.000	2.000	2.000	2.000	2.000	2.000	2.000
5.000	3.000	3.000	3.000	3.000	3.000	3.000	3.000
10.000	4.000	4.000	4.000	4.000	4.000	4.000	4.000
15.000	5.000	5.000	5.000	5.000	5.000	5.000	5.000
20.000	6.000	6.000	6.000	6.000	6.000	6.000	6.000
25.000	7.000	7.000	7.000	7.000	7.000	7.000	7.000
30.000	8.000	8.000	8.000	8.000	8.000	8.000	8.000
35.000	9.000	9.000	9.000	9.000	9.000	9.000	9.000
40.000	10.000	10.000	10.000	10.000	10.000	10.000	10.000
45.000	11.000	11.000	11.000	11.000	11.000	11.000	11.000
50.000	12.000	12.000	12.000	12.000	12.000	12.000	12.000
55.000	13.000	13.000	13.000	13.000	13.000	13.000	13.000
60.000	14.000	14.000	14.000	14.000	14.000	14.000	14.000
65.000	15.000	15.000	15.000	15.000	15.000	15.000	15.000
70.000	16.000	16.000	16.000	16.000	16.000	16.000	16.000
75.000	17.000	17.000	17.000	17.000	17.000	17.000	17.000
80.000	18.000	18.000	18.000	18.000	18.000	18.000	18.000
85.000	19.000	19.000	19.000	19.000	19.000	19.000	19.000
90.000	20.000	20.000	20.000	20.000	20.000	20.000	20.000
95.000	21.000	21.000	21.000	21.000	21.000	21.000	21.000
100.000	22.000	22.000	22.000	22.000	22.000	22.000	22.000
105.000	23.000	23.000	23.000	23.000	23.000	23.000	23.000
110.000	24.000	24.000	24.000	24.000	24.000	24.000	24.000
115.000	25.000	25.000	25.000	25.000	25.000	25.000	25.000
120.000	26.000	26.000	26.000	26.000	26.000	26.000	26.000
125.000	27.000	27.000	27.000	27.000	27.000	27.000	27.000
130.000	28.000	28.000	28.000	28.000	28.000	28.000	28.000
135.000	29.000	29.000	29.000	29.000	29.000	29.000	29.000
140.000	30.000	30.000	30.000	30.000	30.000	30.000	30.000
145.000	31.000	31.000	31.000	31.000	31.000	31.000	31.000
150.000	32.000	32.000	32.000	32.000	32.000	32.000	32.000
155.000	33.000	33.000	33.000	33.000	33.000	33.000	33.000
160.000	34.000	34.000	34.000	34.000	34.000	34.000	34.000
165.000	35.000	35.000	35.000	35.000	35.000	35.000	35.000
170.000	36.000	36.000	36.000	36.000	36.000	36.000	36.000
175.000	37.000	37.000	37.000	37.000	37.000	37.000	37.000
180.000	38.000	38.000	38.000	38.000	38.000	38.000	38.000
185.000	39.000	39.000	39.000	39.000	39.000	39.000	39.000
190.000	40.000	40.000	40.000	40.000	40.000	40.000	40.000
195.000	41.000	41.000	41.000	41.000	41.000	41.000	41.000
200.000	42.000	42.000	42.000	42.000	42.000	42.000	42.000

Fig. 3.5 Sample Output T₃*, 5/9/64 00Z

values. The program accurately produced temperature departures such that $[T^*] = 0$.

The logic involved in program DAGRI3 was quite a bit more complex than CRTSHR. DAGRI3 handled all of the spherical harmonic inputs. Programming for the solution of (2.20) followed the algorithm for its solution described in Lorenz (1978). Once the stream functions were produced, DAGRI3 used a centered-finite difference scheme to produce zonal velocities and the meridional velocity departures. Figures 3.6 - 3.8 show sample outputs for V_1^* , V_3^* and the actual shear between the layers, $U_1 - U_3$, for July 9, 1966 at 00Z.

A good check on the accuracy of the algorithm for solving (2.20) is the sum of V_1^* or V_3^* around a latitude circle, because $\left[\frac{\partial \psi}{\partial x} \right] = 0$. In all cases checked, that sum was zero or within .1 or .2 meters/second of zero.

Program FINAL merged the outputs of CRTSHR and DAGRI3 into the quantities of eq. (2.8), those outputs having been stored separately on the NCAR computing facility mass store device (TMS-4). Table 3.2 shows how this was accomplished. The X parameter, hereafter referred to as X, defined by
$$X = \frac{U_1 - U_3}{U_c}$$
 for the two layer model, was calculated after the shear and critical shears were smoothed latitudinally. Once this was done, the $20^\circ \Delta T$ was squared and multiplied by X to produce the right hand side of (2.8) for each of the four latitude bands. Statistics were kept on U_c because numerous small U_c 's would have abnormally dominated the

MERIDIONAL VELOCITIES FROM PULSAR SAMPLE TABLE 1

	0	1	2	3	4	5	6	7	8	9
0.000	45.0	45.0	45.0	45.0	45.0	45.0	45.0	45.0	45.0	45.0
5.000	45.0	45.0	45.0	45.0	45.0	45.0	45.0	45.0	45.0	45.0
10.000	45.0	45.0	45.0	45.0	45.0	45.0	45.0	45.0	45.0	45.0
15.000	45.0	45.0	45.0	45.0	45.0	45.0	45.0	45.0	45.0	45.0
20.000	45.0	45.0	45.0	45.0	45.0	45.0	45.0	45.0	45.0	45.0
25.000	45.0	45.0	45.0	45.0	45.0	45.0	45.0	45.0	45.0	45.0
30.000	45.0	45.0	45.0	45.0	45.0	45.0	45.0	45.0	45.0	45.0
35.000	45.0	45.0	45.0	45.0	45.0	45.0	45.0	45.0	45.0	45.0
40.000	45.0	45.0	45.0	45.0	45.0	45.0	45.0	45.0	45.0	45.0
45.000	45.0	45.0	45.0	45.0	45.0	45.0	45.0	45.0	45.0	45.0
50.000	45.0	45.0	45.0	45.0	45.0	45.0	45.0	45.0	45.0	45.0
55.000	45.0	45.0	45.0	45.0	45.0	45.0	45.0	45.0	45.0	45.0
60.000	45.0	45.0	45.0	45.0	45.0	45.0	45.0	45.0	45.0	45.0
65.000	45.0	45.0	45.0	45.0	45.0	45.0	45.0	45.0	45.0	45.0
70.000	45.0	45.0	45.0	45.0	45.0	45.0	45.0	45.0	45.0	45.0
75.000	45.0	45.0	45.0	45.0	45.0	45.0	45.0	45.0	45.0	45.0
80.000	45.0	45.0	45.0	45.0	45.0	45.0	45.0	45.0	45.0	45.0
85.000	45.0	45.0	45.0	45.0	45.0	45.0	45.0	45.0	45.0	45.0
90.000	45.0	45.0	45.0	45.0	45.0	45.0	45.0	45.0	45.0	45.0
95.000	45.0	45.0	45.0	45.0	45.0	45.0	45.0	45.0	45.0	45.0
100.000	45.0	45.0	45.0	45.0	45.0	45.0	45.0	45.0	45.0	45.0
105.000	45.0	45.0	45.0	45.0	45.0	45.0	45.0	45.0	45.0	45.0
110.000	45.0	45.0	45.0	45.0	45.0	45.0	45.0	45.0	45.0	45.0
115.000	45.0	45.0	45.0	45.0	45.0	45.0	45.0	45.0	45.0	45.0
120.000	45.0	45.0	45.0	45.0	45.0	45.0	45.0	45.0	45.0	45.0
125.000	45.0	45.0	45.0	45.0	45.0	45.0	45.0	45.0	45.0	45.0
130.000	45.0	45.0	45.0	45.0	45.0	45.0	45.0	45.0	45.0	45.0
135.000	45.0	45.0	45.0	45.0	45.0	45.0	45.0	45.0	45.0	45.0
140.000	45.0	45.0	45.0	45.0	45.0	45.0	45.0	45.0	45.0	45.0
145.000	45.0	45.0	45.0	45.0	45.0	45.0	45.0	45.0	45.0	45.0
150.000	45.0	45.0	45.0	45.0	45.0	45.0	45.0	45.0	45.0	45.0
155.000	45.0	45.0	45.0	45.0	45.0	45.0	45.0	45.0	45.0	45.0
160.000	45.0	45.0	45.0	45.0	45.0	45.0	45.0	45.0	45.0	45.0
165.000	45.0	45.0	45.0	45.0	45.0	45.0	45.0	45.0	45.0	45.0
170.000	45.0	45.0	45.0	45.0	45.0	45.0	45.0	45.0	45.0	45.0
175.000	45.0	45.0	45.0	45.0	45.0	45.0	45.0	45.0	45.0	45.0
180.000	45.0	45.0	45.0	45.0	45.0	45.0	45.0	45.0	45.0	45.0
185.000	45.0	45.0	45.0	45.0	45.0	45.0	45.0	45.0	45.0	45.0
190.000	45.0	45.0	45.0	45.0	45.0	45.0	45.0	45.0	45.0	45.0
195.000	45.0	45.0	45.0	45.0	45.0	45.0	45.0	45.0	45.0	45.0
200.000	45.0	45.0	45.0	45.0	45.0	45.0	45.0	45.0	45.0	45.0

Fig. 3.6 Sample Output V_1^* , 7/9/66 00Z

Table 3.2

Two-Layer Model Programming, Program FINAL

<u>Quantity Produced</u>	<u>Equation in Text</u>	<u>Inputs</u>
Eddy Flux	(2.25)	$V_1^*, V_3^*, T_1^*, T_3^*$
X Parameter Times Temperature Gradient Squared	(2.8)	$20^\circ\Delta T, U_1 - U_3, U_C$

Fourier spectrum to be produced. It was found that only .0015% of the smoothed U_c 's were less than .1 in absolute value. (A small percentage were negative.)

FINAL calculated the eddy flux from (2.25) for each grid point, then did the 10° smoothing for each latitude band. In each case, the smoothing was performed by averaging the three values at, and 5° either side of, the latitude at the center of the band.

Figures 3.9 and 3.10 display sample output from FINAL, eddy flux in joules/m/sec and X times $(\Delta T)^2$ in $^{\circ}K^2$, for April 1, 1963 at 00Z.

3.4 Spectral Decomposition and Analysis of Variance

Program SPECTRA was written to produce the variance, covariance, and correlation coefficient spectra for eq. (2.8). Two major algorithms are found within. SPECTRA first produces the zonal Fourier representations of the left and right hand sides of (2.8). Then, using the coefficients as inputs, it produces the space-time spectra desired by making use of Lorenz' (1979) poor man's spectral analysis of variance. In order to make use of the poor man's analysis technique, the time series were required to be in powers of two. Following Lorenz, we truncated the output data of the program FINAL for input into the program SPECTRA. Each year thus became 256 days in length (Dec 1 - Aug 13, except in leap years),

X TIMES TEMP GRADIENT SQUARED (S.E. MEASURED) OVER	WIDTH OF LATITUDE BAND
0.000	55.0
5.625	56.0
11.250	57.0
16.875	58.0
22.500	59.0
28.125	60.0
33.750	61.0
39.375	62.0
45.000	63.0
50.625	64.0
56.250	65.0
61.875	66.0
67.500	67.0
73.125	68.0
78.750	69.0
84.375	70.0
90.000	71.0
95.625	72.0
101.250	73.0
106.875	74.0
112.500	75.0
118.125	76.0
123.750	77.0
129.375	78.0
135.000	79.0
140.625	80.0
146.250	81.0
151.875	82.0
157.500	83.0

Fig. 3.0 Sample Output, X times Temp. Gradient Squared, 4/1/63 00Z

and we made use of the first four and last four years only, discarding Dec 1, 1966 - Aug 13, 1967. More discussion about this point follows below.

3.4.1 Fourier Analysis in Latitude Bands

The left and right hand sides of (2.8) were analyzed into zonal Fourier series as follows, where m = zonal wave-number, λ = longitude, ϕ = latitude, t = time.

$$X \cdot (\Delta T)^2 (\lambda, \phi, t) = A_0(\phi, t) + \sum_{m=1}^N (A_m(\phi, t) \cos m\lambda + B_m(\phi, t) \sin m\lambda) \quad (3.2)$$

$$\text{Eddy Flux } (\lambda, \phi, t) = C_0(\phi, t) + \sum_{m=1}^N (C_m(\phi, t) \cos m\lambda + D_m(\phi, t) \sin m\lambda) \quad (3.3)$$

Figures 3.9 and 3.10 show the exact input structure of the data in (3.2) and (3.3), which is also just the output of program FINAL. Fast Fourier analysis yields the Fourier transforms for 32 wavenumbers (1/2 the number of input points) from which the coefficients can be directly calculated. For each observation and latitude band, 32 sine coefficients and 32 cosine coefficients are produced. The A_0 and C_0 terms are the zonally averaged cases, the sine coefficients being zero for $m = 0$ and $m = 32$. Hence, (3.2) and (3.3) produce time series of Fourier coefficients for introduction into

the temporal analysis scheme.

3.4.2 Poor Man's Time Spectral Analysis

Lorenz (1979) describes this nifty analysis of variance which is performed separately for each spatial wavenumber and latitude band. The reader should refer to his paper for more complete details; we shall just summarize it here.

Assume that the data to be processed consists of a 2^K successive values, and we wish to find the covariance spectrum of the scalar variables X and Y. We define

$$[X, Y]_k = J^{-1} \sum_{j=0}^{J-1} \left[\ell^{-1} \sum_{L=0}^{\ell-1} X_{(\ell j+i)} \right] \left[\ell^{-1} \sum_{L=0}^{\ell-1} Y_{(\ell j+i)} \right], \quad (3.4)$$

where $k = 0, \dots, K$; $L = 2^k$; and the data are subscripted beginning at 0 running through $L - 1$. We note that $\ell = 2^k$ and $J = L/\ell$. Then

$$(X, Y)_k = [X, Y]_k - [X, Y]_{k+1} \quad (3.5)$$

by definition, for $k < K$. Observing that $[X, Y]_0$ is the mean product of X and Y, while $[X, Y]_K$ is the product of the means, we find the covariance as a sum:

$$\sum_{k=0}^{K-1} (X, Y)_k = [X, Y]_0 - [X, Y]_K. \quad (3.6)$$

when $Y = X$, we calculate the variance spectrum. Our observations are twice daily so that $(X, Y)_k$ is the covariance of 2^{k-1} day averages within 2^k day periods, $k=0, \dots, K-1$. The

analysis scans the spectrum with overlapping filters whose corresponding periods center about 1 day, 2 days, etc. up to 1024 days for our data set. The components $(X,Y)_8$, $(X,Y)_7$ down to $(X,Y)_0$ select contributions to the covariance within years, higher order components average between years. In this way the seasonal cycle (forced eddy behavior) is pronounced, and there is no interruption in the spectrum as there would be in a conventional time series analysis. It is for this reason the data was organized into 2^8 day (2^9 observations) blocks stacked year to year. The seasonal cycle is thus represented as the contrast between winter (Dec 1 - April 7) and summer (April 8 - Aug 13). Shorter period cycles are represented as contrasts between, for example, the first and last halves of summer and winter, etc. Longer period cycles-- 2^9 , 2^{10} and 2^{11} days--are contrasts between years.

For our case, the X's are the $A_m(\phi,t)$ and $B_m(\phi,t)$, and the Y's are the $C_m(\phi,t)$ and $D_m(\phi,t)$. The components of variance of the eddy flux can thus be written as $((C_m, C_m) + (D_m, D_m))_k$, in analogy with (3.6). (This is not the eddy flux energy spectrum.) The components of variance of $X \cdot (\Delta T)^2$ are $((A_m, A_m) + (B_m, B_m))_k$, and the components of the covariance are just $((A_m, C_m) + (B_m, D_m))_k$. Finally, the relevant correlation coefficient is given by

$$r_{mk} = \left(\frac{(A_m, C_m) + (B_m, D_m)}{\sqrt{((A_m, A_m) + (B_m, B_m)) \cdot ((C_m, C_m) + (D_m, D_m))}} \right)_k \quad (3.7)$$

It should be understood that no statistics are produced across scale: only coefficients with the same zonal wavenumber are correlated. Thus, in producing analyses of variance in time for each zonal scale, the spatial scales are resolved as well.

We can, however, produce correlation coefficients representing the sum over all zonal wavenumbers for a given time scale, or, the sum over all k for a given m . We can also produce a total correlation coefficient by computing the total variances and covariances, which are their respective sums over all space and time scales analyzed. These sum and total statistics will be discussed in the next chapter.

Lorenz (1979) describes the algorithm by which the analysis is programmed. SPECTRA follows his logic by introducing the proper Fourier coefficients as they are produced directly into the analysis of variance. Once the dataset is read, the entire analysis is complete. This eliminates the need to store the coefficients before processing by the analysis of variance. Appendix A provides a FORTRAN IV listing of the code.

CHAPTER FOUR
DESCRIPTION OF CORRELATION SPECTRA

In this and the next chapter we will describe and discuss the results of our study. This chapter will be devoted to determination of the degrees of freedom in the various space and time scales in the problem, a description of the raw output of the program SPECTRA, and an organized graphical presentation of the correlation spectra themselves. Chapter Five will discuss the results and conclusions to be drawn from the output and graphical analyses.

4.1 Determination of Degrees of Freedom and Description of Spectral Tables

In order to have some measure of the statistical significance of the correlation spectra, it is necessary to analyze the number of degrees of freedom involved in calculating the coefficients. The most simple approach is to assume statistical independence in the observations. Recalling that for our case the observations are time series of Fourier coefficients, we see that to accurately measure the interdependence of successive observations is difficult. Meteorological data sets are known to exhibit autocorrelation in time because, for instance, today's 500 mb map is not independent of yesterday's. In our case, however, except for the smallest time scales ($k = 0, 1, 2$ where the period = 2^k), we can

assume independence, because processes whose characteristic scales are about 4 days or greater are essentially independent. With thousands of observations at short time scales in our data set, an adjustment in degrees of freedom via calculation of an autocorrelation function would increase the 95% and 99% confidence values only a small amount. Hence we choose to assume statistical independence and use caution in making our conclusions.

The analysis ((3.4), (3.5) and (3.6)) computes the contribution of the covariance of pairs of data to the total covariance. Each pair has one degree of freedom for zonal wavenumber $m = 0$ or $m = 32$, and 2 degrees of freedom for $0 < m < 32$. This is because only cosine coefficients contribute when $m = 0$ or 32 , but both sine and cosine coefficients contribute (independently) to the covariance when $0 < m < 32$. Hence, for $k = 0$, there are 2048 pairs of observations, and when $m = 0$ or 32 there are 2048 degrees of freedom. When, for $k = 0$, $0 < m < 32$, we have 4096 degrees of freedom.

Figures 4.1 - 4.11 display the spectral tables output by the program SPECTRA for latitude band 1 ($\phi = 35^\circ$). Selected tables for latitude bands 2, 3, and 4 ($\phi = 45^\circ$, 55° and 65° , respectively) may be found in Appendix B. The first nine tables consist of the analyses of variance and covariance, and the last two of the correlation spectrum. In each case wavenumber m proceeds down the left-hand column, time period k proceeds across the top. In the analyses of variance

	10	11	12	TOTAL
28	1.4486255557E+02	1.4486255557E+02	1.4486255557E+02	1.4486255557E+02
29	1.4486255557E+02	1.4486255557E+02	1.4486255557E+02	1.4486255557E+02
30	1.4486255557E+02	1.4486255557E+02	1.4486255557E+02	1.4486255557E+02
31	1.4486255557E+02	1.4486255557E+02	1.4486255557E+02	1.4486255557E+02
32	1.4486255557E+02	1.4486255557E+02	1.4486255557E+02	1.4486255557E+02
TOTAL	1.4486255557E+02	1.4486255557E+02	1.4486255557E+02	1.4486255557E+02
CONTINUATION				
1	1.4486255557E+02	1.4486255557E+02	1.4486255557E+02	1.4486255557E+02
2	1.4486255557E+02	1.4486255557E+02	1.4486255557E+02	1.4486255557E+02
3	1.4486255557E+02	1.4486255557E+02	1.4486255557E+02	1.4486255557E+02
4	1.4486255557E+02	1.4486255557E+02	1.4486255557E+02	1.4486255557E+02
5	1.4486255557E+02	1.4486255557E+02	1.4486255557E+02	1.4486255557E+02
6	1.4486255557E+02	1.4486255557E+02	1.4486255557E+02	1.4486255557E+02
7	1.4486255557E+02	1.4486255557E+02	1.4486255557E+02	1.4486255557E+02
8	1.4486255557E+02	1.4486255557E+02	1.4486255557E+02	1.4486255557E+02
9	1.4486255557E+02	1.4486255557E+02	1.4486255557E+02	1.4486255557E+02
10	1.4486255557E+02	1.4486255557E+02	1.4486255557E+02	1.4486255557E+02
11	1.4486255557E+02	1.4486255557E+02	1.4486255557E+02	1.4486255557E+02
12	1.4486255557E+02	1.4486255557E+02	1.4486255557E+02	1.4486255557E+02
13	1.4486255557E+02	1.4486255557E+02	1.4486255557E+02	1.4486255557E+02
14	1.4486255557E+02	1.4486255557E+02	1.4486255557E+02	1.4486255557E+02
15	1.4486255557E+02	1.4486255557E+02	1.4486255557E+02	1.4486255557E+02
16	1.4486255557E+02	1.4486255557E+02	1.4486255557E+02	1.4486255557E+02
17	1.4486255557E+02	1.4486255557E+02	1.4486255557E+02	1.4486255557E+02
18	1.4486255557E+02	1.4486255557E+02	1.4486255557E+02	1.4486255557E+02
19	1.4486255557E+02	1.4486255557E+02	1.4486255557E+02	1.4486255557E+02
20	1.4486255557E+02	1.4486255557E+02	1.4486255557E+02	1.4486255557E+02
21	1.4486255557E+02	1.4486255557E+02	1.4486255557E+02	1.4486255557E+02
22	1.4486255557E+02	1.4486255557E+02	1.4486255557E+02	1.4486255557E+02
23	1.4486255557E+02	1.4486255557E+02	1.4486255557E+02	1.4486255557E+02

Fig. 4.2 Continuation of Fig. 4.1

24	7.0174449E+01	7.1113546E+01	5.2727712E+01	1.75746107E+01	7.11642405E-01	1.27880398E+01	1.71213371E+04
25	7.01130581E+03	6.27271170E+02	1.50775495E+01	5.31061484E+01	1.97702379E+00	1.15496437E+01	1.70805447E+04
26	7.01495102E+01	5.55677181E+01	2.60719195E+01	7.21601565E+00	1.61264046E+00	3.72246262E+00	1.70545598E+04
27	5.00740002E+01	3.55107556E+01	1.55472146E+01	1.12123055E+01	1.07740081E+00	5.59740117E+00	1.69335677E+04
28	7.01471237E+01	5.6590467E+01	1.01102052E+01	1.01364749E+00	1.64334431E+00	6.43614425E+00	1.68833234E+04
29	6.01532224E+01	4.02106782E+01	2.01146520E+01	1.14456209E+01	1.14456209E+01	7.73517915E+00	5.11022829E+00
30	1.00911457E+01	4.00700788E+01	1.01644617E+01	1.01396128E+01	1.01396128E+01	5.49979342E+00	1.66904672E+04
31	7.02363213E+01	5.63495461E+01	1.01155952E+01	1.01301134E+00	1.73554020E+00	3.47614290E+00	1.66646142E+04
32	7.52134401E+01	3.2566371E+01	2.10167449E+01	1.02267572E+01	1.50942774E+00	5.72353956E-02	1.66667184E+04
TOTAL	1.01358030E+04	7.02446022E+04	1.762470219E+04	1.04215442E+04	1.40725276E+04	1.77212170E+05	
BRAYD TOTAL			1021.564862				

Fig. 4.3 Continuation of Fig. 4.1

COMPUTED VALUES OF $(C_m, C_n) + (D_m, D_n)_k$ IN ANALYSIS OF VARIANCE OF EDDY FLUX FOR LATITUDE BAND 1. UNITS ARE DIMENSIONLESS PERIOD.

k	1	2	3	4	5
1	1.412525251E+14	1.044511586E+14	8.358178072E+13	1.484771584E+14	
2	8.215411222E+13	6.258602245E+13	2.742728895E+13	2.853426987E+13	
3	7.805111222E+13	6.617321805E+13	2.825845971E+13	2.321513189E+13	
4	5.010212461E+13	7.234447514E+13	3.444731039E+13	3.821651845E+13	
5	2.064455040E+13	7.583624856E+13	3.924443577E+13	4.379462377E+13	
6	4.203442424E+13	7.873466131E+13	4.203442424E+13	3.615512185E+13	
7	3.406312166E+13	7.806653701E+13	3.406312166E+13	3.056761319E+13	
8	3.571567357E+13	7.876578665E+13	3.571567357E+13	2.336657633E+13	
9	3.15550390E+13	7.807365051E+13	3.15550390E+13	2.728108111E+13	
10	3.646719319E+13	7.827397100E+13	3.646719319E+13	2.421021895E+13	
11	2.762478642E+13	7.667701661E+13	2.762478642E+13	1.2224451330E+13	
12	4.592123577E+13	7.839758191E+13	4.592123577E+13	1.118993194E+13	
13	1.325653126E+13	7.84237755E+13	1.325653126E+13	6.297405773E+13	
14	1.333427293E+13	7.813342729E+13	1.333427293E+13	8.185487424E+13	
15	8.15005230E+13	7.813342729E+13	8.15005230E+13	4.415965002E+13	
16	6.343806556E+13	7.813342729E+13	6.343806556E+13	3.133006556E+13	
17	4.675270552E+13	7.813342729E+13	4.675270552E+13	3.149041207E+13	
18	3.74339622E+13	7.813342729E+13	3.74339622E+13	1.732423993E+13	
19	6.22952222E+13	7.813342729E+13	6.22952222E+13	8.22952222E+13	
20	1.567326839E+13	7.813342729E+13	1.567326839E+13	1.826659949E+13	
21	7.458080693E+13	7.813342729E+13	7.458080693E+13	6.017493372E+13	
22	8.613066019E+13	7.813342729E+13	8.613066019E+13	3.137867465E+13	
23	6.26603744E+13	7.813342729E+13	6.26603744E+13	5.516974027E+13	
24	2.979866779E+13	7.813342729E+13	2.979866779E+13	1.833033377E+13	
25	2.834044987E+13	7.813342729E+13	2.834044987E+13	1.329614457E+13	
26	1.853177198E+13	7.813342729E+13	1.853177198E+13	9.53233169E+11	
27	1.120502945E+13	7.813342729E+13	1.120502945E+13	4.891342875E+11	
28	3.034710105E+11	7.813342729E+13	3.034710105E+11	5.361759616E+11	

Fig. 4.4 Components $((C_m, C_n) + (D_m, D_n))_k$ in Analysis of Variance of eddy flux for latitude band 1.

COMPONENTS (Covariance) OF THE ANALYSIS OF EDDY FLUX WITH X TIMES DELTA T SQUARED
FOR LATITUDE BAND 1 (20°N-30°N) (1960-1969)

UNITS ARE DEGREES SQUARED PER YEAR-DECADE

K	1	2	3	4	5	6
9
10
11
12
13
14
15
16
17
18
19
20
21
22
23
24
25
26
27

Fig. 4.7 Components $((A_m, C_m) + (B_m, D_m))_k$ in Analysis of Covariance of eddy flux with X times temp. gradient squared for latitude band 1.

24	-1.057727E+01	4.001317E+01	1.171017E+01	7.806700E+00	5.100683E+04	2.40510900E+05	-6.165139148E+06
25	1.009480E+05	1.507710E+05	2.11265015E+05	1.707313015E+05	1.243459875E+05	9.062869956E+05	-4.125563915E+05
26	9.50671060E+05	9.37031235E+05	4.64654161E+05	1.75733791E+05	6.51895047E+04	5.743099733E+04	-6.217199206E+06
27	8.75261919E+05	8.76617220E+05	6.0082655E+05	4.3223253E+05	5.437056621E+04	5.75865365E+04	-6.42688644E+06
28	4.8292037E+05	4.34763193E+05	1.80635476E+05	1.47270151E+05	8.7374317E+05	-1.75961962E+05	-6.219257197E+05
29	-1.37133702E+06	-1.17514779E+06	5.1357444E+05	4.7217575E+05	4.169125624E+05	-2.873082363E+05	1.917010490E+06
30	1.009480E+05	1.070605E+06	7.40603300E+05	2.00787127E+04	1.066620535E+05	2.63652089E+05	5.315434692E+06
31	-4.79066E+01	-1.4420607E+05	2.4441239E+05	2.20427433E+05	7.7E50240E+05	2.11836291E+05	-2.107147789E+06
32	-1.23571645E+06	-7.70245465E+05	4.60301335E+05	-1.054623655E+05	1.047743003E+05	-3.199104218E+04	9.401187426E+05
TOTAL	0.000000E+00	0.000000E+00	0.000000E+00	0.000000E+00	0.000000E+00	0.000000E+00	0.000000E+00
GRAND TOTAL	1714307.44000						

Fig. 4.9 Continuation of Fig. 4.7

CORRELATION COEFFICIENTS OF δ WITH X-LIBRA I SQUARED, FOR INDIVIDUAL SPACE-TYPE COMPONENTS, FOR COLUMN AND ROW TOTALS, AND EQ. GRAN
FOR LATITUDE BAND 1 (EQUATORIAL BAND COMPONENTS)
UNITLESS

K	COEFFS FOR SUM OVER K										
	FOR EACH WAVELENGTH										
	1	2	3	4	5	6	7	8	9	10	11
0	.0000	.0000	.0000	.0000	.0000	.0000	.0000	.0000	.0000	.0000	.0000
1	.0000	.0000	.0000	.0000	.0000	.0000	.0000	.0000	.0000	.0000	.0000
2	.0000	.0000	.0000	.0000	.0000	.0000	.0000	.0000	.0000	.0000	.0000
3	.0000	.0000	.0000	.0000	.0000	.0000	.0000	.0000	.0000	.0000	.0000
4	.0000	.0000	.0000	.0000	.0000	.0000	.0000	.0000	.0000	.0000	.0000
5	.0000	.0000	.0000	.0000	.0000	.0000	.0000	.0000	.0000	.0000	.0000
6	.0000	.0000	.0000	.0000	.0000	.0000	.0000	.0000	.0000	.0000	.0000
7	.0000	.0000	.0000	.0000	.0000	.0000	.0000	.0000	.0000	.0000	.0000
8	.0000	.0000	.0000	.0000	.0000	.0000	.0000	.0000	.0000	.0000	.0000
9	.0000	.0000	.0000	.0000	.0000	.0000	.0000	.0000	.0000	.0000	.0000
10	.0000	.0000	.0000	.0000	.0000	.0000	.0000	.0000	.0000	.0000	.0000
11	.0000	.0000	.0000	.0000	.0000	.0000	.0000	.0000	.0000	.0000	.0000
12	.0000	.0000	.0000	.0000	.0000	.0000	.0000	.0000	.0000	.0000	.0000
13	.0000	.0000	.0000	.0000	.0000	.0000	.0000	.0000	.0000	.0000	.0000
14	.0000	.0000	.0000	.0000	.0000	.0000	.0000	.0000	.0000	.0000	.0000
15	.0000	.0000	.0000	.0000	.0000	.0000	.0000	.0000	.0000	.0000	.0000
16	.0000	.0000	.0000	.0000	.0000	.0000	.0000	.0000	.0000	.0000	.0000
17	.0000	.0000	.0000	.0000	.0000	.0000	.0000	.0000	.0000	.0000	.0000
18	.0000	.0000	.0000	.0000	.0000	.0000	.0000	.0000	.0000	.0000	.0000
19	.0000	.0000	.0000	.0000	.0000	.0000	.0000	.0000	.0000	.0000	.0000
20	.0000	.0000	.0000	.0000	.0000	.0000	.0000	.0000	.0000	.0000	.0000
21	.0000	.0000	.0000	.0000	.0000	.0000	.0000	.0000	.0000	.0000	.0000
22	.0000	.0000	.0000	.0000	.0000	.0000	.0000	.0000	.0000	.0000	.0000
23	.0000	.0000	.0000	.0000	.0000	.0000	.0000	.0000	.0000	.0000	.0000
24	.0000	.0000	.0000	.0000	.0000	.0000	.0000	.0000	.0000	.0000	.0000
25	.0000	.0000	.0000	.0000	.0000	.0000	.0000	.0000	.0000	.0000	.0000

Fig. 4.10 Correlation Coefficient Spectrum, Latitude Band 1.

26	-.0046	-.0031	.0165	-.0104	-.0174	-.01516	-.0015	-.0154	.0179	-.0267	.0389	-.0688	-.0064
27	-.0039	-.0050	-.0191	-.0030	.0070	-.0044	.0220	.0183	-.0167	-.0112	-.0128	.0199	-.0075
28	-.0062	-.0044	-.0166	.0243	.0111	.0220	-.0085	-.0180	-.0174	-.0249	-.0407	-.0174	-.0006
29	-.0102	.0028	-.0044	.0197	-.0057	.0030	.0172	-.0136	-.0255	.0516	-.0076	.0783	-.0033
30	-.0110	-.0050	-.0071	-.0030	.0127	-.0275	-.0428	.0506	.0048	.0531	.0330	-.0965	-.0084
31	-.0130	-.0180	.0247	.0244	.0176	.0263	-.0359	-.0003	-.0749	-.0670	.0146	-.05478	-.0041
32	-.0090	.0020	-.0026	-.0113	-.0070	.0050	.0458	-.0250	-.0272	-.0300	-.0530	-1.0000	-.0018
COEFFS FOR													
SUM OVER													
Y AT													
EACH K													
TOTAL COEFFICIENT .9525													

Fig. 4.11 Continuation of Fig. 4.10

and covariance, $k = 12$ is actually the squares or products of the means, and to its right TOTAL shows the mean products for the wavenumbers. At the bottom of the wavenumber column, TOTAL gives the sum of the variances or covariances over all wavenumbers for a given k . Looking down column $k = 12$, and over from row TOTAL, we find the grand square or product of the means, and the grand total is just the total mean product. The total variance or covariance is just the grand total minus the grand square or product. We will briefly discuss the variance and covariance spectra in section 4.6.

Figures 4.10 and 4.11 display the correlation spectrum for the band centered at $\phi = 35^\circ$. The rightmost column entitled COEFFS FOR SUM OVER k FOR EACH WAVENUMBER contains the coefficients derived from the two rightmost columns of the analyses of variance and covariance (see discussion above.) The bottom most row contains the coefficients for the sum over m at each k , these being derived from the bottom TOTAL row mentioned above. The TOTAL COEFFICIENT results from the grand totals in the other analyses. The correlation coefficients are all calculated according to (3.7) or modifications thereof.

Before describing all of the correlation spectra in the next few sections, we should conclude our discussion about degrees of freedom, and indicate the 95% and 99% confidence limits on the correlation coefficients. To determine the degrees of freedom assuming independence for the sums

of the k's at each m, just add them up for the individual k's. Similarly add to get the total for the sum over the m's at each k (again assuming independence). The total number of degrees of freedom is computed by adding once again across the other scale. Table 4.1 lists the degrees of freedom in all possible combinations and the total, which is 253890. It also gives the value of the correlation coefficient significant at the 95% and 99% confidence limits for an equal-tails test of hypothesis $r_{mk} = 0$. These limits are either taken directly or interpolated using the inverse square root formula from G.W. Snedecor, Statistical Methods, 4th ed., Ames, Iowa, Iowa State College Press, 1946, p. 351. Thus, a correlation coefficient exceeding one or both limits is significant at the given limit assuming statistical independence.

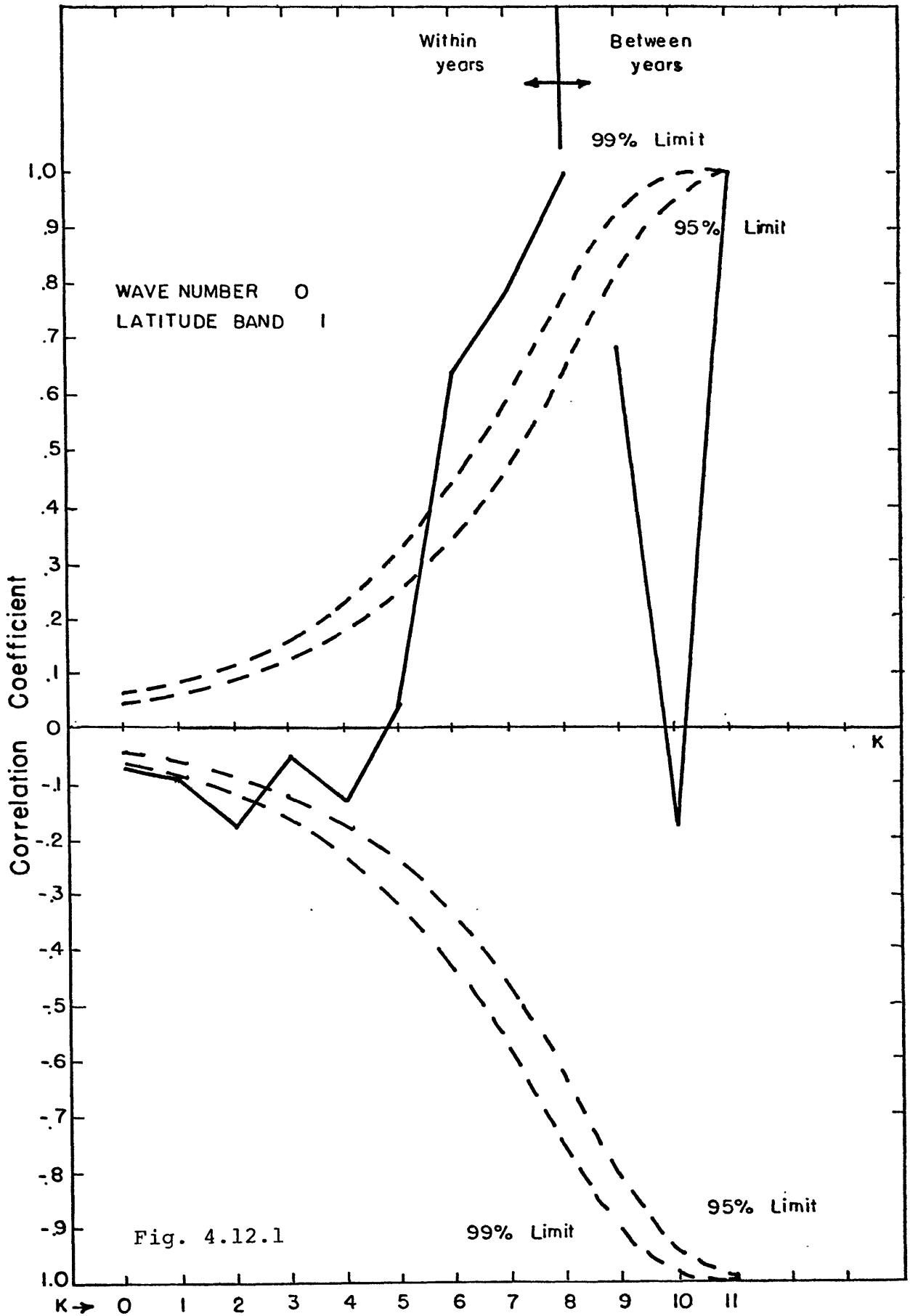
4.2 Correlation Spectra for Individual Wavenumbers and Time Scales by Latitude Band

In this and the next three sections, the important parts of the correlation spectra will be described by means of graphical analysis. Because there is a massive amount of information to be studied, this section will fully describe only spectra for wavenumbers 0 through 5. Wavenumber 5 includes zonal scales ranging from about 6600 KM at 35° to 3400 KM at 65°. This analysis should adequately justify the conclusions to be discussed in the next chapter.

Figures 4.12.1 - 4.12.24 present the correlation spectra by individual wavenumber and time scale for latitude bands 1

Table 4.1
Degrees of Freedom and 95%, 99% Confidence
Limits for Correlation Coefficients

M	K+	K										Sum Over K	D.O.F.		
		0	1	2	3	4	5	6	7	8	9			10	11
0 or 32	D.O.F.	2048	1024	512	256	128	64	32	16	8	4	2	1	4095	D.O.F.
	95%	.043	.061	.087	.122	.172	.242	.338	.468	.632	.811	.950	.997	.031	95%
	99%	.057	.080	.114	.160	.225	.315	.435	.590	.765	.917	.990	1.000	.040	99%
<hr/>															
O<M<32	D.O.F.	4096	2048	1024	512	256	128	64	32	16	8	4	2	8190	D.O.F.
	95%	.031	.043	.061	.087	.122	.172	.242	.338	.468	.632	.811	.950	.022	95%
	99%	.040	.057	.080	.114	.160	.225	.315	.435	.590	.765	.917	.990	.028	99%
<hr/>															
Sum over M	D.O.F.	126976	63488	31744	15872	7936	3968	1984	992	496	248	124	62	Total 253890	D.O.F.
	95%	.0056	.0078	.011	.016	.022	.032	.044	.063	.088	.123	.175	.246	.0039	95%
	99%	.0072	.0102	.014	.020	.029	.041	.058	.081	.115	.162	.229	.320	.0050	99%



Figs. 4.12: Correlation Spectra by Individual Wavenumber and Time Scale K.

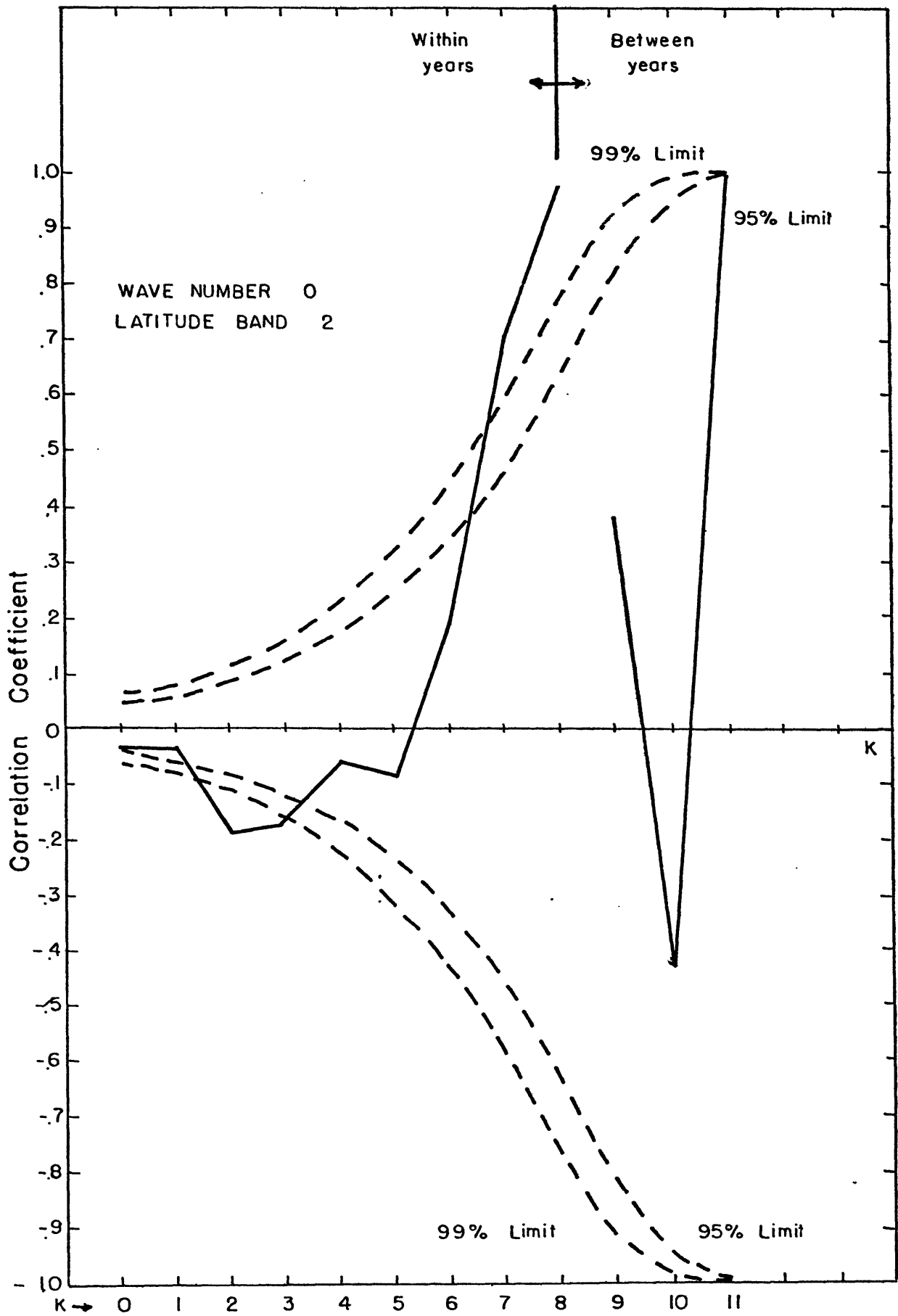


Fig. 4.12.2

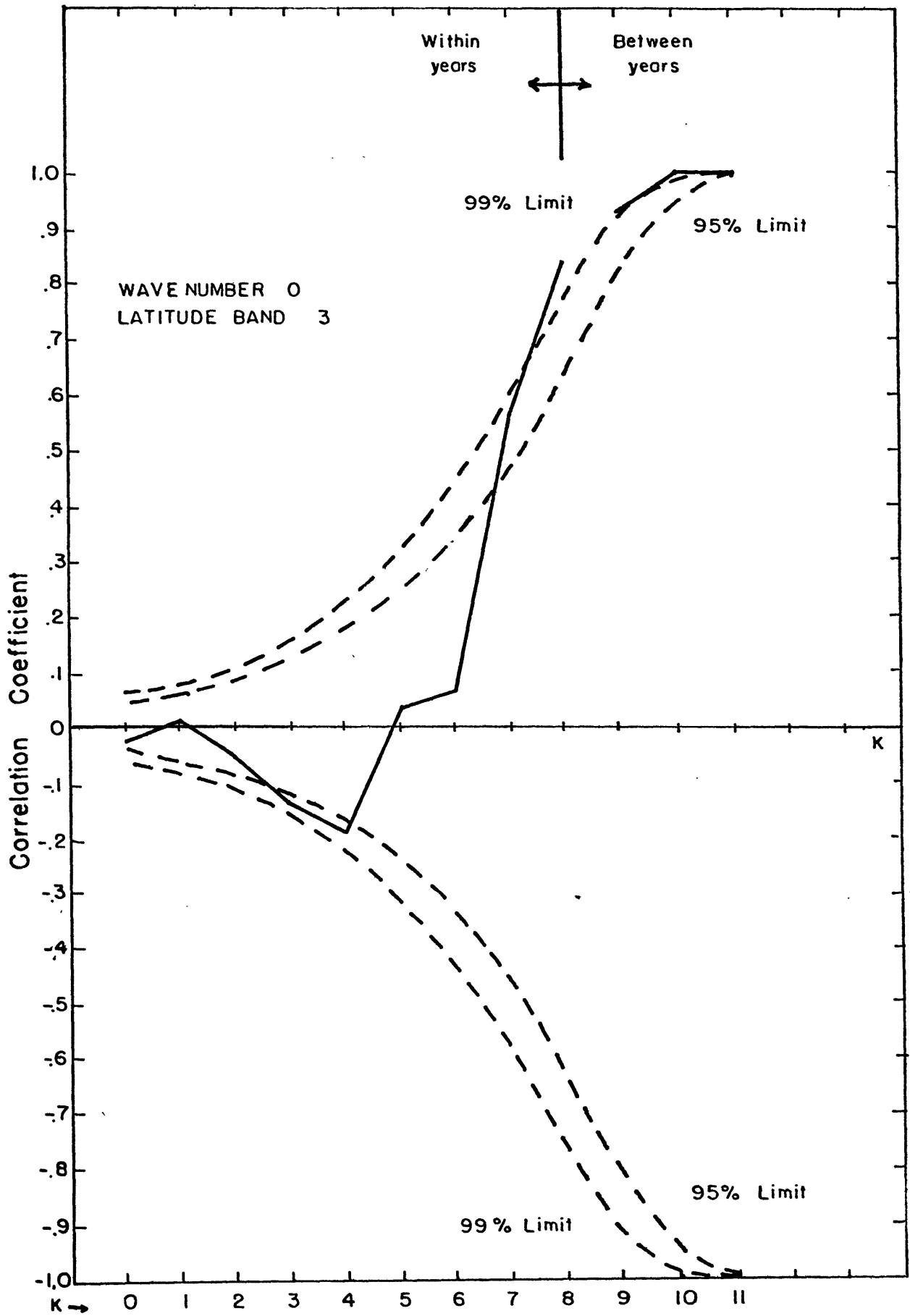


Fig. 4.12.3

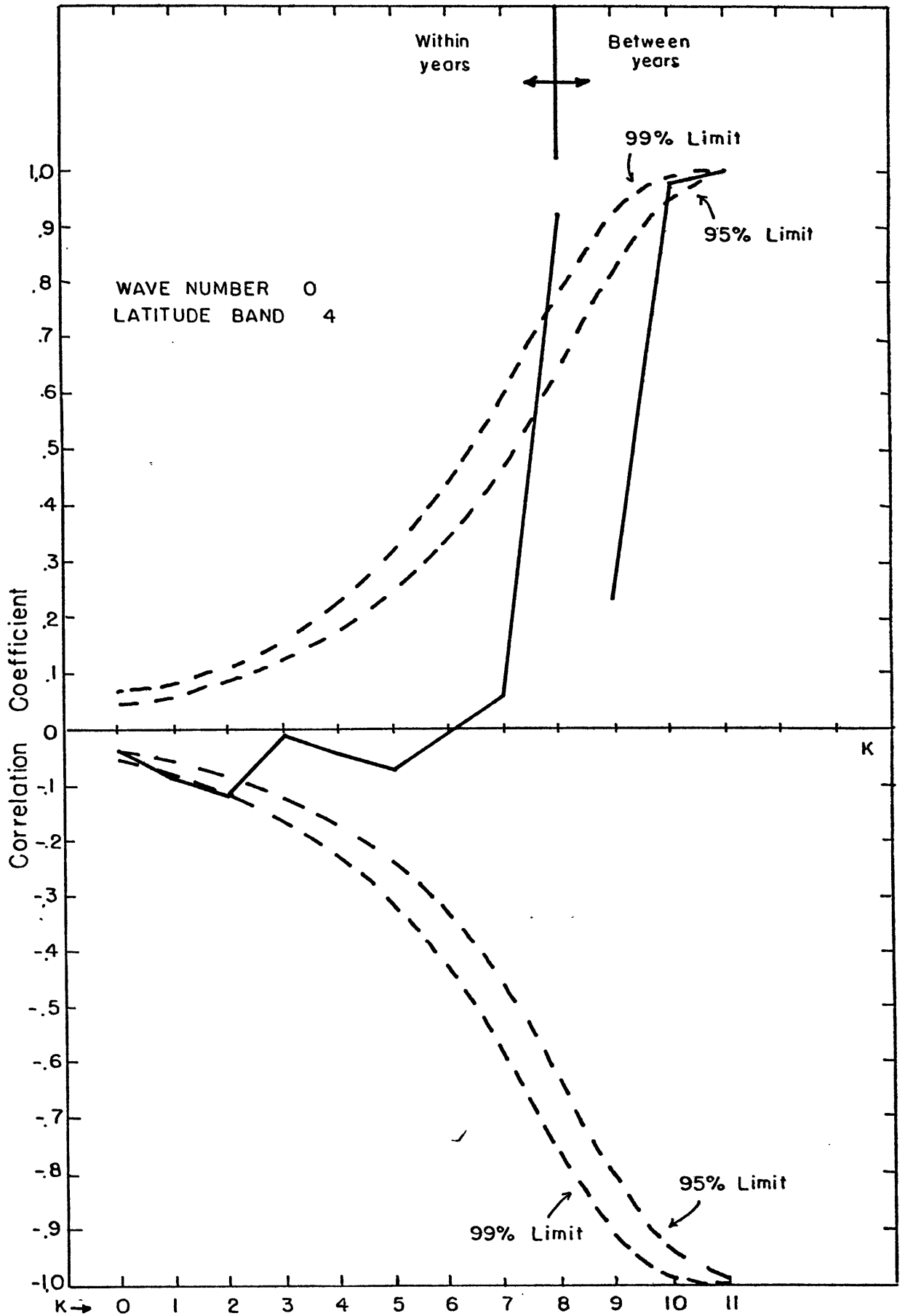


Fig. 4.12.4

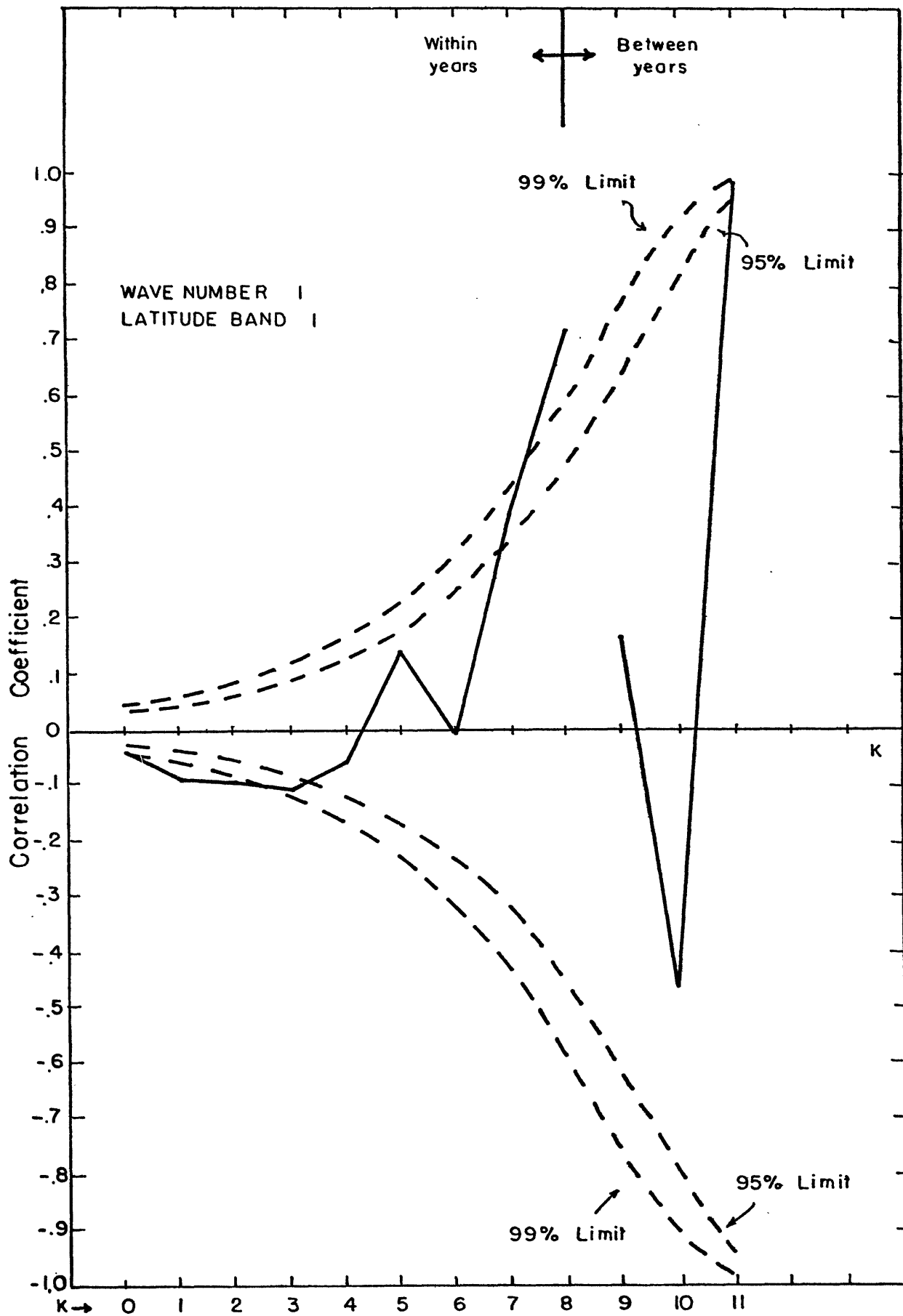


Fig. 4.12.5

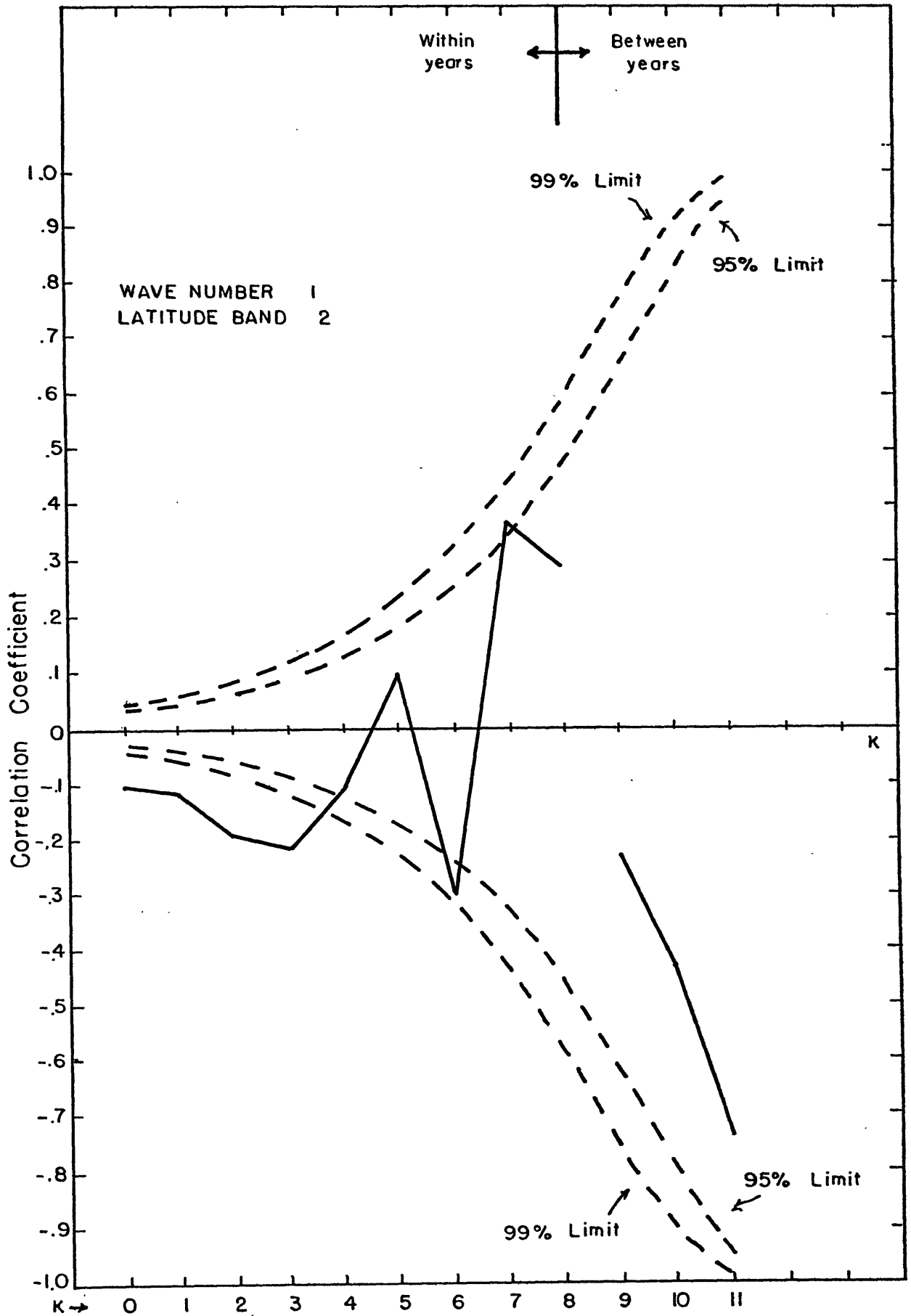


Fig. 4.12.6

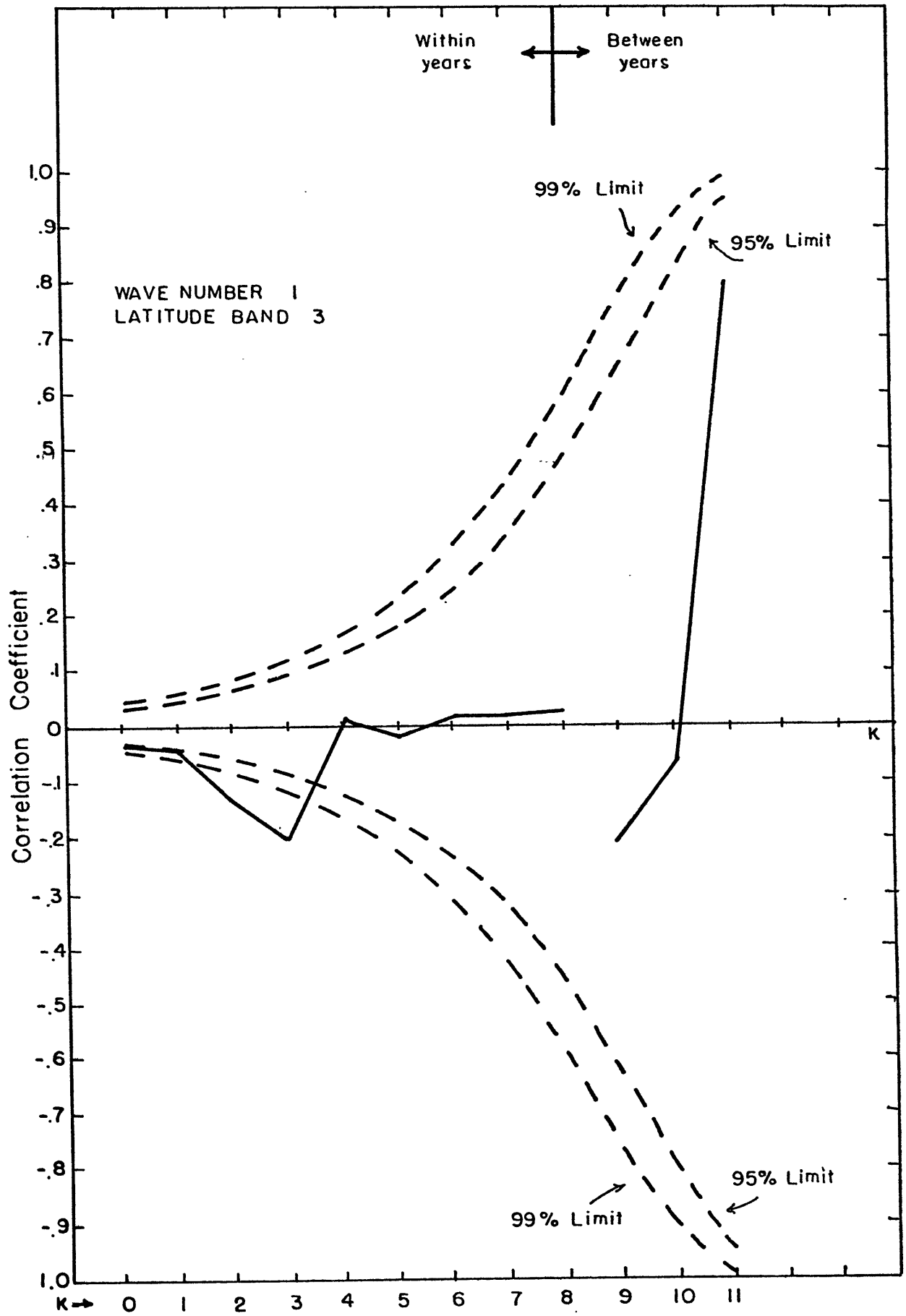


Fig. 4.12.7

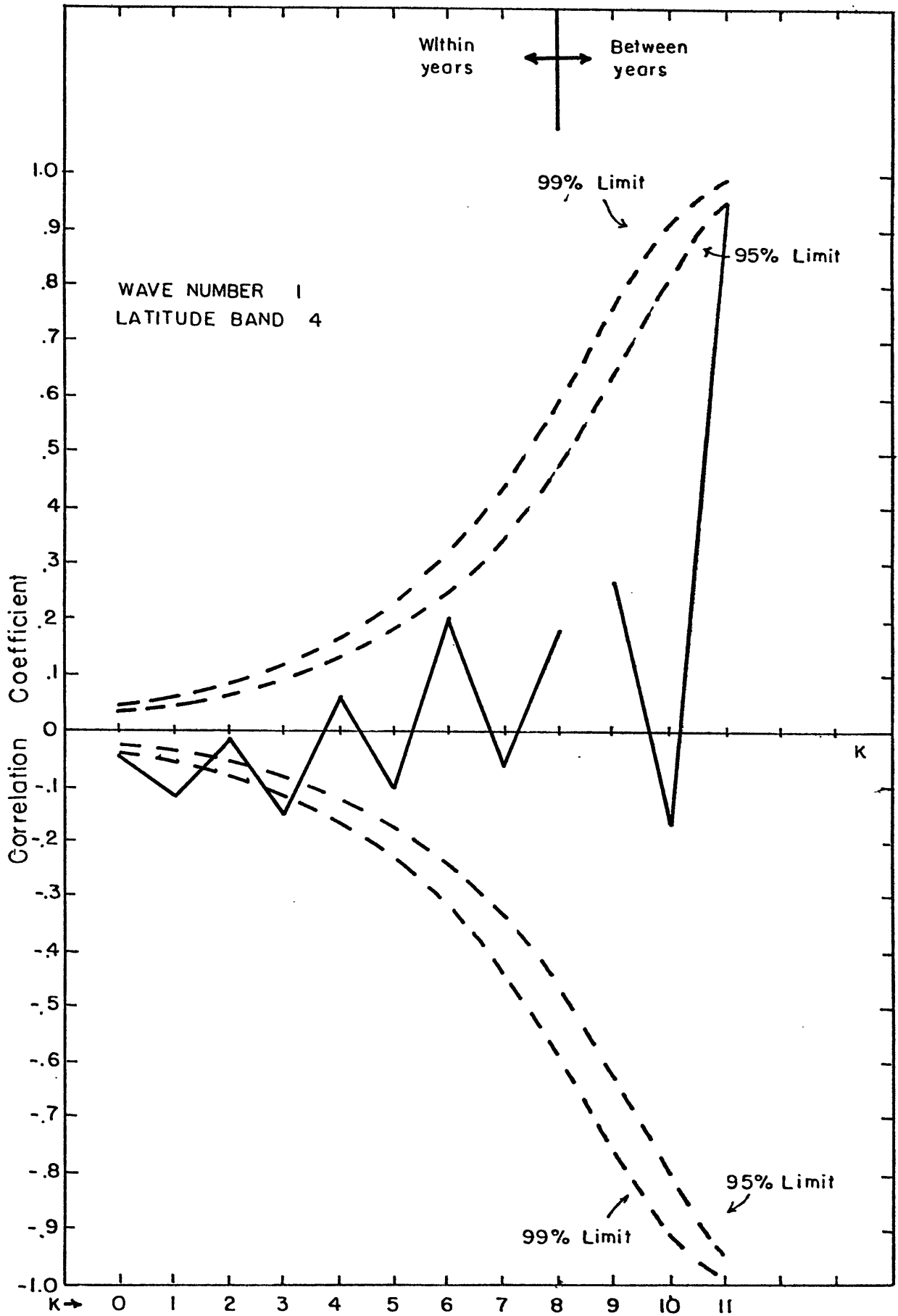


Fig.4.12.8

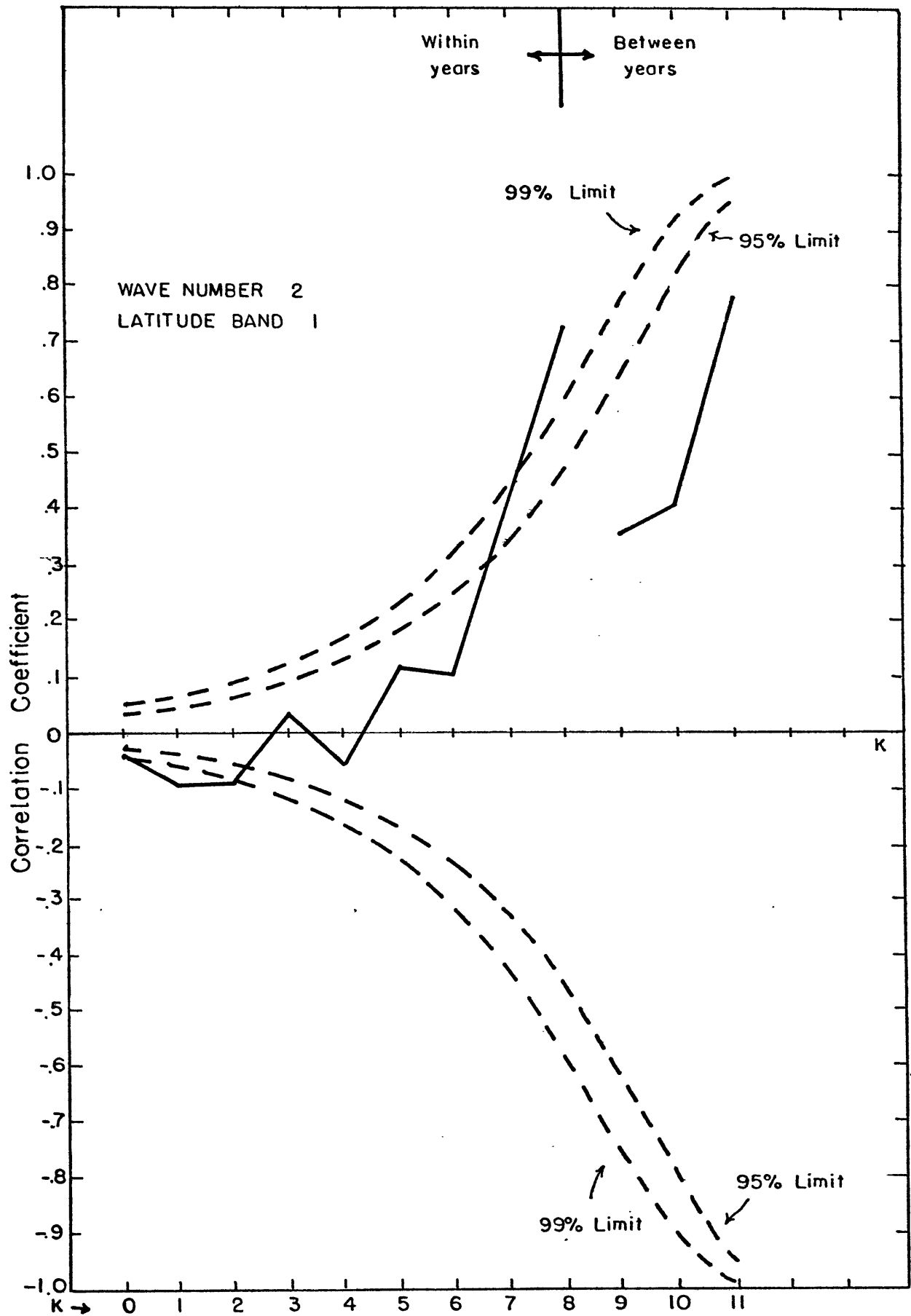


Fig. 4.12.9

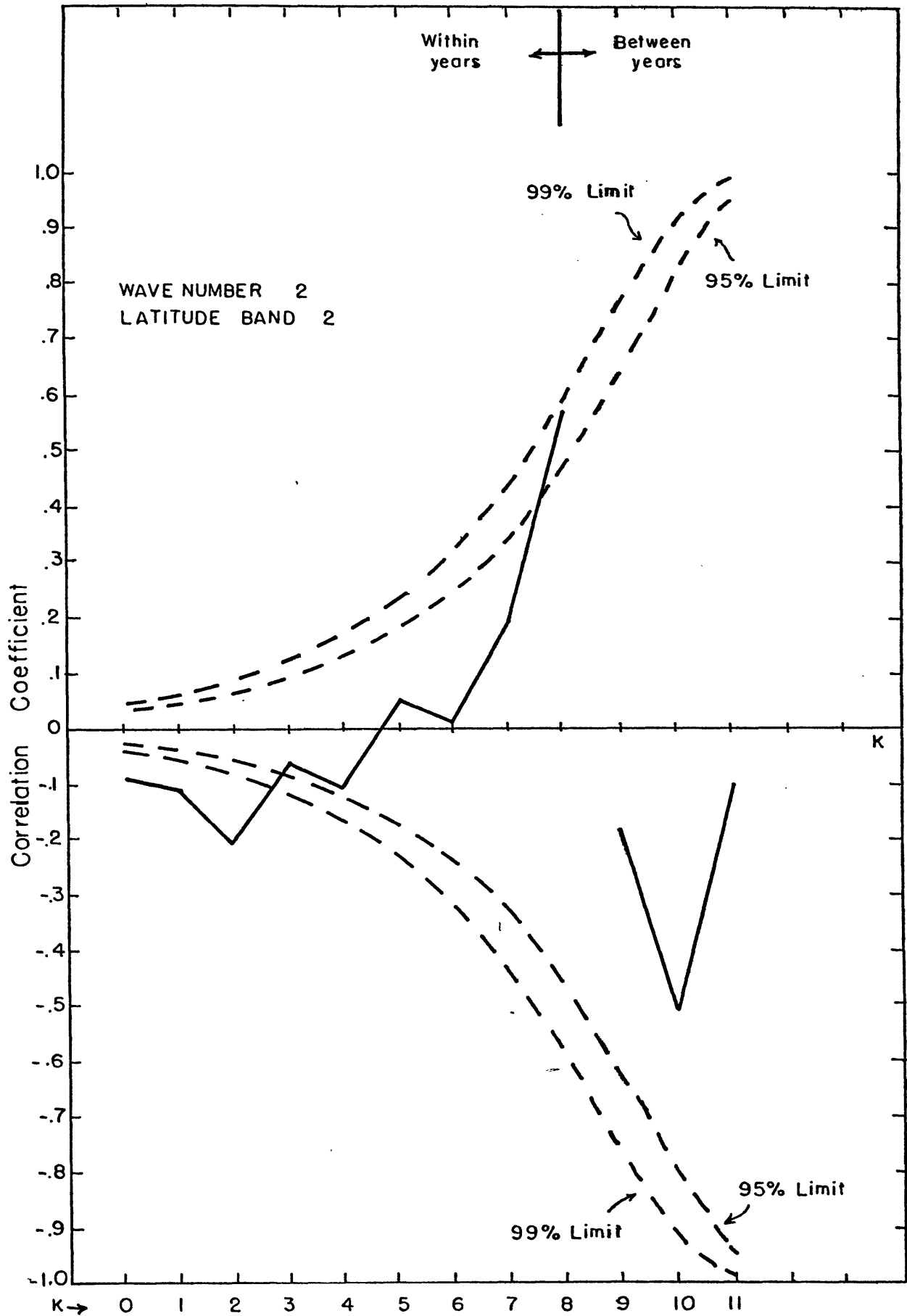


Fig. 4.12.10

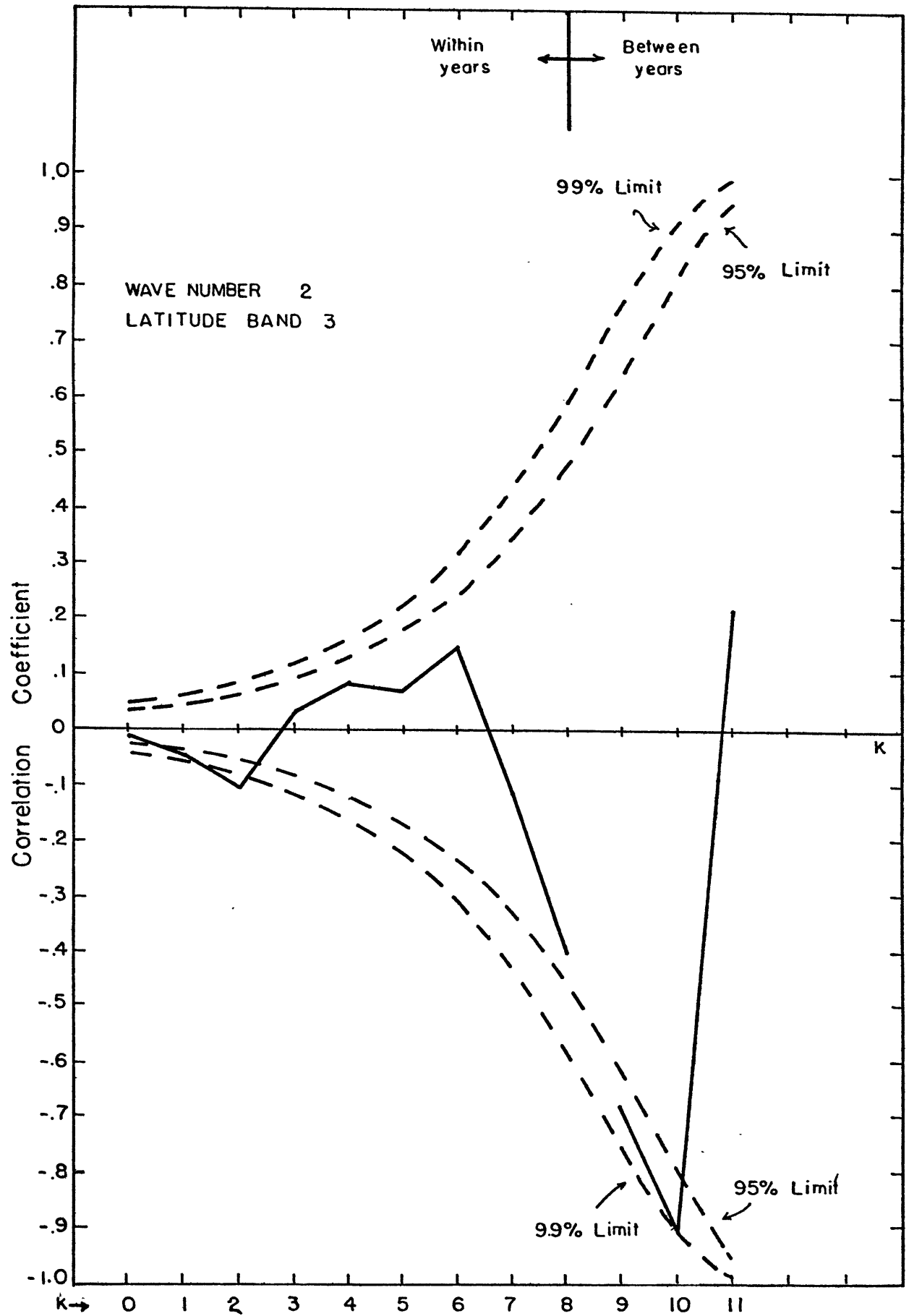


Fig. 4.12.11

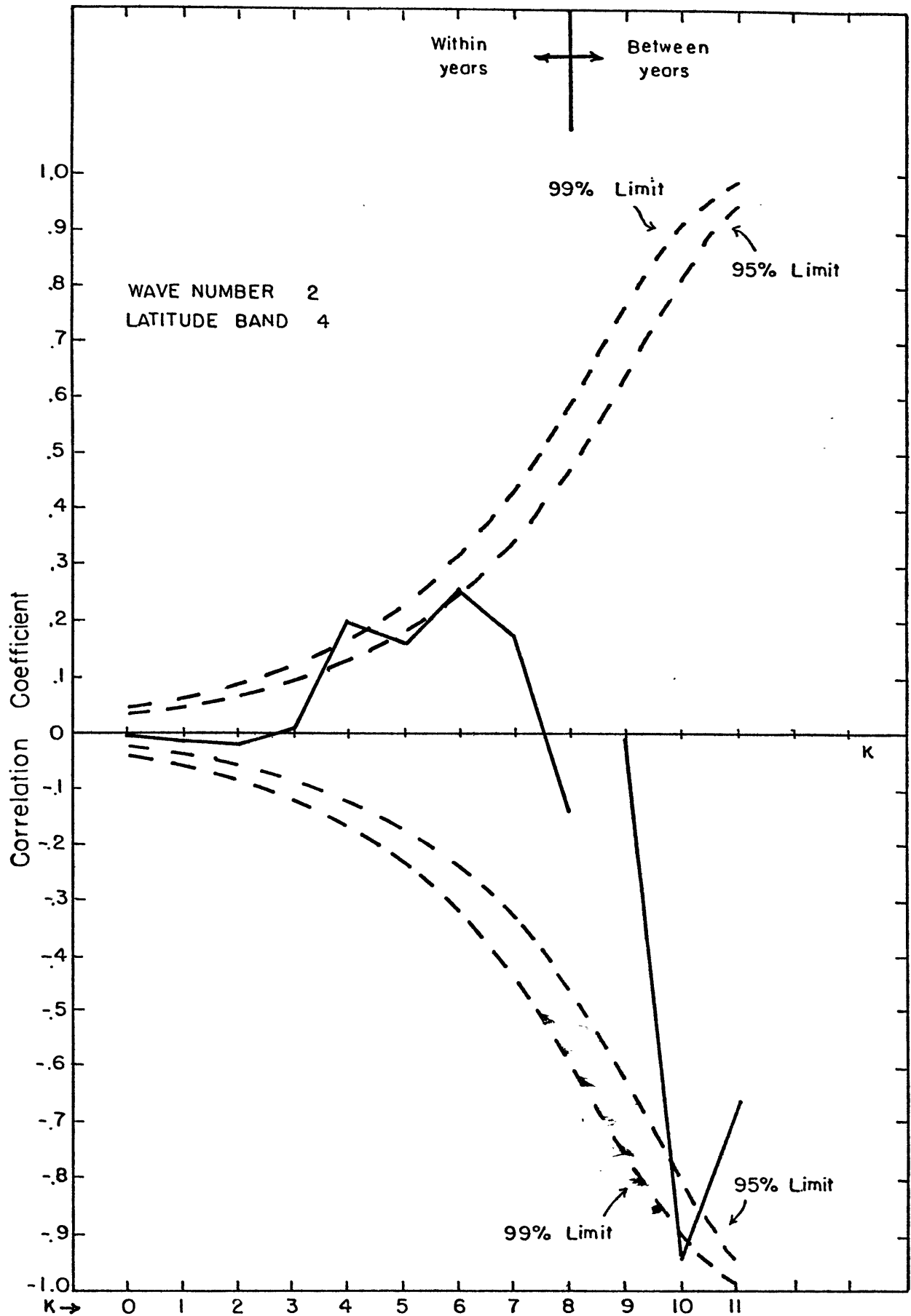


Fig. 4.12.12

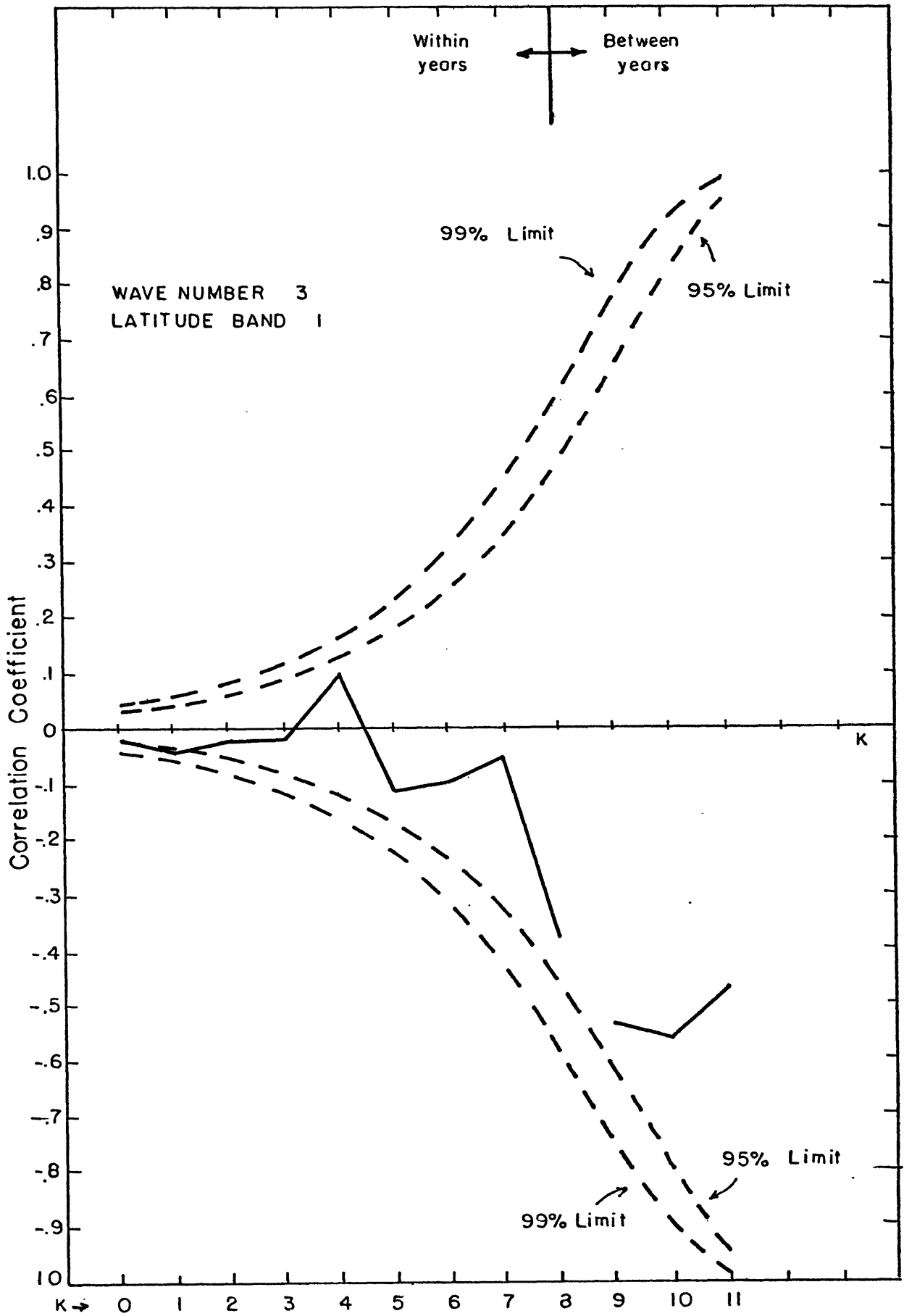


Fig. 4.12.13

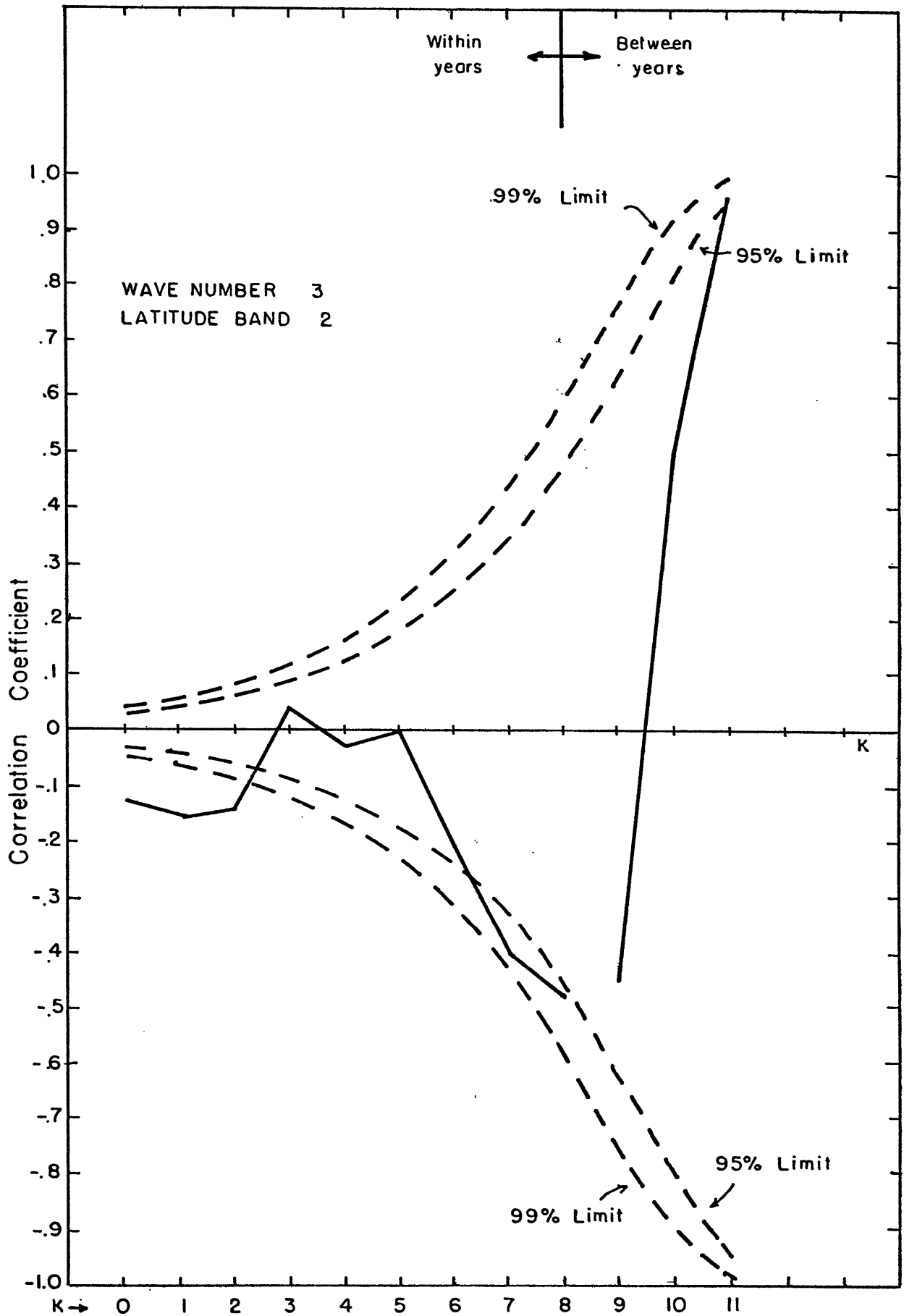


Fig. 4.12.14

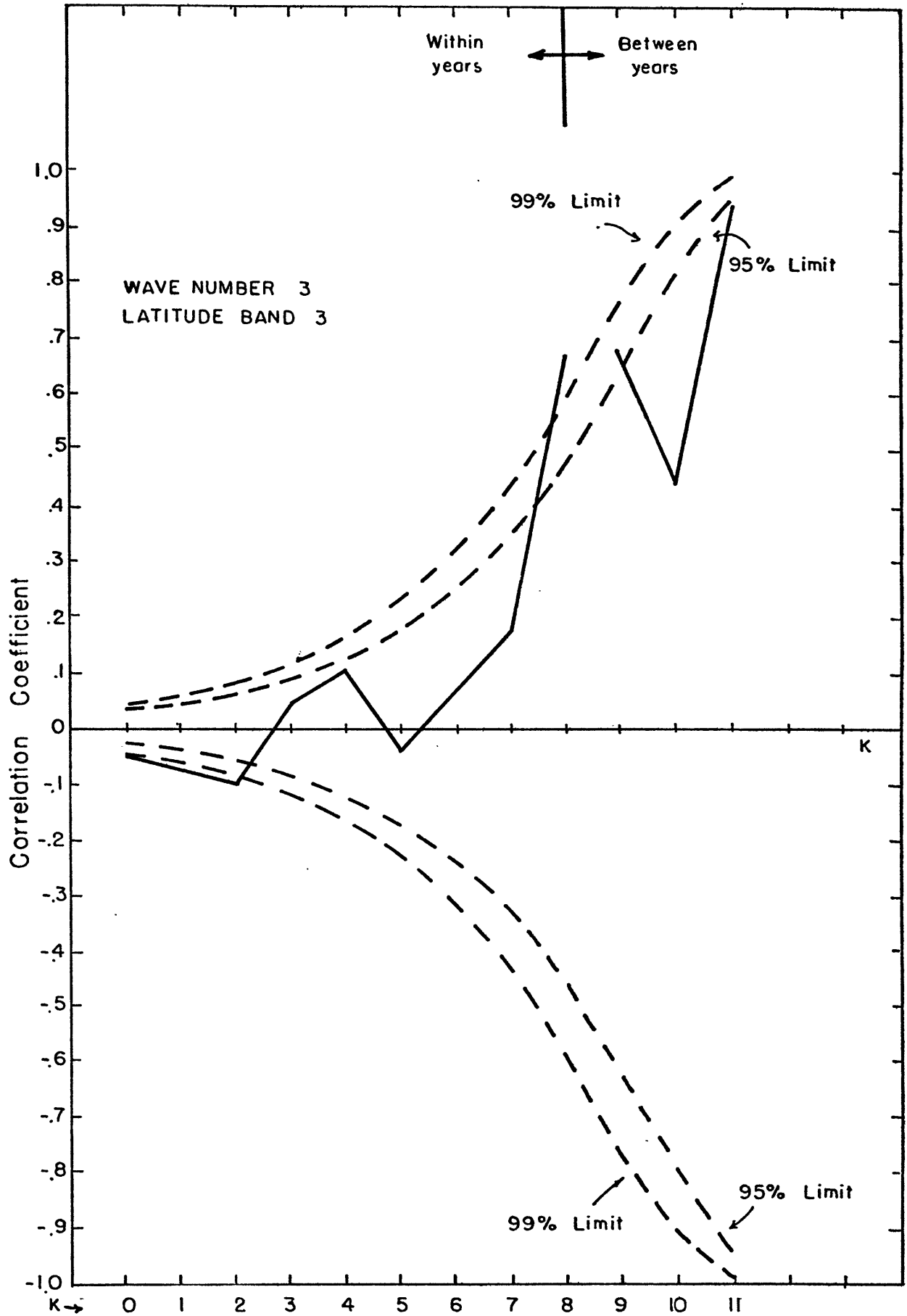


Fig. 4.12.15

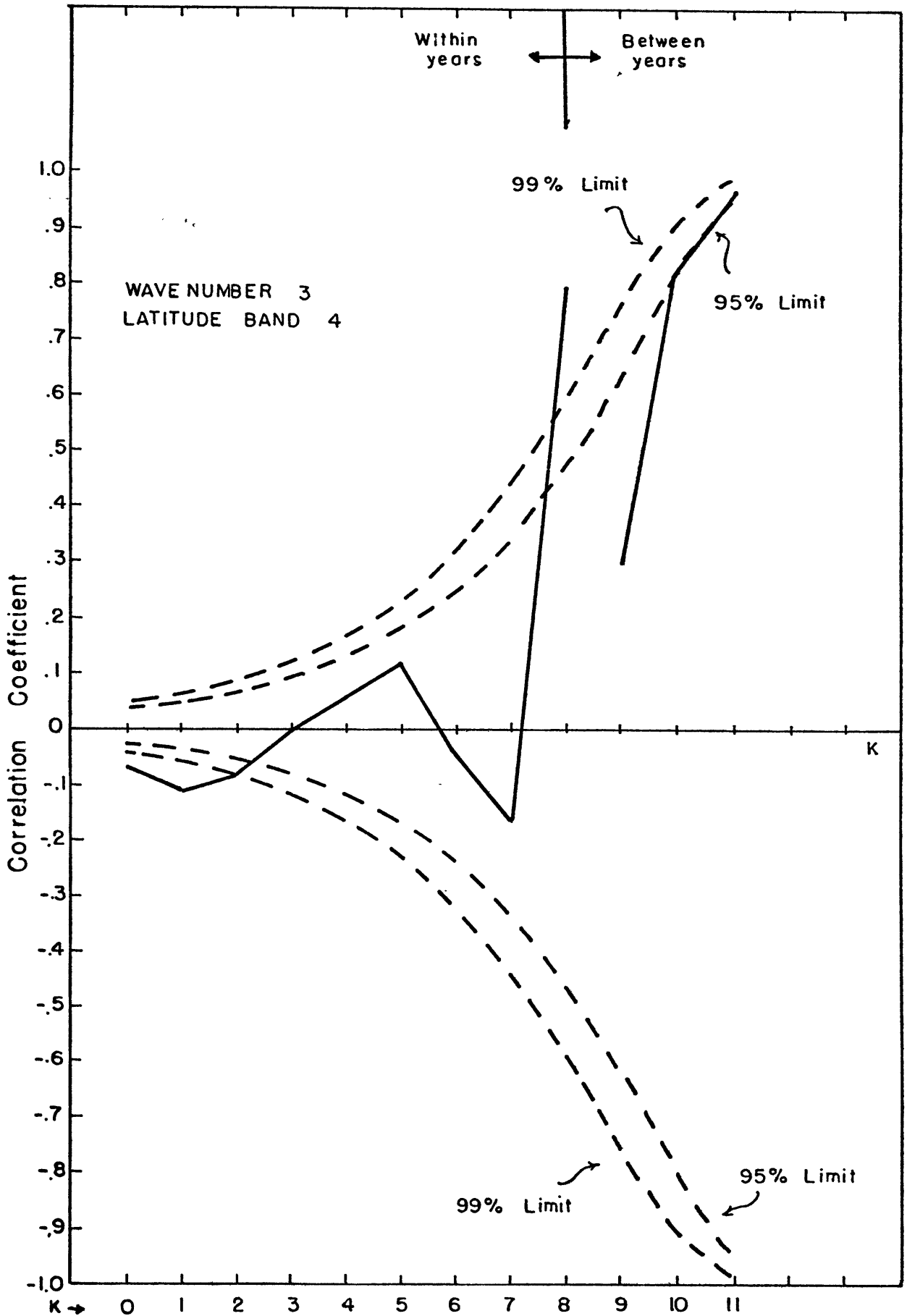


Fig. 4.12.16

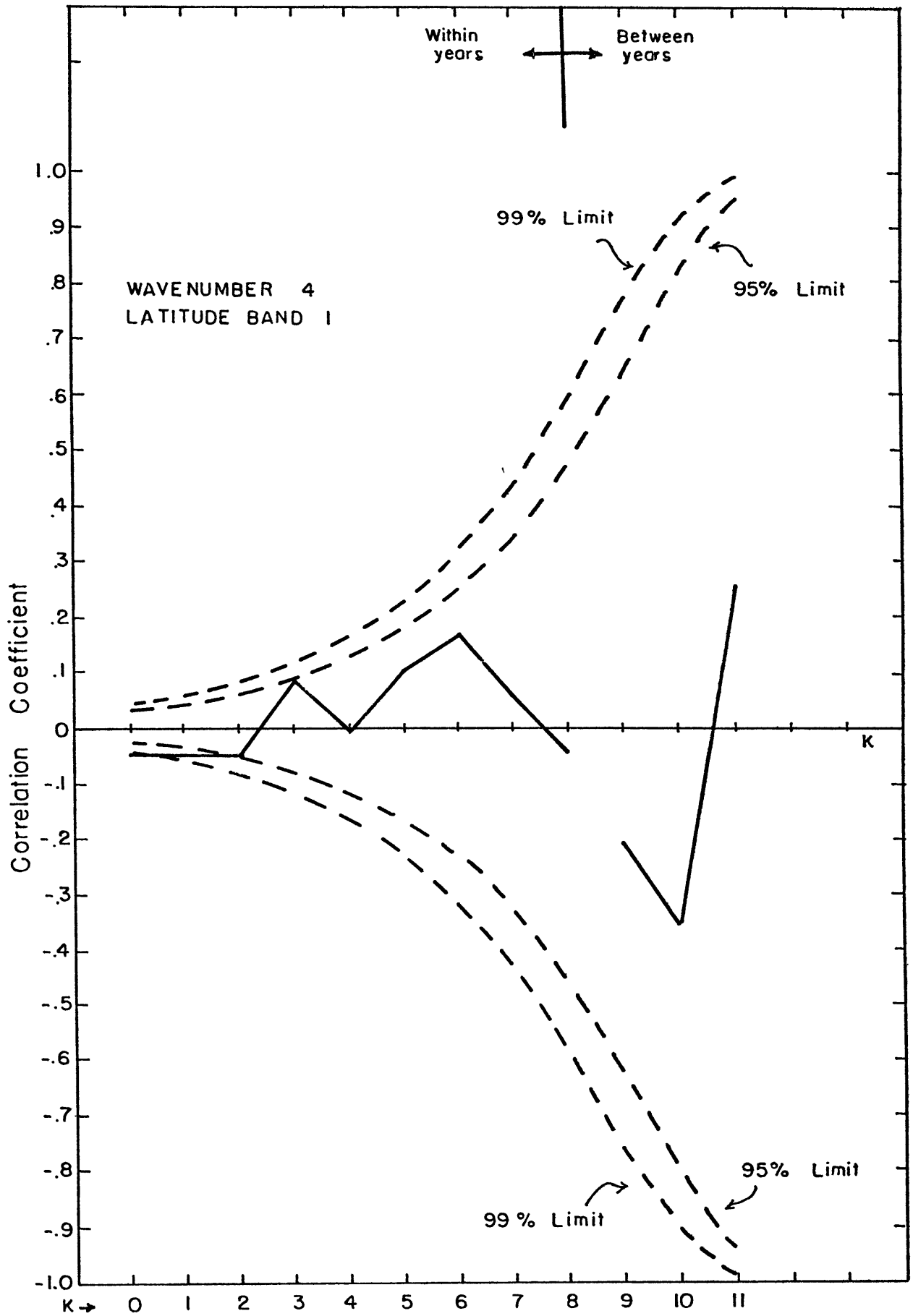


Fig. 4.12.17

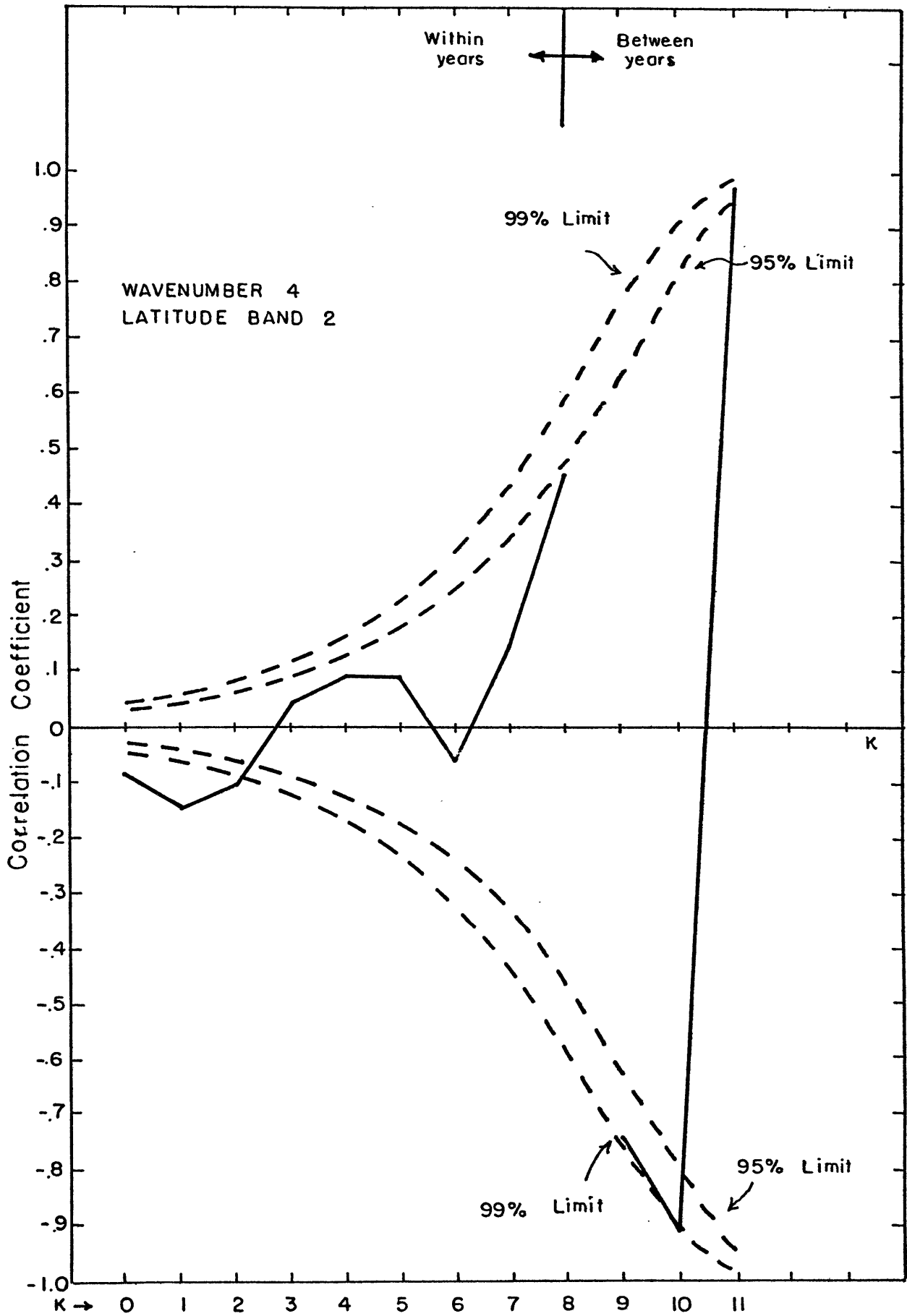


Fig. 4.12.18

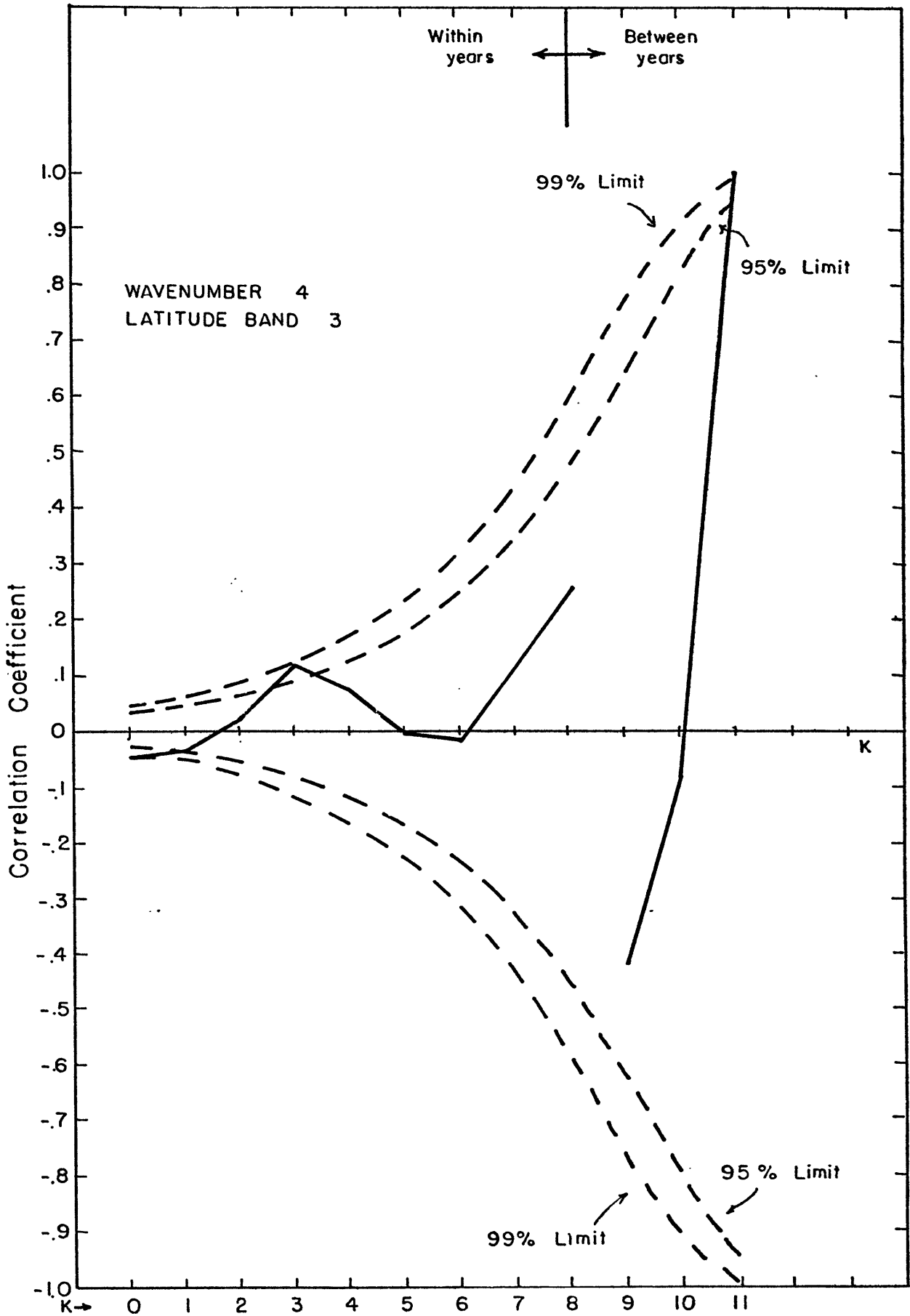


Fig. 4.12.19

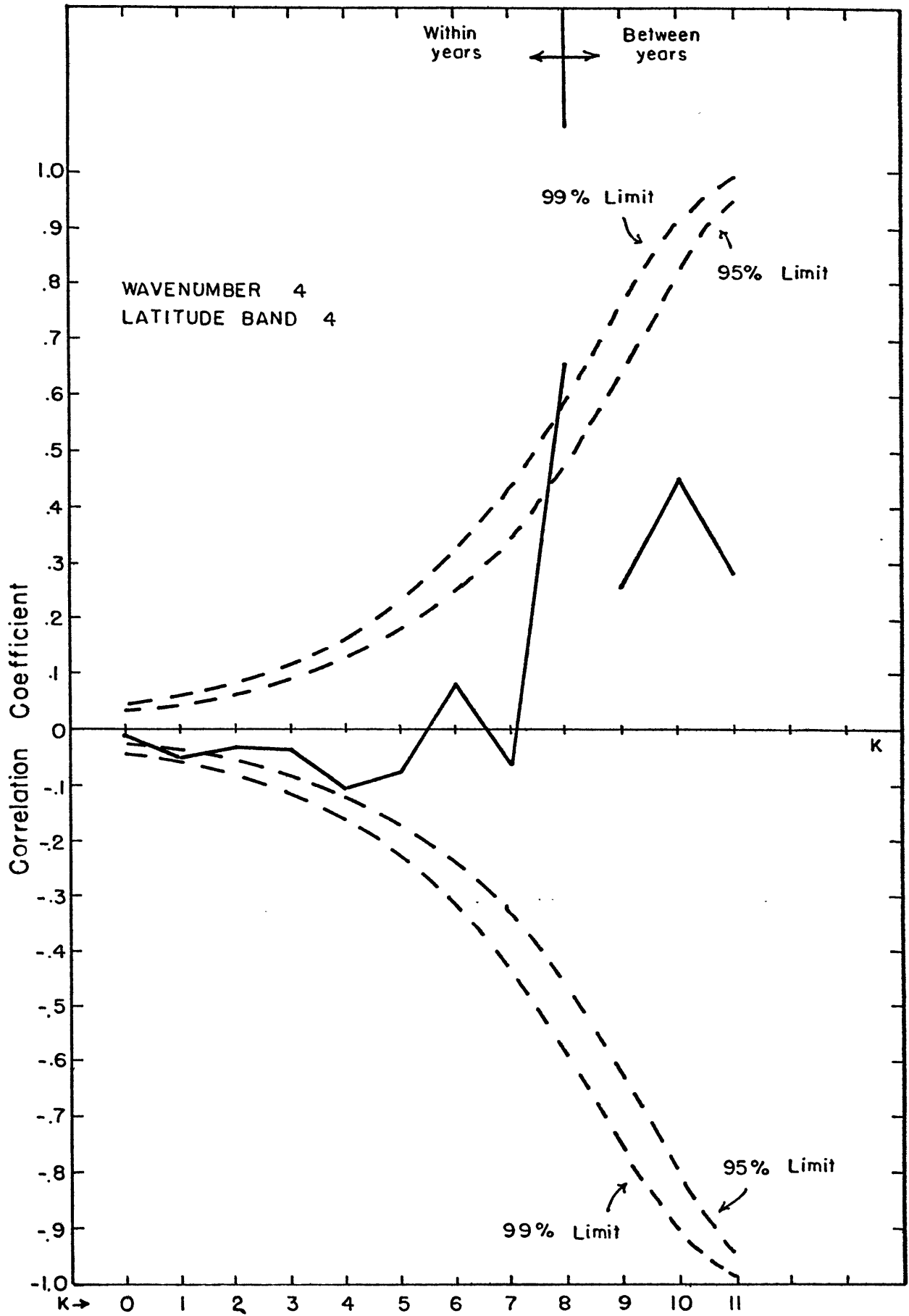


Fig. 4.12.20

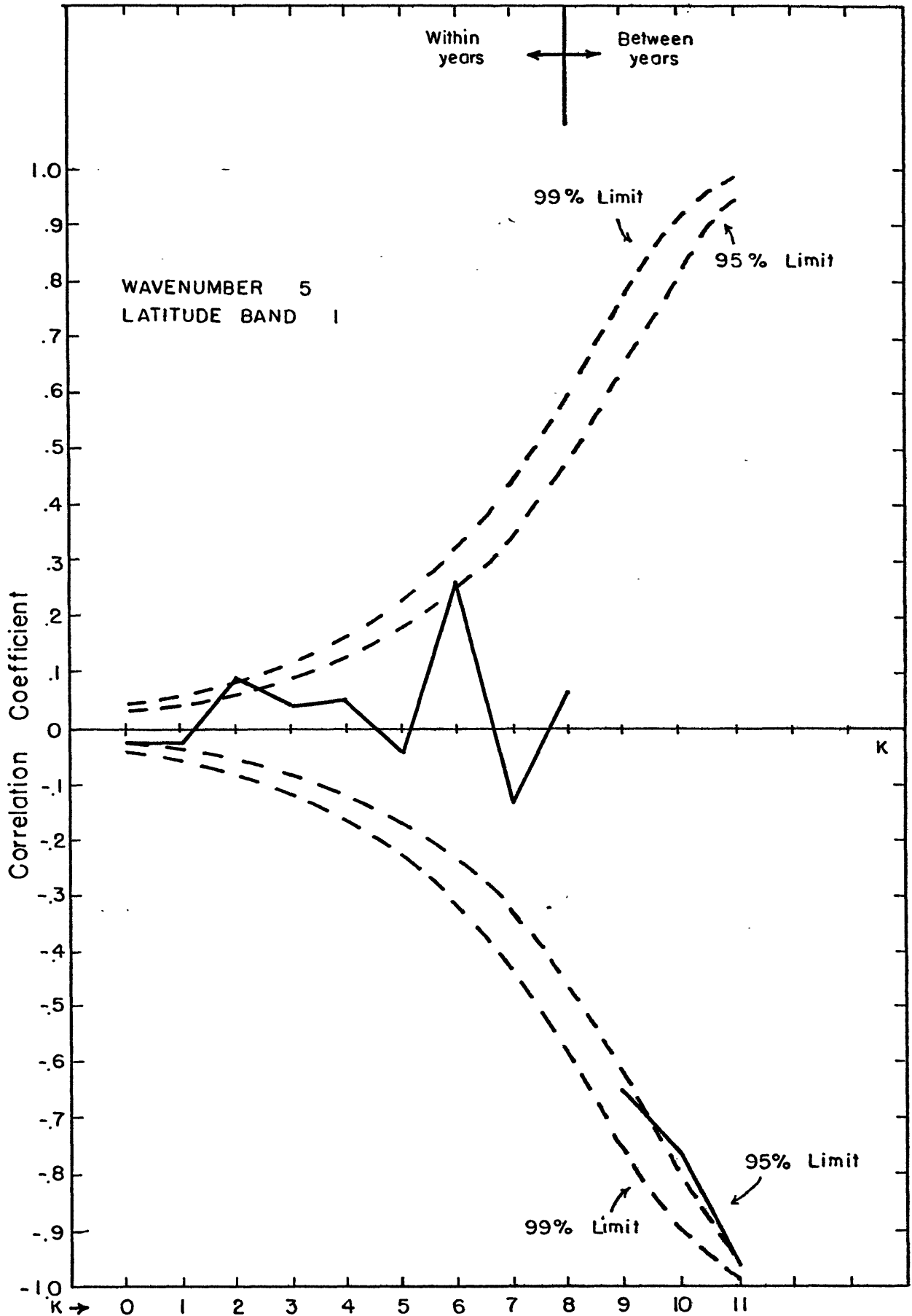


Fig. 4.12.21

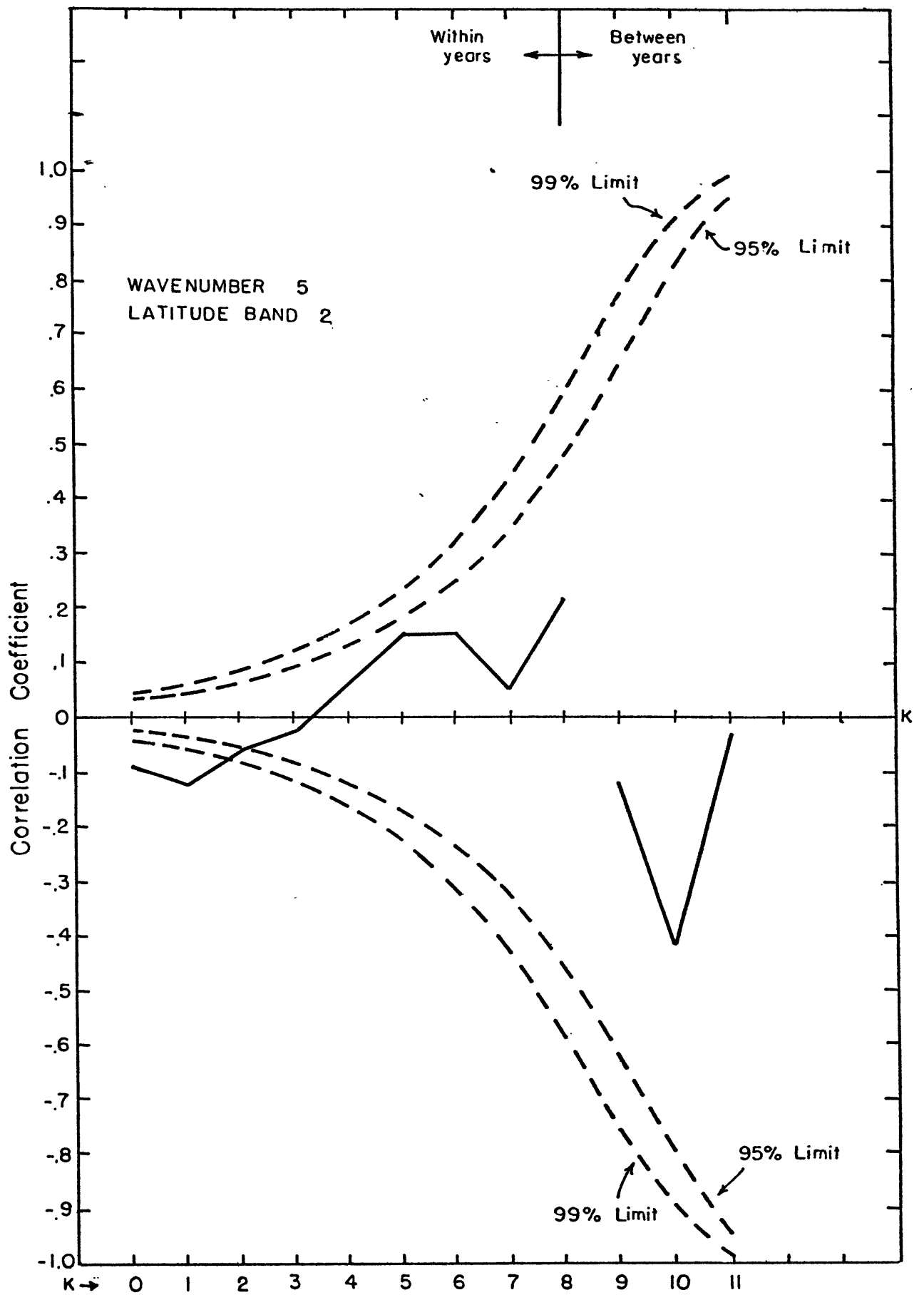


Fig. 4.12.22

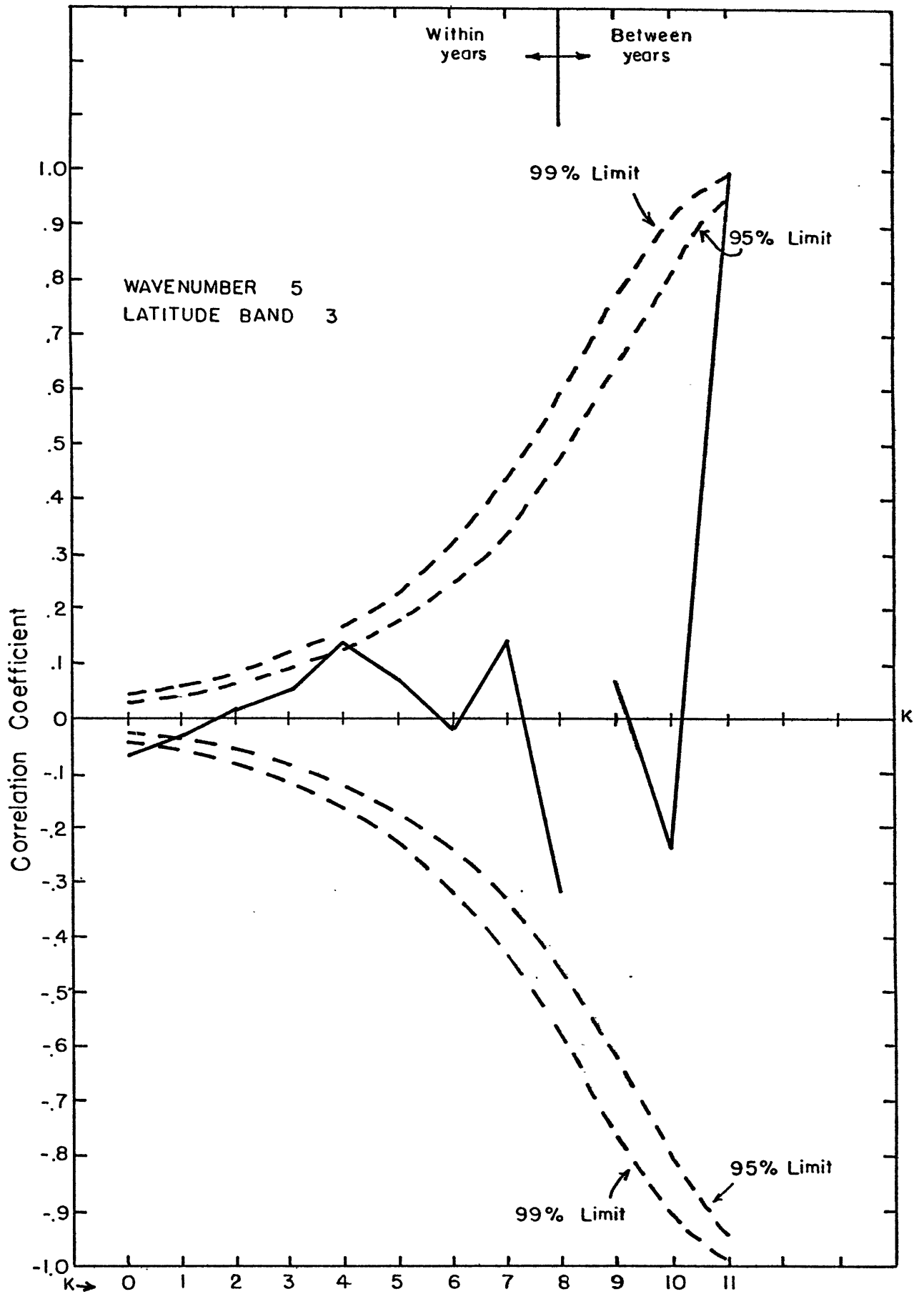


Fig. 4.12.23

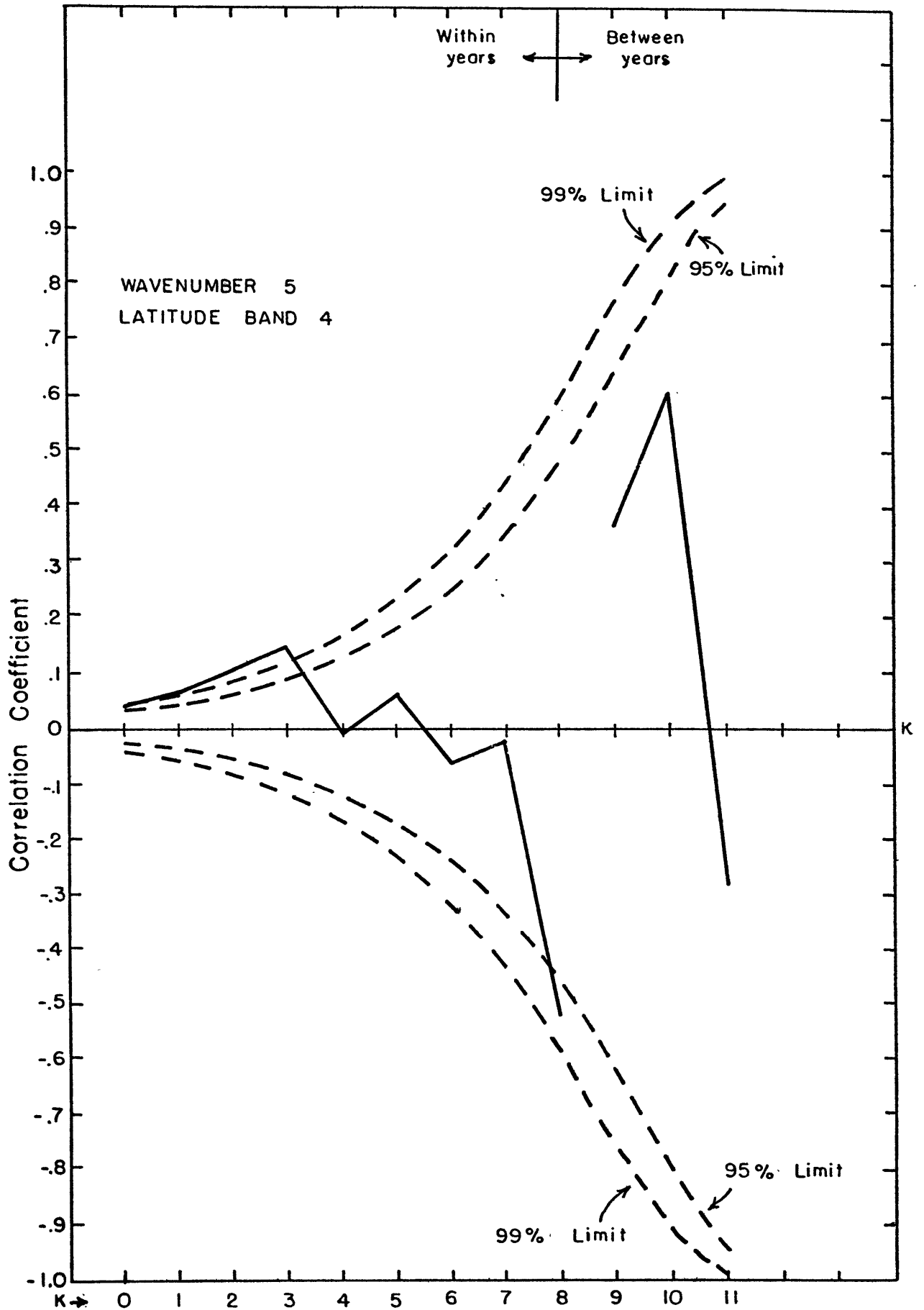


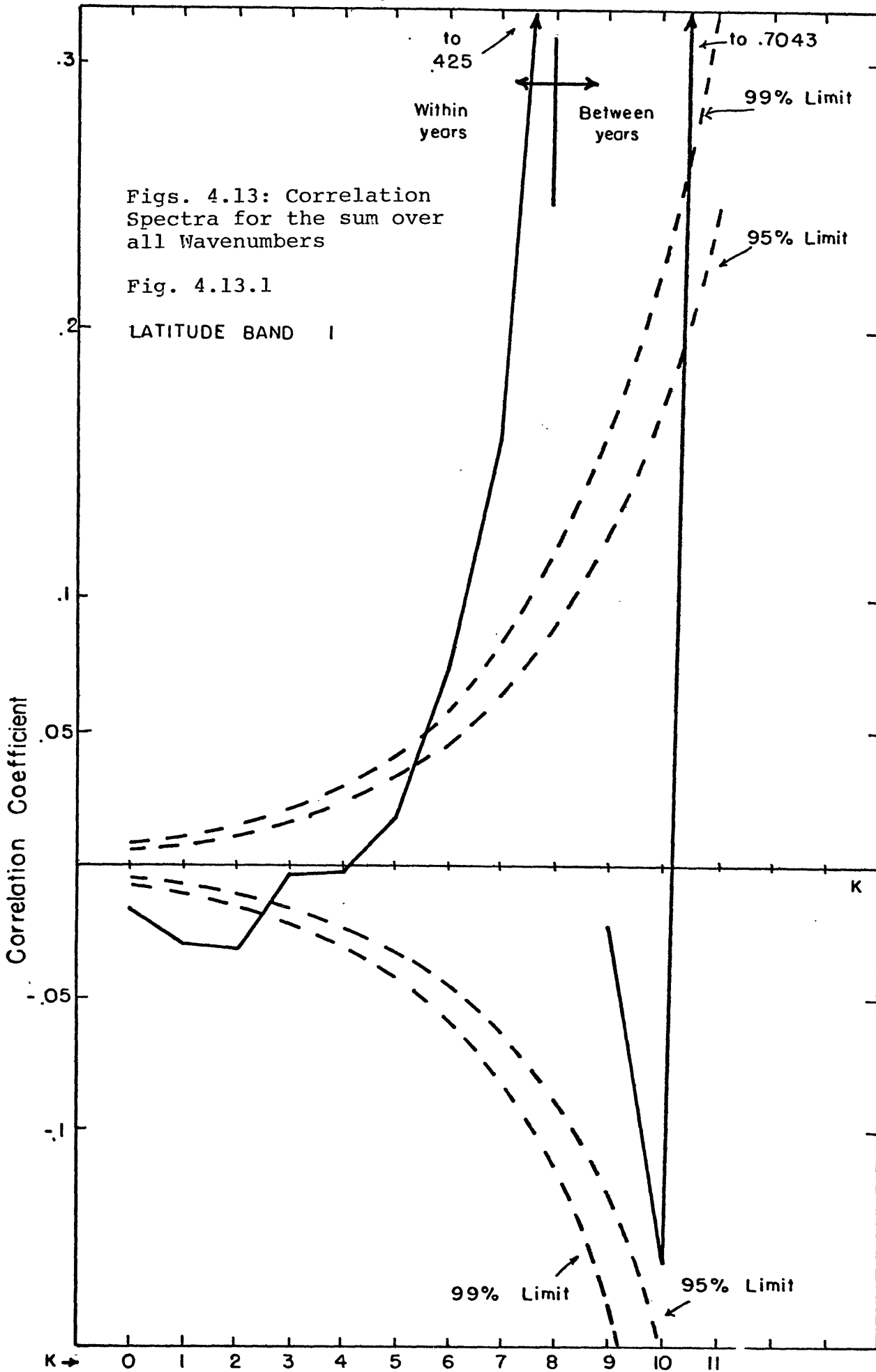
Fig. 4.12.24

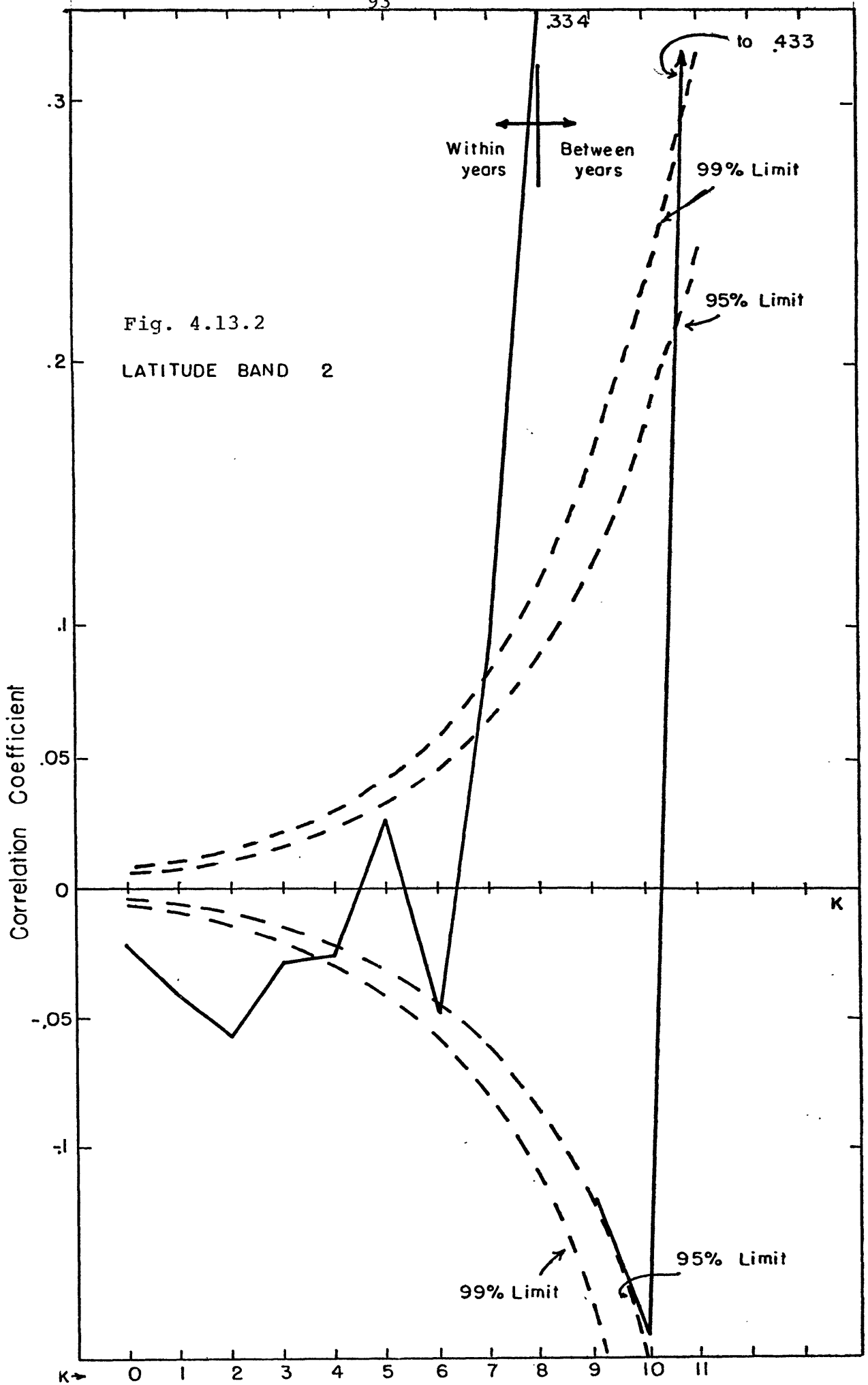
through 4. The confidence limits appear dashed while the coefficients have been connected by solid lines. When $k \leq 8$ the coefficients describe within year processes, when $k > 8$ they are interannual. Hence, we have separated the solid lines to denote these two temporal areas. Fig 4.12.1 shows three significant negative coefficients and two more negative ones for $k \leq 4$, 3 significant positive coefficients and another small positive one for $8 \leq k \leq 5$. For $k > 8$ nothing significant occurs. The coefficient for $k = 11, m = 0$ must be 1.0 because there is only 1 degree of freedom there. For large k , say $k \geq 9$, there are fairly few degrees of freedom so that decisive conclusions about statistical trends are difficult to make.

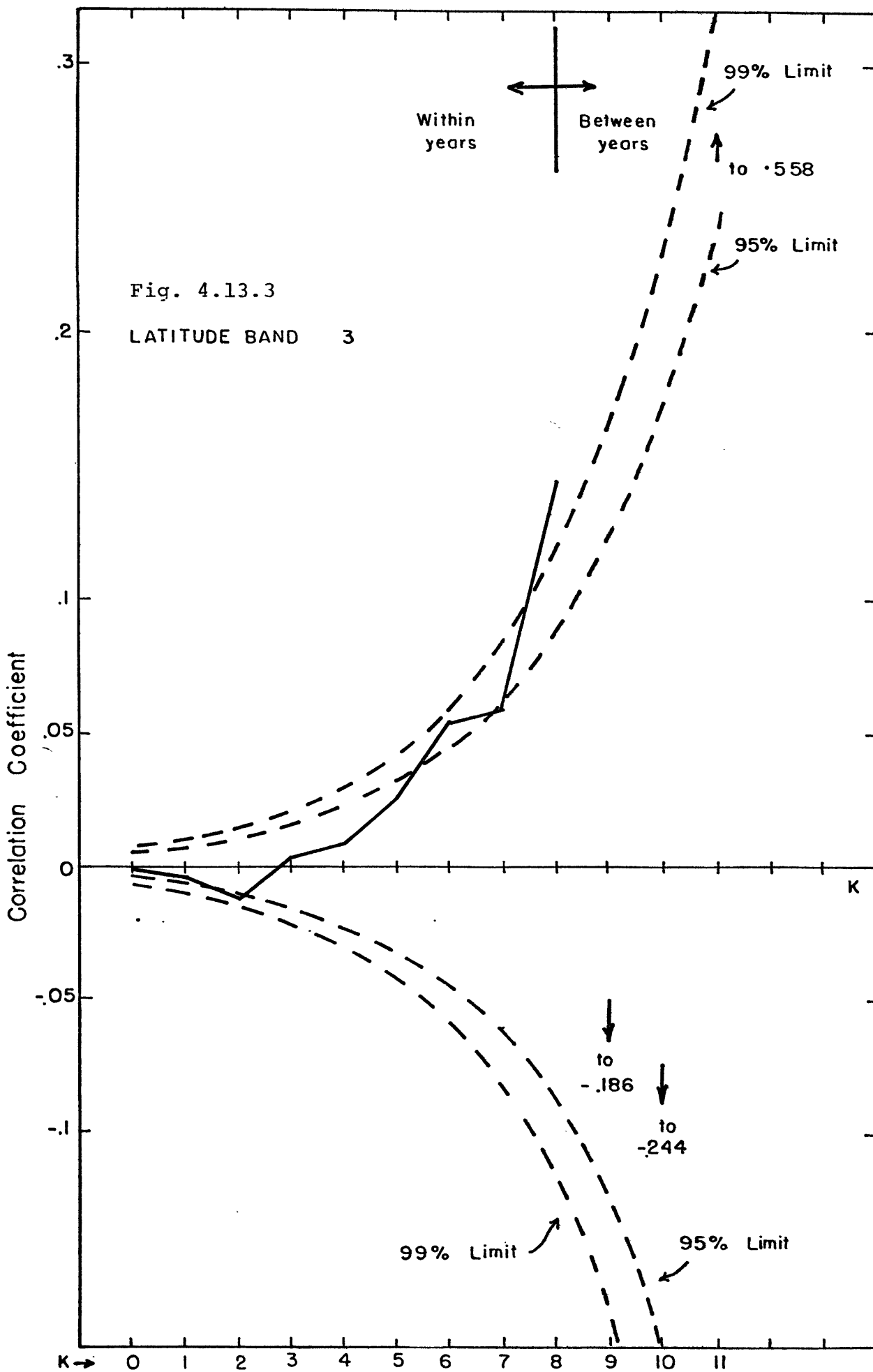
Rather than discuss each graph we will point out a few recognizable traits. In all cases except fig 4.12.24 (wave-number 5, latitude band 4), we observe negative correlations on short time scales. Many are significant at the 99% level. Secondly, we observe significant positive correlations (exception: fig 4.12.24) only on long time scales ($k = 6,7,8$), and only for selected zonal scales. Finally, there is little evidence for significant correlation in the $k > 8$ range of the spectrum.

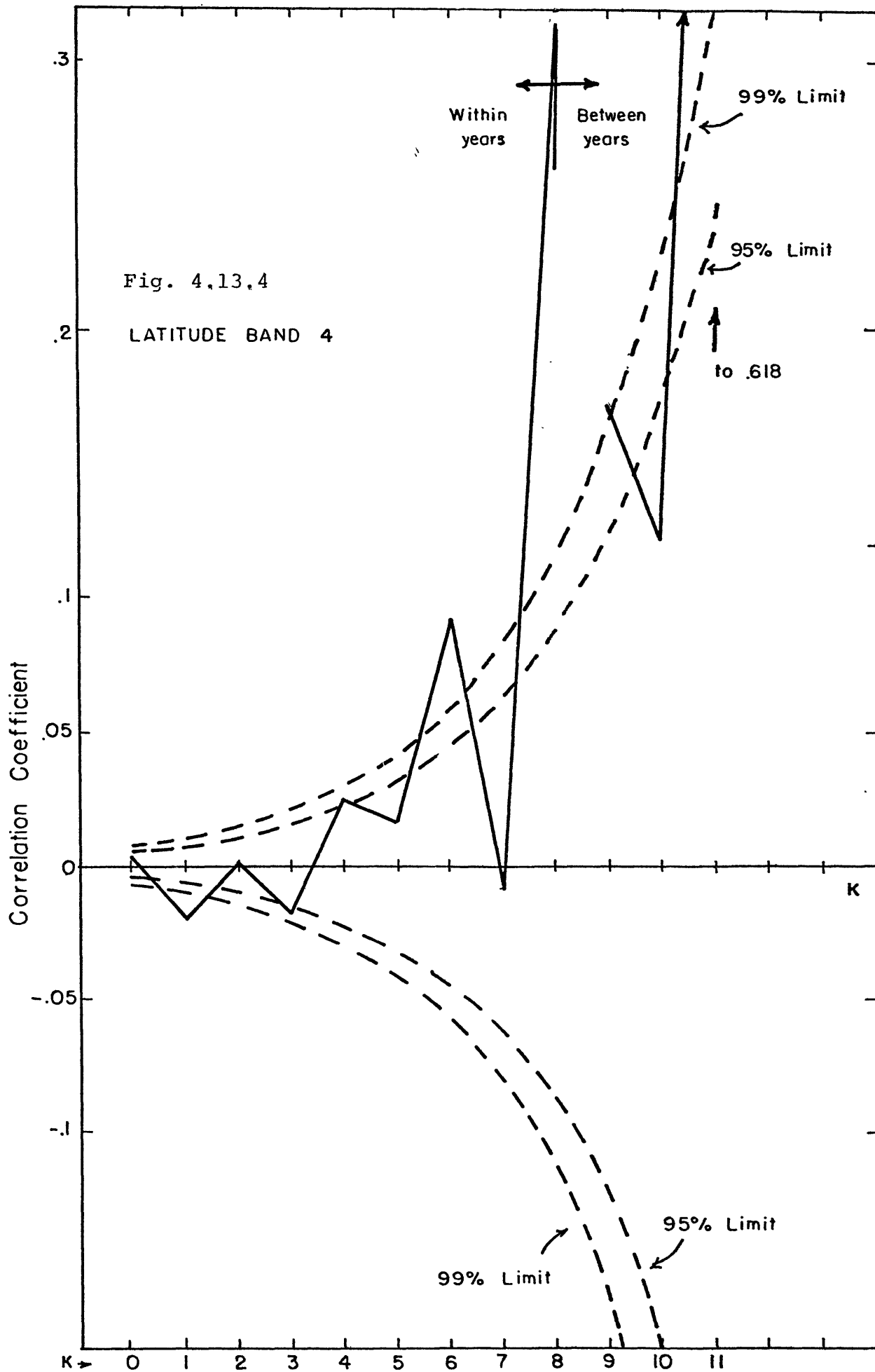
4.3 Correlation Spectra for the Sum Over All Wavenumbers

Figures 4.13.1 - 4.13.4 display these spectra summed over all wavenumbers. The graphs are identical in structure









to those of figure 4.12. Strikingly, all four latitudes show negative correlations on short time scales and positive correlations on long time scales ($k = 6,7,8$), although the trend is less distinct in the two higher latitudes. In contrast to figures 4.12, we do observe significant correlations for the between years scales; however, caution is the word here because of the small number of degrees of freedom.

4.4 Correlation Spectra for the Sum Over All Time Scales

These four spectra, depicted in figs. 4.14.1 - 4.14.4, display correlation coefficient as a function of wavenumber for the sum over all time scales. The reader should observe the expanded ordinate scale between 0 and .1. They describe, in essence, whether positive or negative correlations dominate for the entire range of time scales. Each spectrum is somewhat different; however, in all cases positive correlations are the rule for the zonally averaged flow. Negative correlations are observed to dominate in the 2-5 wavenumber range with a few exceptions. Caution should be taken in broadly interpreting these spectra because they include between year processes ($k > 8$) which are not of significance for this particular study. Latitude band 4 (65°) departs from the patterns established at lower latitudes with high positive correlations between wavenumbers 9 and 17. Referring to Appendix B, output for latitude band 4, we can see that this is caused by a concentrated group of high positive

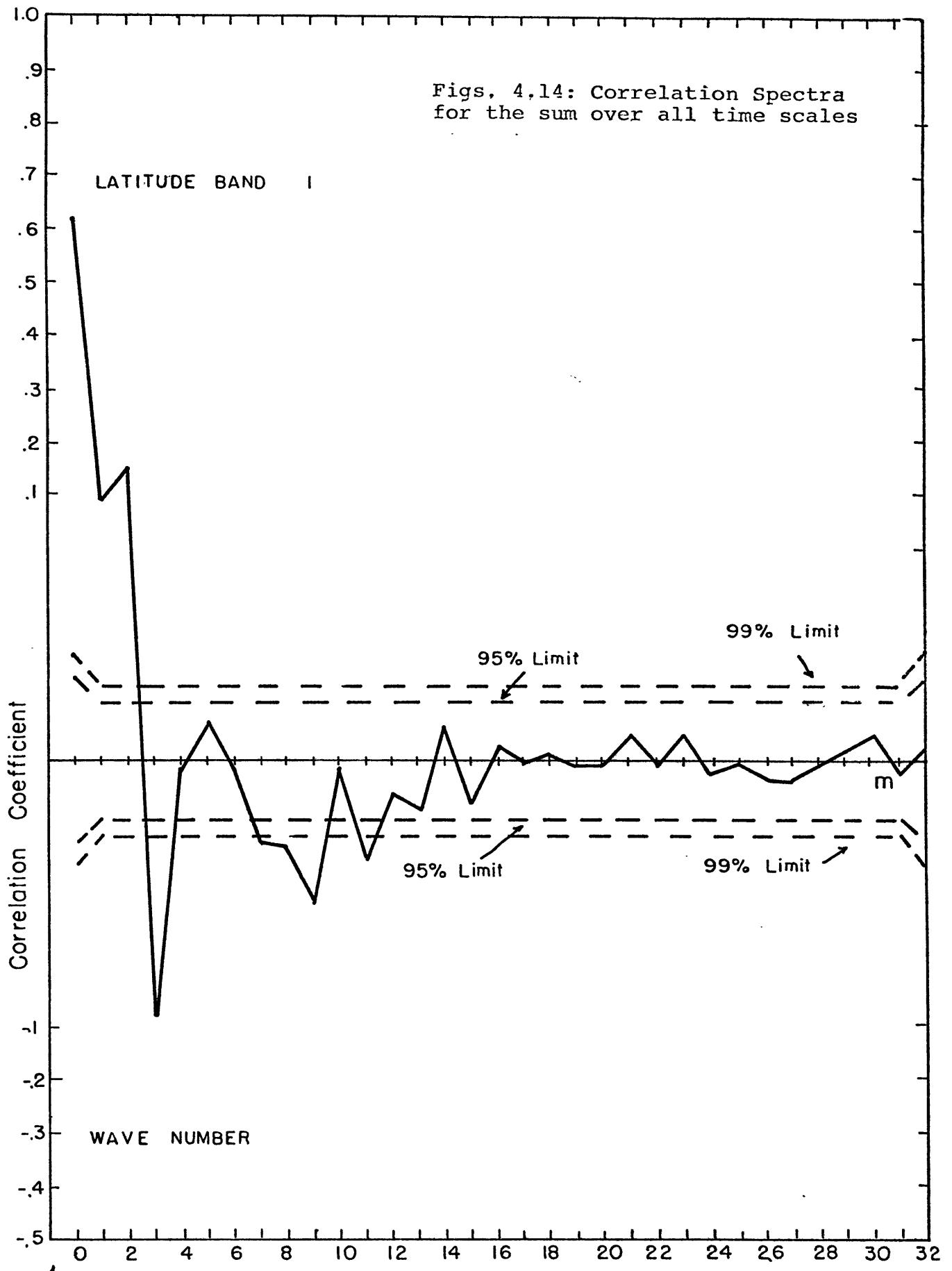


Fig. 4.14.1

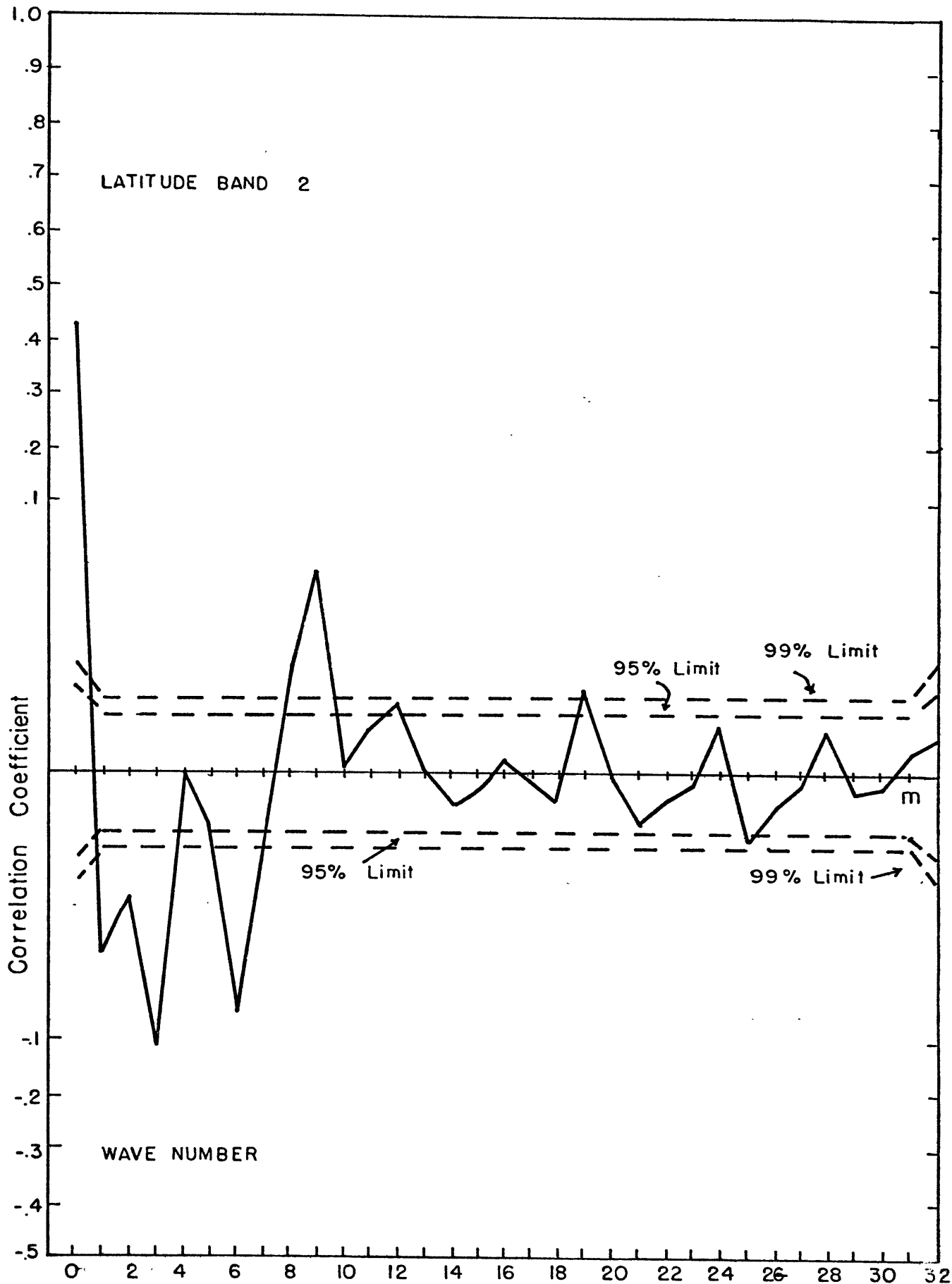


Fig. 4.14.2

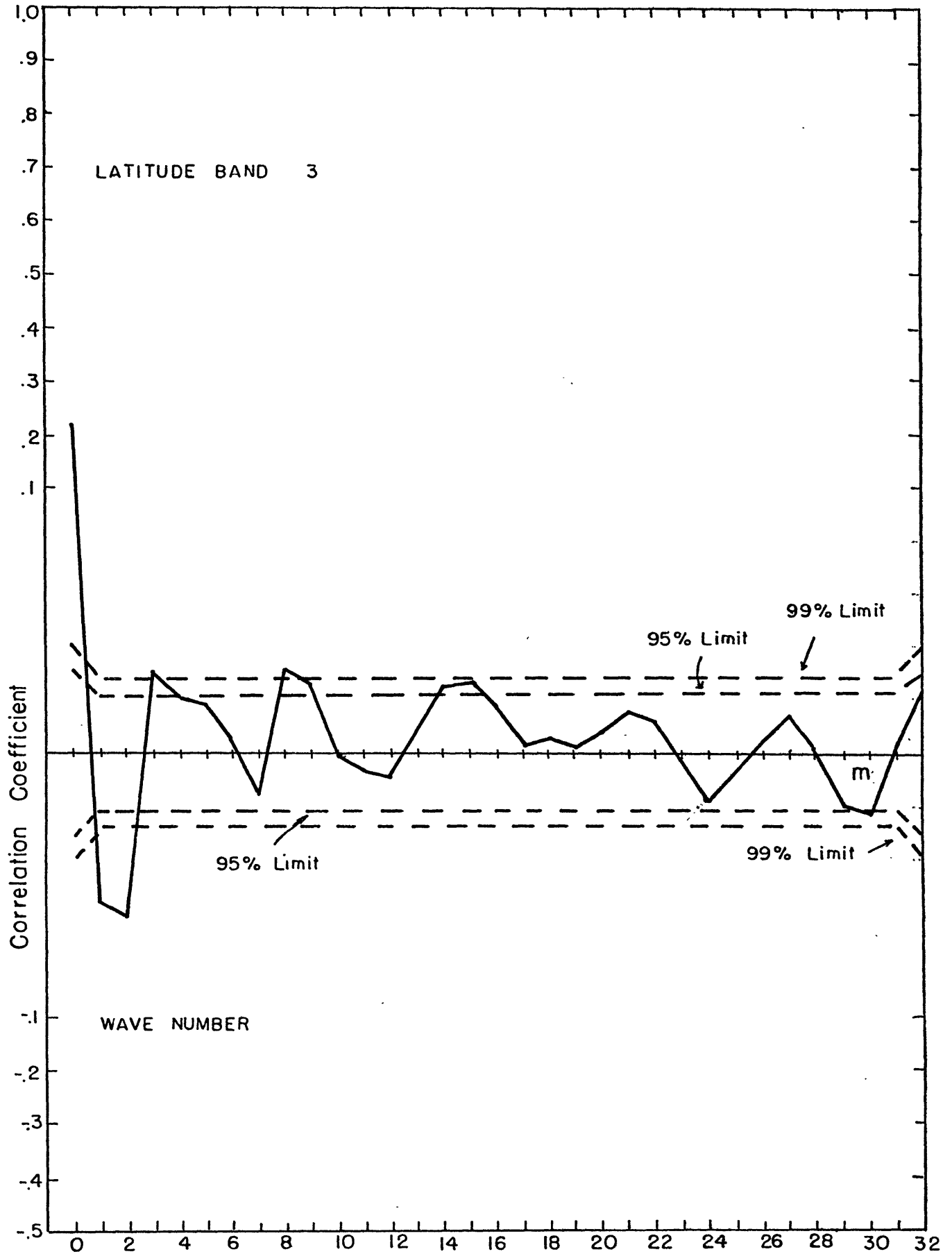


Fig. 4.14.3

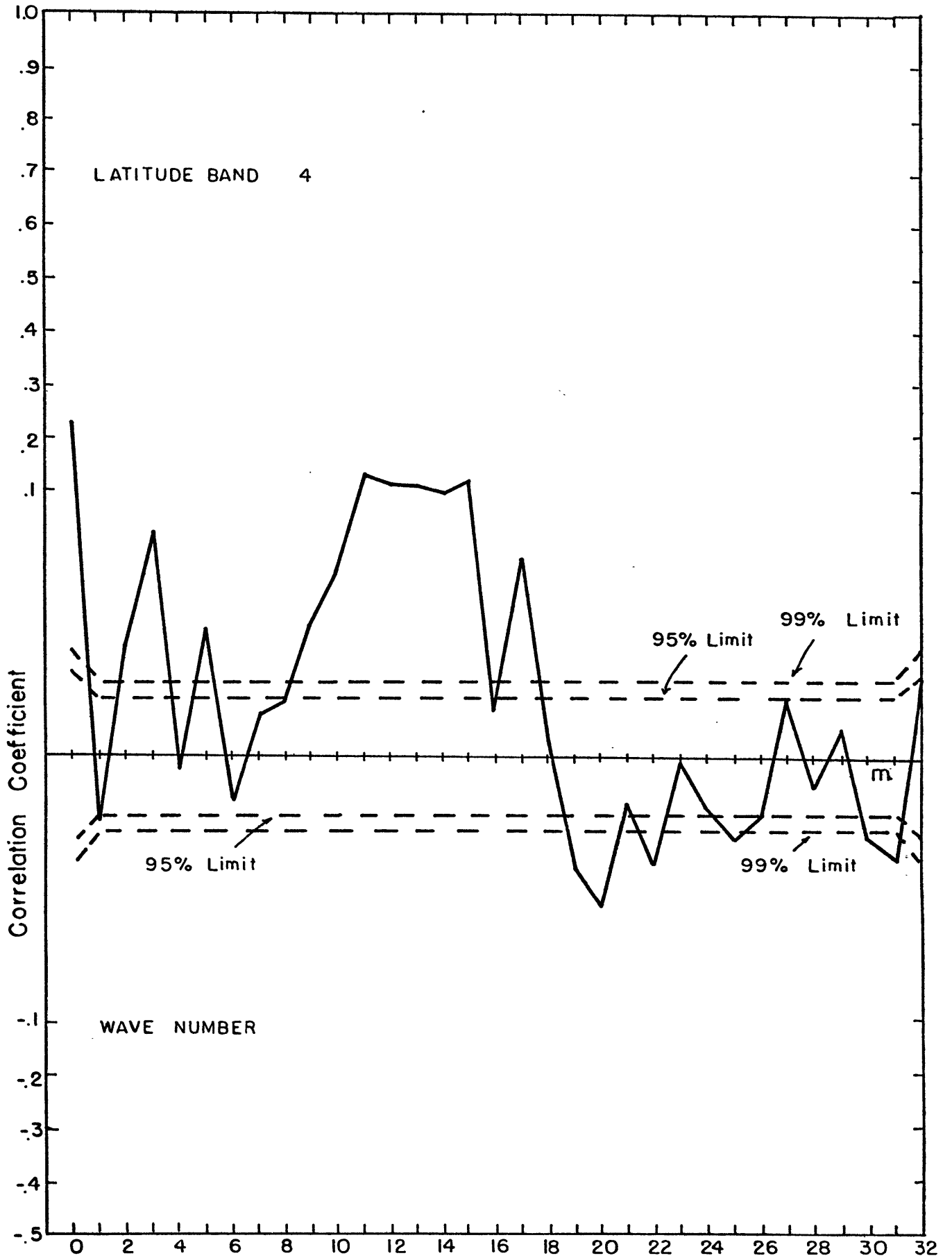


Fig. 4.14.4

correlations within these wavenumbers on short time scales. At 65° , the Zonal Scale is at most 1800 KM ($m = 9$) which approaches the reliable resolution limit of the data. (Hypothetically that limit is $\frac{2\pi a \cos 65^\circ}{32} = 512$ KM, but realistically it is probably twice or even three times that large.) Hence, not too much stock can be placed in significant correlations near this resolution limit. (See Table 5.1, which gives the physical size of the wavenumber domains as a function of latitude.)

4.5 Total Correlations by Latitude Band

Figure 4.15 depicts the total correlation coefficient between the eddy flux and $X \cdot (\Delta T)^2$ as a function of latitude. Little information is to be drawn from this graph because the absolute values of the coefficients are so small, even though they exceed the 99% confidence limit twice. One would not expect a high positive correlation between datasets which are negatively correlated on certain scales and positively correlated on others. These are probably the least meaningful results.

4.6 Variance and Covariance Spectra

Here we will briefly touch on the variance and covariance spectra found in Figures 4.1 - 4.9. In general, the variance of both $X \cdot (\Delta T)^2$ and the eddy flux drops off with increasing wavenumber. Relative maxima may be found, for

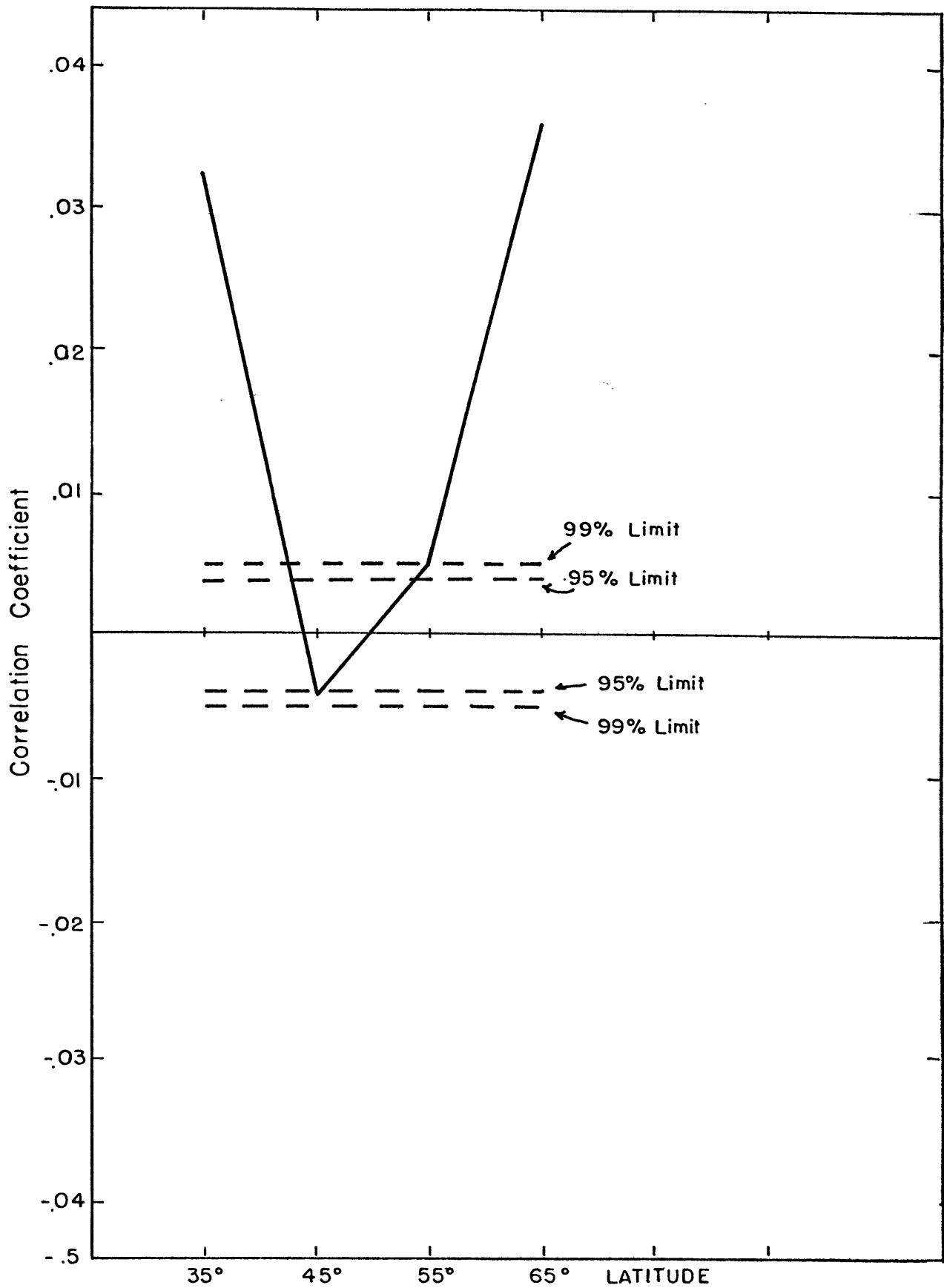


Fig. 4.15 Total Correlations by Latitude Band

instance, for $1 \leq m \leq 9$ and $k = 0$ in the $X \cdot (\Delta T)^2$ variance. Another relative maximum may be found at $m = 0, k = 8$. In the eddy flux case, the variance maximum occurs at $k = 2, m = 9$. The relative maxima described here refer to latitude 35°N only. Lorenz (1979) reports similar findings. In his case the variance in zonally averaged temperature decreased as the meridional scale decreased. Figures 4.7 - 4.9 reveal that the components of the covariance also decrease in magnitude as wavenumber increases. Positive maxima occur near $m = 0$ and $k = 8$, while negative maxima occur near $m = 0, k = 2$.

CHAPTER FIVE

DISCUSSION OF RESULTS AND CONCLUSIONS

5.1 Forced and Free Regimes

We can make use of the figures in the last chapter to draw some conclusions about the forced and free regimes revealed in the parameterization (2.8). In our case, because we correlate the eddy flux with the square of the temperature gradient, positive correlations imply that the variations are forced. For free variations the correlation must be negative, although it is possible to have a negative correlation even though some forcing is present (Lorenz, 1979). For the zonally averaged case, free regimes appear on short time scales and forced regimes appear on seasonal scales. This result solidly verifies both baroclinic adjustment and seasonal forcing within the spectre of the same data set.

For planetary and smaller scale wavenumbers (through $m = 5$), forcing at the seasonal time scale is confined to: wavenumber 1 at 35° and 45° , wavenumber 2 at 35° and 45° , wavenumber 3 at 55° and 65° and wavenumber 4 at 45° (marginal). Because the total eddy flux is modeled, both stationary and transient eddies are included. The wavenumber 3 forcing at high latitudes may very well be due to the topographical (land mass/ocean) forcing of the stationary eddies.

Flux variations which can be explained by this para-

meterization (i.e., which have significant correlations, either positive or negative) are, however, primarily free. At the seasonal time scale, many of the figures reveal no significant correlations. Wavenumber 5 at 65° and wavenumber 3 at 45° are the only seasonal time scales which are marked by negative correlations. As mentioned briefly in the last chapter, it is striking that significant negative correlations occur on all short period time scales except one. We conclude that we have observed what we set out to observe: the eddies also adjust the gradient on scales smaller than the zonally averaged scale!

We feel that we have been successful in effectively displaying the behavior of the eddies by spectrally testing (2.8) on real data. Additionally, we can assess more completely baroclinic adjustment, and make some general conclusions about the validity of (2.8). This we will do in the next two sections.

5.2 Baroclinic Adjustment: A Free Regime Process

By studying the latitudinal and temporal dependence of the eddies for short time scales we can learn a great deal about baroclinic adjustment. First, we will discuss the favored time scale. This is the period at which the eddies are most negatively correlated with $X \cdot (\Delta T)^2$. Secondly, we can examine the zonal scale of the eddies as a function of latitude. Finally we will describe how the

characteristic adjustment period ($= 2^k$ days) is affected by the zonal scale on which the adjustment is occurring.

With the exception of the zonally averaged case, the peak negative correlation begins at $k = 3$ (8 days) and retrogresses with increasing wavenumber until it reaches 1 day for $m = 5$, and finally disappears altogether at 65° for $m = 5$. For the zonally averaged case, the favored time scale is 4 days. This agrees with Lorenz' (1979) results. An average of the zonal and smaller scales could very well suggest 4 days as an overall favored time scale as well. We can offer a simple explanation for the observed retrogression, but must do so in light of the zonal scale of the eddies as a function of latitude.

Table 5.1 illustrates the physical size of the various wavenumber domains as a function of latitude. Referring to Fig 4.10, we see that adjustment is observed up to $m = 11$ for $k = 0$. Here, we define observation of adjustment to include the highest wavenumber exhibiting significant negative correlations for time scales such that $k \leq 4$, and within the reliable resolution limit of the data. This corresponds to a physical scale of about 3000 KM. Comparing this with the highest wavenumber for which adjustment is observed at 65° (see Appendix B) on the same time scale, we get $m = 3$. This corresponds to the physical scale of about 5600 KM. Doing the same for the middle two latitudes yields physical scale "lower limits" of about 3800 KM ($\phi = 55^\circ$) and 4000 KM

Table 5.1
Wavenumber Scales (KM.)*

	$\phi = 35^{\circ}$	45°	55°	65°
m =				
1	32780	28300	22980	16930
2	16390	14150	11490	8465
3	10927	9433	7660	5643
4	8195	7075	5745	4232
5	6556	5660	4596	3386
6	5463	4717	3830	2822
7	4683	4043	3283	2419
8	4098	3537	2872	2116
9	3642	3144	2553	1881
10	3278	2830	2298	1693
11	2980	2573	2089	1539

* Computed using $a = 6.371 \times 10^6 \text{m}$

$$2\pi = 6.28318$$

($\phi = 45^\circ$). A reasonable conclusion is that the zonal scale of the eddies has a lower size limit at around 4000 KM, for time scale $k = 0$ (1 day fluctuations). This result is consistent with baroclinic theory.

As the time scale increases, so does the "lower limit" on the eddy size observed to baroclinically adjust. This is exemplified very nicely at 55° where for $k = 0$, $m = 6$ represented the smallest adjusting eddy, whereas for $k = 3$, $m = 1$ is the smallest adjusting eddy. This transition is very smooth (refer to Appendix B) for $\phi = 55^\circ$ and less smooth but still quite noticeable at all other latitudes.

In light of this we can offer an explanation for the retrogression observed in the preferred time scale. As we move north, the time scale of an eddy at any given wavenumber decreases because the eddy size at that wavenumber decreases towards its lower physical size limit. At any one latitude, the time scale of an eddy decreases as zonal wavenumber increases because the physical size decreases with increasing wavenumber. Two limitations on this process exist. First, the eddies cannot be smaller than their characteristic length scale. In (2.5) that scale is HN/f , where H is the scale height, N the Brünt-Väisälä frequency and f the coriolis parameter. Hence, in fig. 4.12.24, the physical size may be ($m = 5$, $\phi = 65^\circ$ or ~ 3300 KM) too small and no baroclinic eddy is observed. Secondly, their time scale cannot greatly exceed $k = 3$ ($k = 4$ is about maximum) because other physical processes (e.g. stationary eddies) take over the burden of

the heat transport.

We can think of this retrogression in a different way. An eddy of small size is rapidly mixed into eddies of larger sizes -- hence to observe their transport we must search on short time scales. However, a large eddy retains its singular features longer. The largest baroclinic eddies thus exhibit the longest time scales--up to the limit of about $k = 4$ (16 days).

We are satisfied that we have learned a great deal about the zonal scales on which adjustment takes place, and realize that this is due in part to the unique spherical geometry of the earth. In conclusion of this section, Figure 5.1 displays a parametric plot of the preferred eddy time scale in baroclinic adjustment, revealing its retrogressive behavior.

5.3 Validity of the Eddy Flux Parameterization: Eddy Flux Predictors

We can make some general conjectures about the validity of (2.8) in modelling forced variations, which is what it is designed to do. Lorenz (1979) correlated (essentially) the eddy transport with the temperature gradient only, whereas our correlations involved an eddy diffusivity which is supposed to correct for the effect of the free variations by weighting the forced variations. By comparing his correlations with ours we will get a gross measure of the effect of the X parameter on the eddy flux parameterization.

Before doing this we should make clear that the two

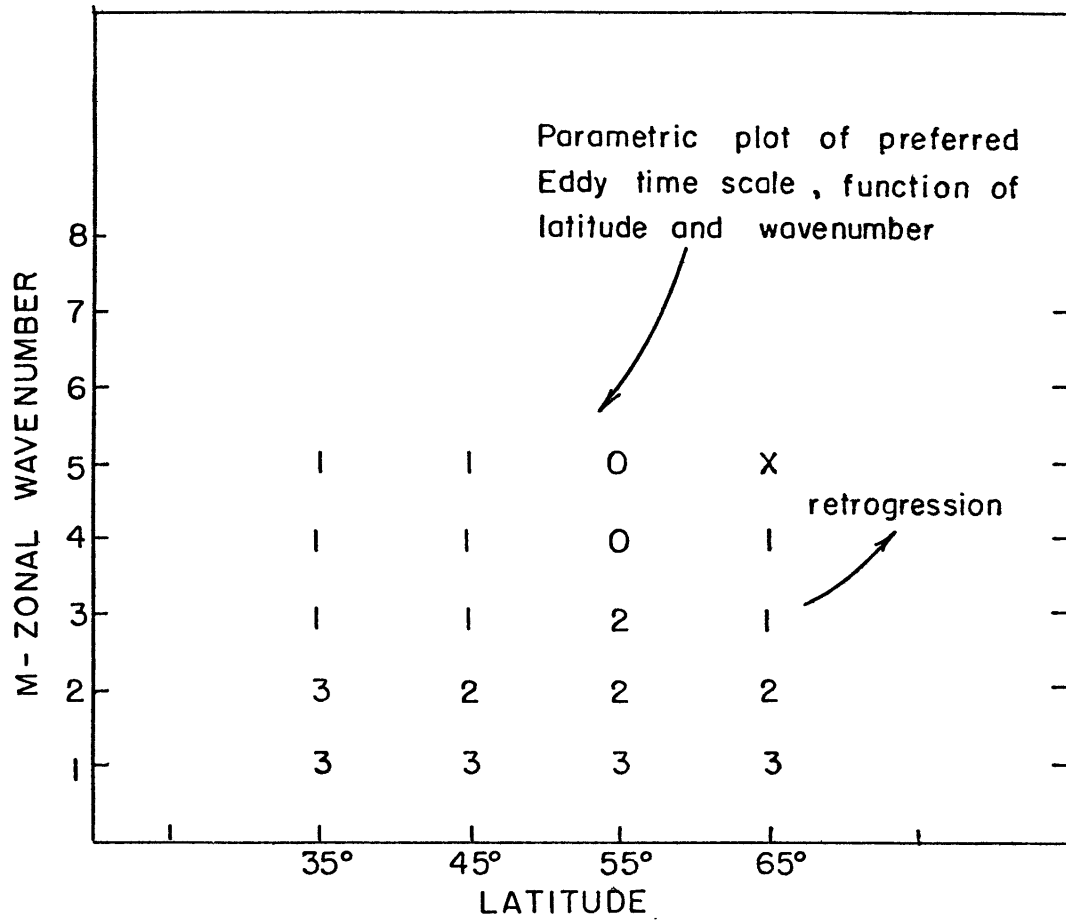


Fig. 5.1 Parametric Plot of preferred eddy time scale in Baroclinic Adjustment*

*k is plotted, time scale is 2^k days

studies are not perfectly compatible. First, Lorenz correlated the two quantities by meridional spectral analysis making use of the Legendre representations of the heat transport and temperature gradient. This effectively isolated the meridional planetary scale ($n=2$, where n is the degree of the Legendre polynomial) which proved to be the scale at which forced variations dominated. Our study correlated the quantities directly within latitude bands, without spectral meridional analysis. Stone and Miller (1979) point out that the characteristic meridional scale of the fluxes is basically the planetary scale when the fluxes are zonally and monthly averaged. Hence, we can be certain that the basic scale involved in our data for $m = 0$ and $k = 7$ or 8 (greater than month-long averages) is the planetary--but our data do not isolate this scale from the others. Hence, small contributions from other scales would decrease our correlations relative to Lorenz's.

Secondly, our data admit latitudinal dependences which Lorenz's does not. Noting that we can compare only the $m = 0$ results, for each time scale we have four correlation coefficients to Lorenz's one. Table 5.2 presents the comparison, where Lorenz's coefficients have been calculated from the tables in his paper. In his case, negative correlations indicate forcing of the flux by the gradient.

Lorenz's coefficients are markedly higher than ours for both time scales. We cannot assess whether this is because

Table 5.2
 Correlation Coefficient Comparison:
 Lorenz (1979) vs. McHenry

m = 0		ϕ	<u>McHenry</u>	<u>Lorenz</u>	<u>N</u>
k = 8		35°	.9834	-.996	2
		45°	.9653		
		55°	.8935		
		65°	.9131		
k = 7		35°	.7813	-.893	2
	45°	.6983			
	55°	.5688			
	65°	.0596			

his parameterization is better than ours, though, because of the above mentioned reason. What we had hoped to show--that ours is better than his--we cannot do either.

We should conclude by mentioning that we set out to test a parameterization which both took account of the β -effect and contained some measure of the zonal scale in its eddy diffusivity. In fact, (2.8) neglects this horizontal scale. We have shown, though, that (2.8) models forced variations well, but cannot determine the impact of X on its ability to model those variations.

In addition, we have presented a graphical analysis which displays both adjustment and seasonal forcing succinctly. We have documented the retrogressive behavior of the characteristic adjustment time scale with the physical eddy size. Finally, we believe the inclusion of X in (2.8) enabled us to better detect the overall behavior of the free regime eddies.

CHAPTER SIX

SUGGESTIONS FOR CONTINUING RESEARCH

In this chapter we will outline several ideas for research related to our study. In the first two sections we will discuss proposals directly related to this research, and in the last section we'll talk about general uses of the program SPECTRA.

6.1 Regional Analysis

Instead of performing correlations in wavenumber space, they could be performed by defining a regional eddy flux and examining specific geographic regions of varying size. The primary advantage of this would lie in better understanding of free variations, because forced variations occur on only the two or three largest longitudinal scales ($m = 0,1,2$).

In this analysis the eddy fluxes are defined regionally and correlations are performed only over the regions of definition. This procedure is undertaken because it is logical to assume that eddy transport (primarily due to transient eddies, in this case) in a region on one side of the globe is not a result of instabilities on the other side, and therefore does not adjust the gradient on the other side. So long as the regions are greater in extent than the appropriate length scale of the transport, illuminating results should be expected.

In order to begin, we define

$$\langle () \rangle = \frac{1}{\lambda_2 - \lambda_1} \int_{\lambda_1}^{\lambda_2} \frac{1}{a \cos \phi} () d\lambda \quad (6.1)$$

as an average over the part of a latitude circle spanned by longitudes λ_1, λ_2 . The regions are thus of extent $a \cdot \cos \phi \cdot (\lambda_2 - \lambda_1)$ in the zonal direction. We now define:

$$\begin{aligned} T^X &= T - \langle T \rangle \\ V^X &= V - \langle V \rangle \end{aligned} \quad (6.2)$$

where the $()^X$ denotes the departure of the field from its average $\langle \rangle$. Assuming a non-divergent geostrophic solution, as before, we find that $\langle V \rangle \neq 0$, and the eddy flux for the region, call it EF_R , now applies only to the region between λ_1 and λ_2 .

To perform the correlations, we might average EF_R over the region, getting $\langle EF_R \rangle$ as a function of time. We could compute and average X over the region, and define ΔT to span its meridional extent. Each region would yield two time series to be correlated. If we chose $\lambda_2 - \lambda_1 = \frac{2\pi}{m}$, we could perform correlations over regions of identical size, obtaining one correlation table for each set of regions of the same size studied. By choosing $\lambda_2 - \lambda_1 = \frac{2\pi}{m}$, we could also directly compare results with the present study for the free variations of short period.

In defining a regional flux, we must account for the fact that the total eddy flux, $\int_0^{2\pi} V^*T^*d\lambda$, is not conserved when the definitions (6.2) are used. A simple expression is now derived which relates the total eddy fluxes as defined each way. As before, let

$$\langle (\) \rangle = \frac{1}{\lambda_2 - \lambda_1} \int_{\lambda_1}^{\lambda_2} \frac{1}{a \cos \phi} (\) d\lambda$$

$()^X$ = departure from regional average

(6.3)

$[]$ = zonal average

$()^*$ = departure from zonal average

The total fluxes are

$$\langle VT \rangle = \langle V \rangle \langle T \rangle + \langle V^X T^X \rangle \quad (\text{region}) \quad (6.4)$$

and

$$[VT] = [V][T] + [V^*T^*] \quad (\text{zonal}) \quad (6.5)$$

Now,

$$\begin{aligned} [VT] &= [\langle VT \rangle] = [\langle V \rangle \langle T \rangle] + [\langle V^X T^X \rangle] \\ &= [\langle V \rangle][\langle T \rangle] + [\langle V \rangle^* \langle V \rangle^*] + [\langle V^X T^X \rangle] \end{aligned} \quad (6.6)$$

Combining the expressions (6.5) and (6.6) we get

$$[VT] = [V][T] + [\langle V \rangle^* \langle T \rangle^*] + [\langle V^X T^X \rangle] \quad (6.7)$$

Again combining, this time (6.7) and (6.5) we arrive at the result desired:

$$[V^*T^*] = [\langle V \rangle^* \langle T \rangle^*] + [V^X T^X] \quad (6.5)$$

We have made use of the fact that $[\langle \rangle] = []$. As it stands (6.8) relates the eddy fluxes as defined both ways, integrated around a latitude circle. The difference term $[\langle V \rangle^* \langle T \rangle^*]$, is the eddy flux resulting from the departure of the regional averages from the zonal averages. We suspect this term involves zonal planetary scale waves, and hence would reveal forced variations if studied over seasonal time scales.

6.2 Multiple Correlation Studies

Because our research did not reveal the affect of the inclusion of an eddy diffusivity on the parameterization (2.8), we feel that a multiple correlation study would be of value. It would be a simple modification to produce three time series: eddy flux, X , and $(\Delta T)^2$, analyze their zonal Fourier components, and correlate them jointly and by pairs. We suspect the results would indicate that X enhances the negative correlations on short time scales, but has only a small effect on seasonal scales since on average X is close to unity. This would confirm the suspected inability of X by itself to model short period free variations, and would point to more complex parameterizations for improved results.

6.3 General Uses of the Program SPECTRA

SPECTRA is a very versatile computer program which can be used to temporally correlate the Fourier coefficients of any two datasets. It is listed in FORTRAN IV in Appendix A. The restrictions are such that the number of datapoints in a set be in powers of two, and that the number of sets in a time series be in powers of two. It is generally easy to interpolate, or truncate, meteorological data sets to fit these requirements.

Instructions are provided in the comment cards on the meaning of the control parameters--there are only three--and on how to adjust the FORMAT statements to fit these parameters. We have found the program to be highly efficient and therefore inexpensive to use.

SPECTRA produces the variance, covariance and correlation coefficient spectra of the input data sets. We can think of many opportunities for its use which would involve only adjustment of the input data sets themselves. For instance, little is known about the cross-correlation spectrum of the eddy heat flux itself. By inputting $V^*(t)$ and $T^*(t)$, this spectrum would be produced in the output table entitled COMPONENTS IN THE ANALYSIS OF COVARIANCE.

APPENDIX A

COMPUTER PROGRAM SPECTRA: LISTING

CARD NUMBER	APPROPRIATE GENERAL LOCATION	PROGRAM
1		FORWARD SELECTA
2		C PROGRAM COMPUTE SPACED-TIME COEFFICIENT AND CORRELATION COEFFICIENTS
3		C FAST FOURIER ANALYSIS TO SPACED AND POOR HAN'S SPECTRAL ANALYSIS
4		C ALTERNATE LOGICALLY FORMATTED DATA SETS ARE CORRELATED
5		C USER MUST SPECIFY LENGTH OF HAN'S AND DIMENSION ARRAYS APPROPRIATELY
6		C ONE IS DEFINED TO BE: BOTH THE ARRAYS ARE ENCLOSED BY ONE
7		C USER MUST ALSO ASSIGN CERTAIN INITIAL STATEMENTS ACCORDING TO THE
8		C VALUES OF LENGTHS AND HAN'S
9		C FOR LOG-SCALE EQUALS NUMBER OF DATA POINTS AROUND A LAT CIRCLE TO BE
10		C FAST FOURIER ANALYSIS MUST BE POWER OF TWO
11		C FOR FOURIER ANALYSIS MUST BE POWER OF TWO
12		C FOR FOURIER ANALYSIS MUST BE POWER OF TWO
13		C FOR FOURIER ANALYSIS MUST BE POWER OF TWO
14		C FOR FOURIER ANALYSIS MUST BE POWER OF TWO
15		C THE COMMON BLOCKS ARE ORGANIZED AS FOLLOWS:
16		C /INP: INPUT GRID
17		C /IHAN: IMAGINARY ARRAYS USED IN FOURIER ANALYSIS ALONG LAT CIRCLE
18		C /OUT: OUTPUT OF FOURIER ANALYSIS WHICH ARE SINE AND COSINE COEFFS
19		C /P: IMPACT ARRAYS USED IN POOR HAN'S SPECTRAL ANALYSIS
20		C /RESULT: OUTPUT OF POOR HAN'S SPECTRAL ANALYSIS
21		C /OUTPUT: OUTPUT APPAYS COMPUTED FOR RESULT
22		C /AP: ARRAYS FOR USE IN PRINT FORMATS AND RESIDUAL CALCULATIONS
23		C /RES: RESIDUAL ARRAYS WITHIN COMMON BLOCKS
24		C /IN (STANDARD)
25		C /IN (STANDARD)
26		C /OUT (STANDARD)
27		C /RES (STANDARD)
28		C EXCEPT CIRCUMFERENCE OF IMPACT-1
29		C /OUTPUT: TOTAL TO STACK WORK AREA (STANDARD)
30		C /TOTAL: TOTAL TO STACK WORK AREA (STANDARD)
31		C /TOTAL: TOTAL TO STACK WORK AREA (STANDARD)
32		C /TOTAL: TOTAL TO STACK WORK AREA (STANDARD)
33		C /TOTAL: TOTAL TO STACK WORK AREA (STANDARD)
34		C /TOTAL: TOTAL TO STACK WORK AREA (STANDARD)
35		C /TOTAL: TOTAL TO STACK WORK AREA (STANDARD)
36		C /TOTAL: TOTAL TO STACK WORK AREA (STANDARD)
37		C /TOTAL: TOTAL TO STACK WORK AREA (STANDARD)
38		C /TOTAL: TOTAL TO STACK WORK AREA (STANDARD)
39		C /TOTAL: TOTAL TO STACK WORK AREA (STANDARD)
40		C /TOTAL: TOTAL TO STACK WORK AREA (STANDARD)
41		C /TOTAL: TOTAL TO STACK WORK AREA (STANDARD)
42		C /TOTAL: TOTAL TO STACK WORK AREA (STANDARD)
43		C /TOTAL: TOTAL TO STACK WORK AREA (STANDARD)
44		C /TOTAL: TOTAL TO STACK WORK AREA (STANDARD)
45		C /TOTAL: TOTAL TO STACK WORK AREA (STANDARD)
46		C /TOTAL: TOTAL TO STACK WORK AREA (STANDARD)
47		C /TOTAL: TOTAL TO STACK WORK AREA (STANDARD)
48		C /TOTAL: TOTAL TO STACK WORK AREA (STANDARD)
49		C /TOTAL: TOTAL TO STACK WORK AREA (STANDARD)
50		C /TOTAL: TOTAL TO STACK WORK AREA (STANDARD)
51		C /TOTAL: TOTAL TO STACK WORK AREA (STANDARD)
52		C /TOTAL: TOTAL TO STACK WORK AREA (STANDARD)
53		C /TOTAL: TOTAL TO STACK WORK AREA (STANDARD)
54		C /TOTAL: TOTAL TO STACK WORK AREA (STANDARD)
55		C /TOTAL: TOTAL TO STACK WORK AREA (STANDARD)
56		C /TOTAL: TOTAL TO STACK WORK AREA (STANDARD)

CARD NUMBER	ALPHA-LATH PROGRAM LOCATION	MODIFICATION
112	127	222
113	127	222
114	127	222
115	127	222
116	127	222
117	127	222
118	127	222
119	127	222
120	127	222
121	127	222
122	127	222
123	127	222
124	127	222
125	127	222
126	127	222
127	127	222
128	127	222
129	127	222
130	127	222
131	127	222
132	127	222
133	127	222
134	127	222
135	127	222
136	127	222
137	127	222
138	127	222
139	127	222
140	127	222
141	127	222
142	127	222
143	127	222
144	127	222
145	127	222
146	127	222
147	127	222
148	127	222
149	127	222
150	127	222
151	127	222
152	127	222
153	127	222
154	127	222
155	127	222
156	127	222
157	127	222
158	127	222
159	127	222
160	127	222
161	127	222
162	127	222
163	127	222
164	127	222
165	127	222
166	127	222
167	127	222
168	127	222

CARD NUMBER	OPERATION	ADDRESS
167	PRINT	131
170	PRINT	131
171	PRINT	131
172	PRINT	131
173	PRINT	131
174	PRINT	131
175	PRINT	131
176	PRINT	131
177	PRINT	131
178	PRINT	131
179	PRINT	131
180	PRINT	131
181	PRINT	131
182	PRINT	131
183	PRINT	131
184	PRINT	131
185	PRINT	131
186	PRINT	131
187	PRINT	131
188	PRINT	131
189	PRINT	131
190	PRINT	131
191	PRINT	131
192	PRINT	131
193	PRINT	131
194	PRINT	131
195	PRINT	131
196	PRINT	131
197	PRINT	131
198	PRINT	131
199	PRINT	131
200	PRINT	131
201	PRINT	131
202	PRINT	131
203	PRINT	131
204	PRINT	131
205	PRINT	131
206	PRINT	131
207	PRINT	131
208	PRINT	131
209	PRINT	131
210	PRINT	131
211	PRINT	131
212	PRINT	131
213	PRINT	131
214	PRINT	131
215	PRINT	131
216	PRINT	131
217	PRINT	131
218	PRINT	131
219	PRINT	131
220	PRINT	131
221	PRINT	131
222	PRINT	131
223	PRINT	131
224	PRINT	131

SAMPLE OUTPUT OF FOURTH COEFFICIENTS AND RECONSTRUCTED GRIDS

CARD NUMBER	APPENDIX	PROGRAM LOCATION	DESCRIPTION
333	2290		PRINT 101,102,103*(LEAND,K)*K*(KCOU2+KCOU3)
334	2310		PRINT 104, GRAND(LEAND)
335	2326		PRINT 105
336	2333		PRINT 111
337	2341		PRINT 102,LEAND
338	2347		PRINT 112
339	2354		LEAND*(12) 404900+956
340	2356	904	PRINT 106*(10+JUTR(1))*(1+FCOU)
341	2370		PRINT 107
342	2365		PRINT 108*(10+JUTR(1))*(1+FCOU)
343	2361		PRINT 107*(10+JUTR(1))*(1+FCOU)
344	2346		PRINT 139
345	2347	405	PRINT 139*(10+JUTR(1))*(1+FCOU)
346	2367		PRINT 105
347	2371		PRINT 131
348	2371		C TOTAL(LEAND)*K*(KCOU2+KCOU3)
349	2372		PRINT 107*(10+JUTR(1))*(1+FCOU)
350	2441		PRINT 108*(10+JUTR(1))*(1+FCOU)
351	2321		PRINT 100
352	2356		PRINT 113
353	2343		PRINT 108,LEAND
354	2377		PRINT 114
355	2377		PRINT 115
356	2304		PRINT 116
357	2321		PRINT 117*(10+JUTR(1))*(1+FCOU)
358	2321		PRINT 115
359	2326		PRINT 118*(10+JUTR(1))*(1+FCOU)
360	2367		PRINT 119
361	2371		PRINT 120
362	2602		PRINT 121
363	2602		PRINT 122
364	2607		PRINT 123*(CORP(LEAND)*K*(1+K*INUS))
365	2624		PRINT 124*(GRACOR(LEAND))
366	2634	200	CONTINUE
367	2630	100	FORMAT(10)
368	2636	101	FORMAT(10),COMPONENTS ((A1P1A1R3*(10+JUTR(1))*(1+FCOU))
369	2637	102	COF VARIANCE OF Y TILES DELTA T SQUARED)
370	2636	102	FORMAT(10),FOR LATITUDE BAND*(13)*PEZOMAL KAPENUMBER*(K*TIME
371	2636	102	CP(10))
372	2636	103	FORMAT(10),SUMS ARE BEC(K, I, I, FOURTY)
373	2636	104	FORMAT(10),K*(1+K*INUS)
374	2636	105	FORMAT(10),K*(1+K*INUS)
375	2636	106	FORMAT(10),TOTAL*(1+K*INUS)
376	2636	107	FORMAT(10),GRAND TOTAL*(1+K*INUS)
377	2636	108	FORMAT(10),COF VARIANCE OF Y TILES DELTA T SQUARED)
378	2636	109	FORMAT(10),COF VARIANCE OF Y TILES DELTA T SQUARED)
379	2636	110	COF VARIANCE OF Y TILES DELTA T SQUARED)
380	2636	111	FORMAT(10),SUMS ARE BEC(K, I, I, FOURTY)
381	2636	112	FORMAT(10),SUMS ARE BEC(K, I, I, FOURTY)
382	2636	113	FORMAT(10),SUMS ARE BEC(K, I, I, FOURTY)
383	2636	114	FORMAT(10),SUMS ARE BEC(K, I, I, FOURTY)
384	2636	115	FORMAT(10),SUMS ARE BEC(K, I, I, FOURTY)
385	2636	116	FORMAT(10),SUMS ARE BEC(K, I, I, FOURTY)
386	2636	117	FORMAT(10),SUMS ARE BEC(K, I, I, FOURTY)
387	2636	118	FORMAT(10),SUMS ARE BEC(K, I, I, FOURTY)
388	2636	119	FORMAT(10),SUMS ARE BEC(K, I, I, FOURTY)
389	2636	120	FORMAT(10),SUMS ARE BEC(K, I, I, FOURTY)
390	2636	121	FORMAT(10),SUMS ARE BEC(K, I, I, FOURTY)
391	2636	122	FORMAT(10),SUMS ARE BEC(K, I, I, FOURTY)
392	2636	123	FORMAT(10),SUMS ARE BEC(K, I, I, FOURTY)
393	2636	124	FORMAT(10),SUMS ARE BEC(K, I, I, FOURTY)
394	2636	125	FORMAT(10),SUMS ARE BEC(K, I, I, FOURTY)
395	2636	126	FORMAT(10),SUMS ARE BEC(K, I, I, FOURTY)
396	2636	127	FORMAT(10),SUMS ARE BEC(K, I, I, FOURTY)
397	2636	128	FORMAT(10),SUMS ARE BEC(K, I, I, FOURTY)
398	2636	129	FORMAT(10),SUMS ARE BEC(K, I, I, FOURTY)
399	2636	130	FORMAT(10),SUMS ARE BEC(K, I, I, FOURTY)
400	2636	131	FORMAT(10),SUMS ARE BEC(K, I, I, FOURTY)
401	2636	132	FORMAT(10),SUMS ARE BEC(K, I, I, FOURTY)
402	2636	133	FORMAT(10),SUMS ARE BEC(K, I, I, FOURTY)
403	2636	134	FORMAT(10),SUMS ARE BEC(K, I, I, FOURTY)
404	2636	135	FORMAT(10),SUMS ARE BEC(K, I, I, FOURTY)
405	2636	136	FORMAT(10),SUMS ARE BEC(K, I, I, FOURTY)
406	2636	137	FORMAT(10),SUMS ARE BEC(K, I, I, FOURTY)
407	2636	138	FORMAT(10),SUMS ARE BEC(K, I, I, FOURTY)
408	2636	139	FORMAT(10),SUMS ARE BEC(K, I, I, FOURTY)
409	2636	140	FORMAT(10),SUMS ARE BEC(K, I, I, FOURTY)
410	2636	141	FORMAT(10),SUMS ARE BEC(K, I, I, FOURTY)
411	2636	142	FORMAT(10),SUMS ARE BEC(K, I, I, FOURTY)
412	2636	143	FORMAT(10),SUMS ARE BEC(K, I, I, FOURTY)
413	2636	144	FORMAT(10),SUMS ARE BEC(K, I, I, FOURTY)
414	2636	145	FORMAT(10),SUMS ARE BEC(K, I, I, FOURTY)
415	2636	146	FORMAT(10),SUMS ARE BEC(K, I, I, FOURTY)
416	2636	147	FORMAT(10),SUMS ARE BEC(K, I, I, FOURTY)
417	2636	148	FORMAT(10),SUMS ARE BEC(K, I, I, FOURTY)
418	2636	149	FORMAT(10),SUMS ARE BEC(K, I, I, FOURTY)
419	2636	150	FORMAT(10),SUMS ARE BEC(K, I, I, FOURTY)
420	2636	151	FORMAT(10),SUMS ARE BEC(K, I, I, FOURTY)
421	2636	152	FORMAT(10),SUMS ARE BEC(K, I, I, FOURTY)
422	2636	153	FORMAT(10),SUMS ARE BEC(K, I, I, FOURTY)
423	2636	154	FORMAT(10),SUMS ARE BEC(K, I, I, FOURTY)
424	2636	155	FORMAT(10),SUMS ARE BEC(K, I, I, FOURTY)
425	2636	156	FORMAT(10),SUMS ARE BEC(K, I, I, FOURTY)
426	2636	157	FORMAT(10),SUMS ARE BEC(K, I, I, FOURTY)
427	2636	158	FORMAT(10),SUMS ARE BEC(K, I, I, FOURTY)
428	2636	159	FORMAT(10),SUMS ARE BEC(K, I, I, FOURTY)
429	2636	160	FORMAT(10),SUMS ARE BEC(K, I, I, FOURTY)
430	2636	161	FORMAT(10),SUMS ARE BEC(K, I, I, FOURTY)
431	2636	162	FORMAT(10),SUMS ARE BEC(K, I, I, FOURTY)
432	2636	163	FORMAT(10),SUMS ARE BEC(K, I, I, FOURTY)
433	2636	164	FORMAT(10),SUMS ARE BEC(K, I, I, FOURTY)
434	2636	165	FORMAT(10),SUMS ARE BEC(K, I, I, FOURTY)
435	2636	166	FORMAT(10),SUMS ARE BEC(K, I, I, FOURTY)
436	2636	167	FORMAT(10),SUMS ARE BEC(K, I, I, FOURTY)
437	2636	168	FORMAT(10),SUMS ARE BEC(K, I, I, FOURTY)
438	2636	169	FORMAT(10),SUMS ARE BEC(K, I, I, FOURTY)
439	2636	170	FORMAT(10),SUMS ARE BEC(K, I, I, FOURTY)
440	2636	171	FORMAT(10),SUMS ARE BEC(K, I, I, FOURTY)
441	2636	172	FORMAT(10),SUMS ARE BEC(K, I, I, FOURTY)
442	2636	173	FORMAT(10),SUMS ARE BEC(K, I, I, FOURTY)
443	2636	174	FORMAT(10),SUMS ARE BEC(K, I, I, FOURTY)
444	2636	175	FORMAT(10),SUMS ARE BEC(K, I, I, FOURTY)
445	2636	176	FORMAT(10),SUMS ARE BEC(K, I, I, FOURTY)
446	2636	177	FORMAT(10),SUMS ARE BEC(K, I, I, FOURTY)
447	2636	178	FORMAT(10),SUMS ARE BEC(K, I, I, FOURTY)
448	2636	179	FORMAT(10),SUMS ARE BEC(K, I, I, FOURTY)
449	2636	180	FORMAT(10),SUMS ARE BEC(K, I, I, FOURTY)
450	2636	181	FORMAT(10),SUMS ARE BEC(K, I, I, FOURTY)
451	2636	182	FORMAT(10),SUMS ARE BEC(K, I, I, FOURTY)
452	2636	183	FORMAT(10),SUMS ARE BEC(K, I, I, FOURTY)
453	2636	184	FORMAT(10),SUMS ARE BEC(K, I, I, FOURTY)
454	2636	185	FORMAT(10),SUMS ARE BEC(K, I, I, FOURTY)
455	2636	186	FORMAT(10),SUMS ARE BEC(K, I, I, FOURTY)
456	2636	187	FORMAT(10),SUMS ARE BEC(K, I, I, FOURTY)
457	2636	188	FORMAT(10),SUMS ARE BEC(K, I, I, FOURTY)
458	2636	189	FORMAT(10),SUMS ARE BEC(K, I, I, FOURTY)
459	2636	190	FORMAT(10),SUMS ARE BEC(K, I, I, FOURTY)
460	2636	191	FORMAT(10),SUMS ARE BEC(K, I, I, FOURTY)
461	2636	192	FORMAT(10),SUMS ARE BEC(K, I, I, FOURTY)
462	2636	193	FORMAT(10),SUMS ARE BEC(K, I, I, FOURTY)
463	2636	194	FORMAT(10),SUMS ARE BEC(K, I, I, FOURTY)
464	2636	195	FORMAT(10),SUMS ARE BEC(K, I, I, FOURTY)
465	2636	196	FORMAT(10),SUMS ARE BEC(K, I, I, FOURTY)
466	2636	197	FORMAT(10),SUMS ARE BEC(K, I, I, FOURTY)
467	2636	198	FORMAT(10),SUMS ARE BEC(K, I, I, FOURTY)
468	2636	199	FORMAT(10),SUMS ARE BEC(K, I, I, FOURTY)
469	2636	200	FORMAT(10),SUMS ARE BEC(K, I, I, FOURTY)

APPENDIX B
ADDITIONAL SPECTRAL OUTPUT

Below we provide the output tables of correlation coefficient spectra for latitude bands 2, 3 and 4, (45° , 55° , 65°).

CORRELATION COEFFICIENTS OF WITH DELTA T SQUARED, FOR INDIVIDUAL SPACE-TIME COMPONENTS, FOR COLUMN AND ROW TOTALS, AND FOR GRAN FOR LATITUDINAL AVERAGE PERIOD

M	COEFFS FOR SUM OVER K												
	0	1	2	3	4	5	6	7	8	9	10		
0	-.0322	-.0322	-.1827	-.1747	-.0694	-.0936	.1183	.6583	.2653	.3174	-.4371	1.0000	-.4262
1	-.1081	-.1203	-.1276	-.2414	-.1110	.0902	-.3030	.3655	-.2873	-.2324	-.4310	-.7309	-.0630
2	-.0237	-.1120	-.2073	-.0609	-.1071	.0535	.0163	.1930	.5671	-.1898	-.5103	-.1000	-.0470
3	-.1222	-.1540	-.1456	-.0415	-.0255	-.0950	-.0165	-.3062	-.4898	-.4931	.4941	-.9568	-.1137
4	-.0443	-.1374	-.1032	-.0046	-.0946	.0223	-.0638	.1500	-.4517	-.7467	-.2092	-.2145	-.0004
5	-.0264	-.1221	-.0658	-.0222	-.0528	.1336	.1506	.0309	.2135	-.1235	-.4211	-.0310	-.0204
6	-.1098	-.1209	-.0675	-.0070	-.1387	-.1580	-.2490	-.3667	.4433	-.0425	.0905	-.7168	-.0897
7	-.0740	-.0822	.1042	-.0075	-.0083	.0198	.7090	-.1703	.1441	-.1121	-.5041	-.4420	-.0212
8	.0025	.0230	.0768	-.0405	-.0409	-.0002	.2355	.0425	.0907	.6685	.8203	.6582	.0306
9	.0637	.0742	.0364	-.0375	.1562	-.1653	.1820	.1646	.3325	.3307	.6889	.5343	.0736
10	.0304	.0463	.0137	-.0204	-.1023	-.1000	.1363	-.1153	.5884	.1627	-.6358	.5108	.0026
11	.0409	.0057	.0307	.0624	.0221	.0481	.0635	-.3098	-.1376	.0714	-.7300	-.4121	.0160
12	.0344	.0290	.0127	.0250	-.0955	.0285	.0294	.0343	-.3485	.1796	.5683	-.0417	.0252
13	.0026	-.0134	-.0525	.0363	-.0506	.0240	.1323	-.0364	.0286	-.0312	-.2268	.6282	.0004
14	-.0268	-.0175	-.0134	.0300	-.0161	.0376	.0548	.0689	.3206	-.2613	-.0802	.9387	-.0106
15	-.0123	-.0082	-.0198	-.0134	-.0424	.0387	.1411	-.2924	.4561	-.0418	.1631	.3000	.0073
16	-.0245	.0206	.0359	-.0402	.0886	-.4149	.1321	.7376	.6459	.5246	.4583	.3498	.0032
17	-.0215	.0172	-.0030	-.0097	.1238	.0059	.0578	.2902	.2253	.1116	.0915	-.7447	-.0027
18	.0121	-.0159	-.0111	.0417	-.0246	-.0382	-.1545	.2471	.1269	.1818	.2864	.2075	-.0109
19	.0215	.0243	.0428	-.0002	.0325	.1594	.2254	-.0161	.1182	.6220	.7701	.6473	.0287
20	-.0016	-.0011	.0345	-.0699	.0465	.0319	.1805	-.0028	.2011	-.1944	.2005	-.2775	.0018
21	-.0213	.0182	-.0199	.0458	.0111	.1204	-.0667	-.1519	-.5483	-.3284	-.6066	-.9684	.0194
22	-.0793	.0075	-.0083	.0031	-.0444	.1462	-.0292	.0609	.2522	.3992	-.1826	.6931	-.0110
23	.0156	-.0370	-.0052	-.0417	-.0372	.0845	.0221	-.0559	-.3242	.6355	.2893	.3338	.0040
24	.0174	-.2024	.0417	.0745	-.1458	.1408	-.1163	-.4748	.1984	.0374	.2763	.9986	.0167
25	-.0348	-.0092	.0325	-.0216	-.0409	.1237	-.0343	-.2931	-.0360	-.2016	-.0563	-.0264	

CORRELATION COEFFICIENTS OF WITH DELTA T SQUARED, FOR INDIVIDUAL SPACE-TIME COMPONENTS, FOR COLUMN AND ROW TOTALS, AID FOR GRAN
 FOR LATITUDE RANGING FROM 30°N TO 30°S, AND TIME PERIOD

K	COEFFS FOR SUM OVER K												
	0	1	2	3	4	5	6	7	8	9	10	11	
0	-.0238	.0099	-.0229	-.1638	-.1974	.0736	.6665	.5585	.8395	.9300	.9979	1.0000	.2183
1	-.0356	-.0464	-.1337	-.0986	.0026	-.0233	.0203	.0262	-.2019	-.0712	-.7827	-.8563	
2	-.0198	.0057	-.1065	.0330	.0787	.0643	.1485	-.1122	-.4147	-.6893	-.9158	-.2198	-.0624
3	-.0437	-.0687	-.0516	.0437	.1026	-.0325	.0662	.1717	.6672	.6749	.4354	.9359	.0300
4	-.0464	-.0377	.0244	.1121	.0752	-.0022	-.0482	.1221	.2555	-.3220	-.0845	.2947	.0208
5	-.0081	-.0385	.0250	.0598	.1376	.0719	-.0207	.1397	-.3209	.0654	-.2335	.2908	.0185
6	-.0370	-.0200	.0237	.0491	.1024	.1512	.1711	-.2970	-.0303	.2060	-.0405	.2735	.0056
7	-.0134	-.0103	-.0390	-.0291	-.1301	.0246	.2383	.1160	.2394	-.3804	-.8343	.2946	-.0162
8	.0271	.0442	.0545	-.0267	.0538	.0035	.2236	.0516	-.1780	.0677	.8837	-.2435	.0312
9	.0104	.0685	.0251	.0492	-.1971	.0021	-.0680	.2365	-.2427	-.0125	.1050	.2368	.0262
10	.0299	-.0021	.0024	.0404	.0952	-.0520	.0040	-.0343	-.2303	-.0874	-.7068	-.1790	-.0017
11	.0163	-.0287	-.0329	.0227	.0355	-.1073	.0769	-.2156	-.0833	.7415	.1023	.0317	-.0075
12	.0390	.0438	.0162	.0205	.0676	-.0644	-.0924	.0434	.1017	.0039	-.3252	.2748	-.0027
13	.0514	.0002	.0433	.0240	-.0460	.0172	-.0310	.0213	-.2621	.1907	-.0228	.1276	.0095
14	.0598	.0176	.0077	.0254	.0146	.0680	-.1017	.0798	-.0669	-.2463	.1095	-.2895	.0255
15	.0206	.0395	.0125	.0428	.0246	.0105	.0450	.1395	.1240	.1020	.1190	.2903	.0269
16	-.0017	.0364	.0261	.0204	.0588	.0443	.0153	-.2549	.3719	-.2349	-.7541	.45512	.0175
17	-.0238	.0276	.0178	.0200	.1027	.0641	.0766	.0558	-.0956	-.0110	-.0953	.49811	.0027
18	-.0191	.0371	.0061	.0059	.0680	.0317	.0180	.0020	.0091	.4467	-.7486	.48172	.0050
19	-.0156	.0220	.0102	.0255	.0367	.0324	.0548	.1013	-.0221	-.0243	.0465	.6909	.0018
20	.0075	.0261	.0121	.0318	.0301	.0656	.0415	.0164	.0265	-.0075	.3596	.4128	.0072
21	.0200	.0055	.0041	.0416	.0573	.0701	.0427	.2364	-.0682	.0779	.2382	.2580	.0156
22	.0019	.0532	.0160	.0228	.0544	.0711	.0097	.1315	-.2014	.1116	-.6358	-.1076	.0113
23	-.0001	.0031	-.0124	.0111	.0880	.0921	.0460	.0093	-.2573	.0271	-.4879	-.10009	-.0032
24	-.0173	.0089	.0037	.0097	.0571	.0982	.0270	-.2468	.3556	-.2363	.7712	.9994	-.0180
25	.0046	-.0051	.0171	.0433	.0508	.0261	.0299	.0804	.0587	.1568	.0305	-.69368	-.0050

26	.0124	-.0053	-.0130	.0021	.0079	-.0041	-.0755	-.1117	.2205	-.4350	-.3162	.9523	.0045
27	.0123	-.0041	.0722	.0525	.1833	-.0591	.0152	-.0767	.0676	.5593	-.3946	.9033	.0134
28	-.0008	-.0175	.0157	.0152	.0509	.1694	.0711	-.1399	-.0102	-.0133	.7112	-.0951	.0003
29	-.1188	-.0574	.0121	-.0227	.1524	-.0950	-.0709	-.1766	.0792	.1458	.0252	-.5412	-.0207
30	-.0210	-.0022	-.0263	-.0463	.0707	-.0290	-.0435	-.0581	.0411	.1665	-.0703	.0196	-.0245
31	.0021	.0223	.0237	.0457	.0076	.0062	-.1133	-.2267	.0110	-.0113	-.0002	.0442	.0026
32	-.0058	.0730	.0223	.0241	.1766	-.0273	.3757	-.0730	-.1526	-.6606	-.0427	-.0000	.0277

COEFFS. FOR
SUM OVER
M AT
EACH K

-.0014 -.0052 -.0122 .0053 .0043 .0243 .0535 .0585 .1428 .1845 .2437 .5577

TOTAL COEFFICIENT .0040

CORRELATION COEFFICIENTS OF 4115 DELTA T SAMPLES, FOR INDIVIDUAL SPACE-TIME COMPONENTS, FOR COLUMN AND ROW TOTALS, AND FOR GRAN
FOR LATITUDE BAND 47-50.0 N. AVERAGING PERIOD
UNITLESS

K	COEFFS FOR SUM OVER K												
	FOR EACH WAVELENGTH												
	1	2	3	4	5	6	7	8	9	10	11		
0	.0411	.0120	.1180	.0140	.0525	.0770	.0027	.0556	.0191	.2283	.9180	1.0090	.2237
1	.0581	.0130	.0910	.0150	.0575	.1080	.0162	.0623	.1278	.2629	.1716	.2927	.0223
2	.0034	.0102	.0152	.0076	.1552	.0553	.0744	.1732	.1116	.0175	.0489	.0611	.0419
3	.0745	.0107	.0024	.0077	.0567	.1167	.0076	.1711	.0752	.2977	.0137	.0690	.0831
4	.0177	.0282	.0230	.0275	.0103	.0783	.0788	.0676	.0523	.2691	.0469	.2725	.0045
5	.0374	.0631	.1055	.1435	.0154	.0513	.0638	.0254	.5287	.3661	.6004	.0253	.0467
6	.0017	.0093	.0043	.0762	.0764	.1288	.1185	.0221	.0066	.02167	.1973	.03984	.0170
7	.0459	.0076	.0105	.0524	.0424	.1261	.0182	.0033	.0520	.3327	.2631	.0634	.0163
8	.0101	.0032	.0036	.0183	.1231	.1027	.0087	.0340	.03754	.04331	.0358	.07660	.0206
9	.0340	.0204	.1333	.0432	.0524	.0602	.0723	.1284	.0372	.00223	.0681	.0379	.0430
10	.0491	.0422	.0316	.1504	.1501	.0522	.0640	.0274	.1592	.5673	.0357	.0944	.0638
11	.0614	.1122	.1761	.1217	.0553	.1075	.0044	.0194	.0228	.1787	.0039	.0602	.1286
12	.0745	.1170	.1279	.1191	.1332	.1432	.0652	.1876	.2056	.3641	.0992	.1016	.1105
13	.1000	.1353	.1111	.0301	.0650	.0636	.1027	.1667	.1611	.0243	.2336	.0092	.1077
14	.0255	.1294	.1212	.0791	.0682	.0650	.0116	.1615	.0031	.0686	.0303	.0443	.0987
15	.1132	.1297	.0459	.0526	.1307	.1310	.1310	.1315	.0285	.0280	.3455	.0917	.1082
16	.0183	.0619	.0334	.0916	.0110	.0582	.0162	.0671	.0597	.0185	.0177	.0280	.0175
17	.0501	.0297	.0034	.0191	.0024	.1577	.0866	.1582	.0290	.0413	.0349	.1380	.0739
18	.0277	.0370	.0287	.0074	.0483	.1170	.0060	.1135	.0278	.01751	.0818	.0177	.0046
19	.0407	.0202	.0171	.0581	.1322	.1847	.1631	.0033	.0332	.0781	.0316	.0228	.0124
20	.0334	.0233	.0583	.1107	.1605	.0091	.1383	.1972	.1563	.0307	.0303	.0705	.0567
21	.0053	.0197	.1129	.0085	.02173	.0640	.1574	.0030	.0221	.0134	.0113	.0216	.0156
22	.0454	.0132	.0374	.0141	.1203	.1482	.0207	.0623	.1343	.0244	.0387	.0588	.0102
23	.0243	.0117	.0027	.0048	.0102	.0114	.0137	.1088	.0604	.0282	.0337	.0110	.0029
24	.0271	.0001	.0164	.0404	.0281	.0110	.01703	.027	.0538	.0137	.0248	.0248	.0200
25	.0123	.0090	.0504	.0287	.0056	.0172	.1654	.0234	.0402	.0400	.0459	.0751	.0307

REFERENCES

- Blackman, M.L., 1976: A climatological spectral study of the 500 mb geopotential height of the northern hemisphere. J. Atmos. Sci., 33, 1607-1623.
- Held, I.M., 1978a: The vertical scale of an unstable baroclinic wave and its importance for eddy heat flux parameterizations. J. Atmos. Sci., 35, 572-576.
- Held, I.M., 1978b: Theories for transient baroclinic eddy fluxes. The General Circulation: Theory, Modelling and Observations, NCAR/CQ-6+1978-ASP, 224-235.
- Holton, J.R., 1972: An Introduction to Dynamic Meteorology, Academic Press, Inc., 319 pp.
- Leith, C.E., 1974: Spectral statistical-dynamical forecast experiments. Proc. Intern. Symp. Spectral Methods in Numerical Weather Prediction, CARP Programme on Numerical Experimentation, Rep. No. 7.
- Lorenz, E.N., 1978: An experiment in non-linear statistical weather forecasting. Mon. Rev., 105, 590-602.
- Lorenz, E.N., 1979: Forced and free variations of weather and climate. J. Atmos. Sci., 36, 1367-1376.
- Phillips, N.A., 1954: Energy transformations and meridional circulations associated with simple baroclinic waves in a two-level quasigeostrophic model. Tellus, 6, 273-286.
- Saltzman, B., 1967: Steady-state solutions for axially-symmetric climatic variables. Research on the theory of climate. Contract Cwb-11389, Rept., Travelers Research Center, 1-38.
- Stone, P.H., 1972: A simplified radiative-dynamical model for the static stability of rotating atmospheres. J. Atmos. Sci. 29, 408-418.
- Stone, P.H., 1978: Baroclinic adjustment. J. Atmos. Sci., 35, 561-571.
- Stone, P.H., and Miller, D.A., 1979: Empirical relations between seasonal changes in meridional temperature gradients and meridional fluxes of heat. MIT Dept. of Meteorology, awaiting publications, 41 pp.

St. Pierre, R., 1979: Correlations between eddy heat fluxes and baroclinic instability. MIT Dept. of Meteorology Master's Thesis, 83 pp.